The University Of Sheffield.

Understanding and modelling low adhesion risk in the wheel-rail interface

Thomas Butcher

A thesis submitted in partial fulfilment of the requirements for the degree of Doctor of Philosophy

The University of Sheffield

Faculty of Engineering

Department of Mechanical Engineering

Submission Date

September 2022

Abstract

As the global drive for more sustainable and environmentally friendly travel continues, rail companies and operators are being put under more pressure to improve safety and reliability, as well as encourage commuters to switch to rail for their commute. Leaves are known to contribute to low adhesion in the wheel-rail interface, which is a massive problem for train operators. These problems include, but are not limited to, wheel sliding, Signals Passed At Danger (SPADs), station overruns and collisions. This project aimed to investigate the current understanding of how leaves get to the railhead and how they bond to the rail while causing low adhesion, including the differences between leaf species. The outcomes of these investigations were then used alongside KPI data from industry to develop a low adhesion risk assessment model.

A literature review and paper grading were conducted to find gaps in the current knowledge and steer the direction of this work. These gaps included; mechanisms of leaf fall, chemical composition of certain deciduous tree species native to the UK and their effects on friction. Specific bonding mechanisms and bond strength also remain unclear. Hypotheses regarding the specific leaf layer formation and low adhesion mechanisms were identified during the literature review. Throughout the autumn period data is gathered, including monitoring leaf levels on trees across the UK using photographs taken by leaf fall observers. These form part of the input to the adhesion prediction(s), which are used by the Train Operating Companies (TOC's), to plan their journeys and timetables. A more detailed, location specific model that takes other physical factors into account is needed, hence the development of the low adhesion risk assessment model in this work.

Through Autumn of 2018 and 2019 ambient humidity, pressure and temperature as well as railhead temperature were recorded at various known low adhesion points across the Supertram network in Sheffield, UK and at several heritage rail locations. This was achieved using a sensor box to record the ambient parameters (air temperature, pressure and humidity) and an infrared thermometer to record railhead temperature. The purpose was to determine which environmental conditions correlate with leaf fall times and low adhesion incidents. These were then fed into the adhesion risk assessment prediction model.

A study was conducted to assess the leaf fall behaviours of three tree species under still and artificially windy conditions. Leaf retention on ballast was tested with dry, slightly wet and fully saturated leaves, where the wind speed at which leaves were

removed was tested. This information was fed into the adhesion risk assessment prediction model.

The bonding and low adhesion hypotheses identified from the literature review were detailed along with their own specific testing plans. The hypotheses were tested using a mixture of mechanical testing, chemical testing and analysis. The findings of these tests contribute to the wider understanding of leaf layer formation.

A large part of this project involved the development of an improved adhesion prediction model. Historical Key Performance Indicator (KPI) data concerning Wheel Slide Prevention (WSP) was provided by Chiltern Railways Company Limited (CRCL) and formed the basis of a case study and initial formation of a leaf layer induced low adhesion risk assessment model. Locations on the CRCL network were organised by the frequency of WSP activation, then split into high, medium and low groups. A combination of Google maps and physical site visits were used to assess the vegetation levels and physical track parameters. The scores for half of the locations were mathematically analysed in order to rank the impact of the parameters. The model was then applied to the second half of the locations to validate the parameter rankings. Outcomes of the other parts of work looking at leaf fall classification, times and associated weather conditions as well as friction and bonding hypotheses also fed into the scoring method where applicable.

Acknowledgements

The author of this work would like to express immense gratitude to Professor Roger Lewis, Dr Joseph Lanigan, Mr Louis Schmandt and Mr Anup Chalisey for their guidance and support throughout the project.

Additional thanks must be given to the EPSRC and RSSB for funding the work, to the ARG for providing a means of dissemination and communication of the work at various stages and to CRCL for supplying information that was crucial in the low friction risk assessment model development. The integrated tribology CDT also deserves special thanks as without it, the author would not be in a position to carry out this PhD project, with additional thanks to the CDT manager Ms Kimberly Matthews-Hyde.

The author would like to thank their fellow PhD students and research associates for providing an encouraging and helpful atmosphere and a strong sense of community.

Special recognition must be given to technician Mr David Butcher and the rest of the support staff in the Mechanical Engineering department, without whom this project would have been far more difficult.

Last but not least the author must thank all of his friends, family and amazing girlfriend Cait Griffiths for their unwavering support during the thesis writing.

Abbreviations

ARG	Adhesion Research Group
AWG	Adhesion Working Group
BBP	Brown leaf Black Precipitate
BLE	Brown Leaf Extract
BLF	Black Leaf Film
ESCA	Electron Spectroscopy for Chemical Analysis
FSR	Full-Scale Rig
FT-IR	Fourier Transform Infrared spectroscopy
GBP	Green leaf Black Precipitate
GLE	Green Leaf Extract
KPI	Key Performance Indicator
LRS	Laser Raman Spectroscopy
NwR	Network Rail
RAIB	Rail Accident Investigation Branch
rpm	revolutions per minute
RSSB	Rail Safety and Standards Board
SPAD	Signal Passed At Danger
SUROS	Sheffield University ROlling Sliding test rig
UMT	Universal Mechanical Tester
v	Velocity (m/s)
WSP	Wheel Slide Protection
Wt.%	Weight Percentage of a substance in a mixture
XPS	X-ray Photoelectron Spectroscopy
XRD	X-ray Diffraction spectroscopy
μ	Friction /Adhesion/Traction coefficient

Contents

1. INTRODUCTION

1.1 Overview and context of the project

As the global drive for more sustainable and environmentally friendly travel continues, rail companies and operators are being put under more pressure to improve safety and reliability, as well as encouraging people to switch to rail for their commute. The rail network in the UK is responsible for 4 million journeys daily [1], with this number predicted to double over the next 25 years. Covid has of course had a major impact on the entire world, including the rail industry. An industry finance report from the Office of Rail and Road (ORR) found that in the 2020/21 financial year, fares income in dropped from £10.2 billion to £1.8 billion due to the impact of the pandemic [2].

Low adhesion in the wheel-rail interface causes traction problems which significantly affect network performance each autumn, as traction is reduced, acceleration out of stations is reduced, leading to delays. Braking is also affected, which is a major safety concern (leading to rail squats, wheel flats due to sliding, SPADS, station overruns, collisions etc.). The annual cost of low adhesion to the UK rail industry has been estimated to exceed £350 million [3]. Examples of what this cost is attributed to include:

- £0.5 million for safety risks and associated injury costs (e.g. rapid response teams, staff training and briefing),
- £290.5 million for autumn performance dip and leaf fall timetable,
- £64.5 million for seasonal fleet costs, manual rail cleaning, damage repair, lineside vegetation management and autumn driver training [4].

Figure 1: Black leaf layer bonded to the railhead (left), and clean railhead (right).

The problematic leaf layer (see Figure 1 above) adheres strongly to the railhead and while not being the only source of low adhesion (others include: water, grease, pollution etc.) significantly reduces adhesion at the wheel-rail interface [5]. This causes a reduction in braking effectiveness, which can result in signals being passed at danger

(SPADs), station overruns and collisions two examples are covered in these Rail Accident Investigation Branch (RAIB) reports 18/2011 and 26/2014 [6], [7].

Current mitigation methods include feeding to the wheel-rail interface sand (sometimes via emergency braking) or traction gel, wire brush 'scrubbing', as well as high-pressure water jetting. From a review of the current literature on the 'leaves on the line' problem, it is clear that there is a lack of understanding as to the specific chemical and tribological mechanisms responsible for the bonding of the layer to the railhead. This is also true for the mechanisms of low adhesion between the wheel and the leaf layer. When a better understanding of this is found then solutions could be provided for better mitigation and forecasting information to Train Operating Companies (TOCs) and other rail companies (Network Rail etc.).

1.2 Aims

The aims of the project were to widen the understanding of low adhesion caused by leaves to include various effects. This included: different leaf chemistries, times of the year that particular leaves fall and related weather conditions (as this information was not found during the literature review). This was achieved with a combination of lab and field testing alongside the use of KPI's containing information on WSP[1], a train borne mitigation technique. Then to use the information gathered to develop a model for predicting the risk of leaf induced low adhesion at different locations.

The objectives set out to achieve this project were mapped out by work packages (WP) listed below:

- WP1 - Review literature to assess the current understanding of leaf friction, bonding mechanisms and chemistry of different leaf types
- WP1 - Identify gaps in the literature that need to be investigated, then form hypotheses to be tested
- WP2 - Determine the necessary data to be collected throughout the autumn period and devise an efficient method for achieving this
- WP3 - Design and carry out a test plan to investigate bonding and low friction hypotheses
- WP4 - Observe and analyse the process of leaf fall (from the branch to the railhead) and investigate leaf properties and fall characteristics for different species

[1] WSP is an electronic system fitted to most modern passenger trains that is there to protect wheels from damage and improve braking distance.

- WP5 - Carry out a case study on the Chiltern Network using KPI data on WSP activity to identify sites with varying incident characteristics
- WP5 - Combine autumn data with friction and bonding data to develop a computational model for assessing the risk of leaf induced low adhesion

The project was split into five work packages, outlined above in Figure 2.

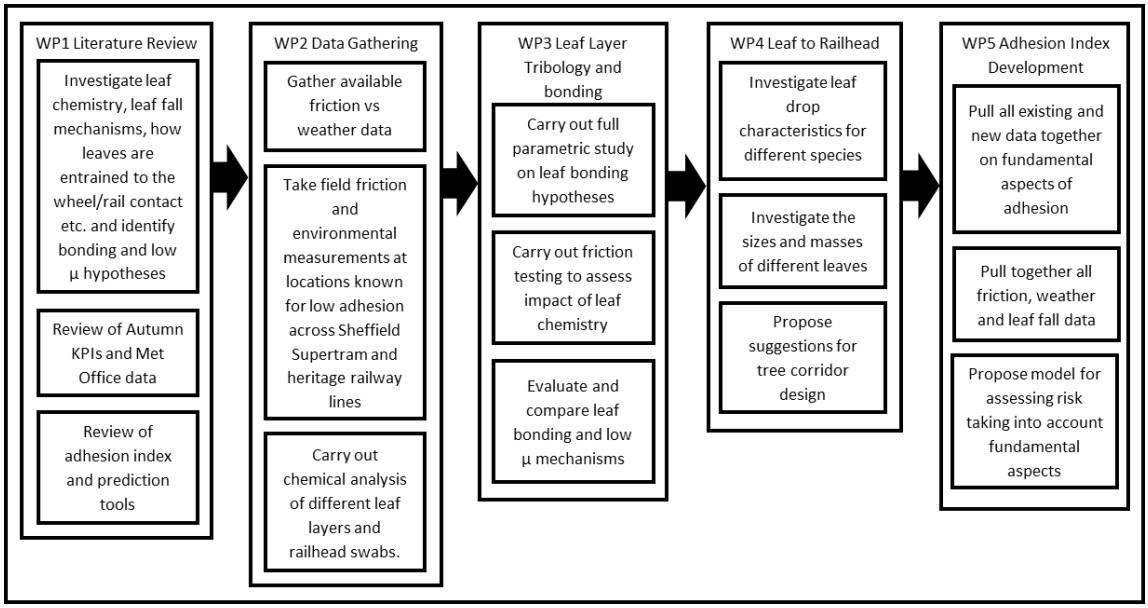

Figure 2: Project flow chart.

1.3 Novelty and impact

Novel aspects of this work include:

- The development of an open source low adhesion risk assessment model.
- The leaf fall characteristics study comparing leaves of different species.
- The leaf HPT friction test outcomes comparing species and against graphite.
- The SUROS friction tests on leaves with and without an acidity controller to inhibit acidic gel formation.
- The SUROS layer formation/friction tests on leaves with and without a metal ion capturing agent to reduce reactions with Fe ions.
- The comparison of steel and titanium specimens to confirm the role of iron in leaf layer formation.

The open source low friction risk assessment model will benefit the industry by potentially improving financial (delay minutes) and safety (e.g. the Salisbury rail collision in 2021 [8]) factors, the outcomes of the leaf fall study could help steer

vegetation management (to target specific areas/physical features and/or tree species) and railhead cleaning timetables (to coincide with leaf fall at locations with higher risk).

The outcomes of the HPT tests comparing friction of different leaf species against graphite coupled with the PBS and EDTA experimental outcomes give greater understanding of the lubrication and bonding mechanisms of leaves. The supercritical water testing and the comparison of steel and titanium specimens to confirm the role of iron in leaf layer formation all provide mechanistic insight into how contaminants cause low friction in the wheel-rail interface.

1.4 Thesis outline

This thesis contains the following chapters:

Literature review

A full literature review has been carried out to establish at what level the current understanding of the different aspects of the problem are. The main topics investigated included leaf species, leaf senescence, operational data analysis, leaf friction and bonding. The material reviewed also underwent a paper grading process to assess its quality and relevance to the project.

Approach to project

To ensure the success of the project, the distinct phases were carefully planned out in advance with a clear path from start to finish. This chapter details how and why the work packages were chosen, and certain parameters were investigated.

Autumn data collection

This chapter describes the planning and recording of the natural leaf fall and weather conditions. This included the Sheffield 'Supertram' metro network throughout the autumn seasons of 2018 and 2019. Also, data was recorded at two heritage railway sites where available, where it was also possible to record railhead friction data (friction data could not be recorded on the Supertram network due to safety and logistical reasons).

Leaf fall study

The leaf fall study investigated the falling mechanisms and spread of different leaf species under various conditions. Leaf removal tests (using simulated wind) were also used to compare leaf species/types in terms of natural friction to ballast.

The aim of this section of work was to investigate how leaves reach the track and identify suggestions for vegetation management and leaf corridor design for Network Rail (NwR) vegetation control methods.

Layer formation/bonding hypotheses testing

The proposed hypotheses behind the bonding of a leaf layer to the railhead and the resulting low friction in the wheel-rail interface were listed and discussed in the literature review chapter of this thesis (section 2.7). Appropriate mechanical testing and chemical analysis methods were proposed for each hypothesis.

Low friction (μ) hypothesis testing

Different methods for leaf layer generation in the laboratory were proposed and tested. The leaf layers generated were then compared to naturally formed leaf layers and to those of different leaf species. Bond strength hypotheses were investigated and discussed in this chapter, with different analysis methodologies utilised for each hypothesis. Low friction hypotheses were investigated in a similar manner to the bond strength hypotheses.

A subsection of this chapter was used for a comparison of friction levels arising from different species, which was achieved as a result of the investigation into the "Compressed leaf solid lubricant" hypothesis investigation using the High-Pressure-Torsion HPT test rig.

Chiltern Railways Company Limited (CRCL) study and model development

Through collaboration with CRCL, KPI data on WSP activation on their passenger trains was obtained. This data was used for a case study that sorted the locations by frequency and length of WSP activation incidents and then investigated the locations. Half of them were scored using parameters that were thought to contribute to a higher risk, the outcomes were then fitted to the frequency data in order to rank the parameters. This was then validated against the second half of the data and a model was developed using Microsoft Excel.

Discussion

This chapter expands upon the main findings of the research carried out in the previous chapters and relates them to the original project specification, as well as listing any limitations. Links are also made with literature, to further assess and validate the outlined hypotheses.

Conclusions

The conclusion summarises the project outcomes, as well as scope for future work.

1.5 Contributions

The contributions of other members of the research group towards this project are listed below in Table 1.

Table 1: Contribution of researchers.

Name of researcher	**Contribution**
Dr Will Skipper	Conducted all of the HPT tests.
Mr Ali Almaskati	Assisted in the conduction of the leaf drop tests under the direction and supervision of the author.

1.6 Publications and presentations

Conference paper

A short paper titled "Development of a model to assess the risk of low adhesion at different rail sites" was submitted to the Railways 2022 conference, alongside the presentation in August of 2022. Publication of the conference proceedings is expected for October of 2022.

Presentations

- Presentation to ARG, hosted by RSSB in London in June of 2018
- Presentation to ARG, hosted by the University of Sheffield in March of 2019
- Presentation to ARG, hosted online in May of 2020
- Presentation at ARG, hosted online in February of 2021
- Presentation at ARG, hosted online in February of 2022
- Presentation to the Railways 2022 conference in August of 2022

Journal paper

A journal paper is being prepared on the low adhesion risk assessment model development.

2. LITERATURE REVIEW

2.1 Introduction

The aims of this literature review were to assess the understanding of low adhesion caused by leaves to include effects of different leaf chemistries, times that certain species of leaves fall and related weather conditions. Gaps found in the literature will suggested a lack of understanding in certain areas, these gaps were used to steer the research.

The objectives chosen to achieve the aims of the review were to:

- Assess the current understanding of leaf friction, bonding mechanisms and chemistry of different leaf types.
- Identify current hypotheses regarding bonding and low μ and assess testing methods available to ensure appropriate tests are planned.
- Assess current autumn data and identify gaps in data sets to plan more comprehensive autumn data collection for the future.
- Identify key information required to track the progress of leaves from the branch to the railhead.
- Produce a paper grading map to visually identify areas lacking in peer reviewed research (this is expanded on later in this chapter).

2.1.1 Data sources used

Multiple data sources were utilised in this literature review, such as, Network Rail, review papers, scientific journal publications, Key Performance Indicators (KPIs) and field reports from industry. Due to size of the rail industry in the UK being so large, there is a wealth of information on failures and their causes, for example accident reports, leaf fall data, autumn KPIs etc. KPIs come in documents and contain measurable values that reflect on how a company or industry is performing and if they are achieving business objectives. KPIs take various forms, such as spreadsheets, reports or presentations and provide feedback with evidence which can then be used to steer the industry in the most suitable direction. Autumn KPI's cover topics including Signals Passed At Danger (SPADs), station overruns, Wrong Side Track Circuit Failures (WSTCFs), collisions etc.

2.1.2 Paper Grading

The paper grading was conducted to quantitively assess the research carried out and give an indication on the volume and quality of work that has been conducted on a particular area. Peer reviewed publications were preferential, but not always available. It is important to note that papers are being assessed based on their quality, as well as their relevance to the research aims of this project and whether or not the conclusions are validated by the testing and or modelling work.

Papers were assessed against 7 "yes" or "no" criteria, the sum of the scores were split into three categories, either C (0-2), B (3-4) or A (5-7). Categories with a higher score indicate a more representative and relevant source. The knowledge-map was useful for visualising what areas are lacking in appropriate research, in turn helping to steer this research to fill these gaps. The paper grading method used came from the literature [9], [10], and was originally developed by Harmon & Lewis [10].

2.2 Leaves

2.2.1 Trackside tree species

The range of tree species in the UK is extensive for both deciduous and coniferous sub-species, however, a key feature of deciduous trees is their seasonal loss of leaf canopy. According to a recent AWG[2] manual [11], some of the most troublesome trees are; sycamore, horse chestnut, sweet chestnut, ash, poplar and lime. Both silver birch and English oak are listed as possible species that can only be planted >10m from the outside rail, while sycamore and ash are listed as species that should not be planted near live track at all [11]. The reasoning behind the classification of tree species as either troublesome or not troublesome primarily comes from anecdotal data supplied by train drivers and other relevant parties. This could be partially attributed to there being a higher frequency of particular tree species, therefore higher numbers of leaves and leaf layers being generated and observed. It is possible that some species generate layers that bond more strongly to the railhead and/or reduce friction to different levels, however, this would require specific testing to find out. Another possibility is that the physical shape and/or size of leaves of different species plays a role in them landing or being blown onto the railhead and remaining there, again this would require specific testing to assess any differences between species.

[2] AWG is a "*cross-industry focus group formed in 1995 with the sole objective of researching and developing initiatives to combat the effects of low wheel / rail adhesion and promoting awareness of the low adhesion issue within the industry and key stakeholders.*"

It is apparent when using the railway network in the UK that there are many different trackside tree species, with some species being locally native to certain areas [11]. English oak, silver birch, ash and sycamore have been identified as being among the most popular trees in the UK, they also represent two tree species from each category described in the above paragraph and the 2018 AWG manual [3].

A 2007 RSSB report into the characteristics of railhead leaf contamination, by Poole [12] investigated sycamore, oak and horse chestnut leaves. The aims of the report included;

- Understanding the bonding mechanism of leaf film to the railhead with an aim of improving existing, or providing new, means of leaf film removal
- Measuring leaf film and simulated film hardness and moisture properties in relation to adhesion and track circuit operation
- Specification of low adhesion measurement requirements and development of a related Guidance Note
- Specification of low adhesion simulation requirements and development of a related Guidance Note

The direction of the investigation was to improve the understanding and define the leaf contamination and bonding mechanisms of three different leaf types, with a view to treat or prevent leaf contamination in the future [12]. This is particularly relevant to this current project. More details of the outcomes of this report will be discussed later on in this review.

A 2017 paper on mapping (allergenic pollen) vegetation in the UK [13] has, along with the UK pollen network, produced maps of tree taxa density in England and Wales. The taxa density is defined as the numerical density of a specific species in a certain area relative to other species. Those of Oak, Ash and Birch have been extracted and are shown below in Figure 3. Sycamore trees were not included in the survey as they are not a pollen risk and are not covered by the pollen network. The units for the maps are in number of trees per 1km x 1km grid square and the quantile sizes change for each species.

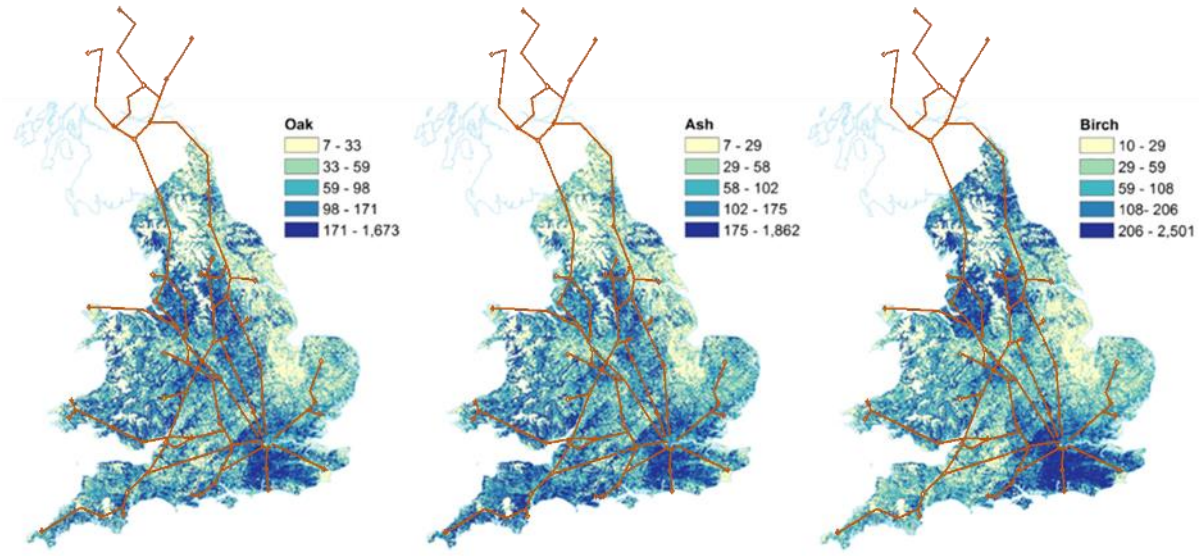

Figure 3: Maps of Oak, Ash and Birch tree density in England and Wales [13], [14]**, with a diagram of the major rail lines in the UK superimposed** [15]**.**

Figure 3 indicates that Oak has lower measured numbers, when compared to Ash, while Birch has the highest of the three species. It is clear when looking at the data that the highest densities for all three species occur around the southeast, northeast and northwest.

The Forestry Commission completed a National Forestry Inventory (NFI) report [16] estimating the quantities of broadleaved species in British woodlands, with a special focus on Ash (possibly due to Ash die back disease, meaning that restrictions are in place for cutting down healthy Ash trees [17]). Some of the relevant key findings of this report include that;

- Ash accounts for approximately 14% of total broad-leaved standing volume in Great Britain.
- There are approximately 1.4 billion broadleaved trees in British woodlands of over 0.5 hectares, of which ash trees are estimated to number 126 million.

It is not clear from this report if lineside species were included, due to them being in potentially restricted areas. Instead, it contains "estimates derived from areas of woodland located outside the NFI woodland map" [16].

The report also provides data on the numerical distribution of broadleaf tree species, see Figure 4 (left), where oak (9%), sycamore (8%), ash (9%) and birch (18%) make up a total of 44%. The standing volume distribution of the same species is shown in Figure 4 (right), where oak (30%), sycamore (11%), ash (14%) and birch (9%) make up a total of 64%. It is interesting that birch represent 18% of the number of broad-leaf trees, but

only occupy 9% of the volume, this could be due to birch trees being generally smaller in size than other species.

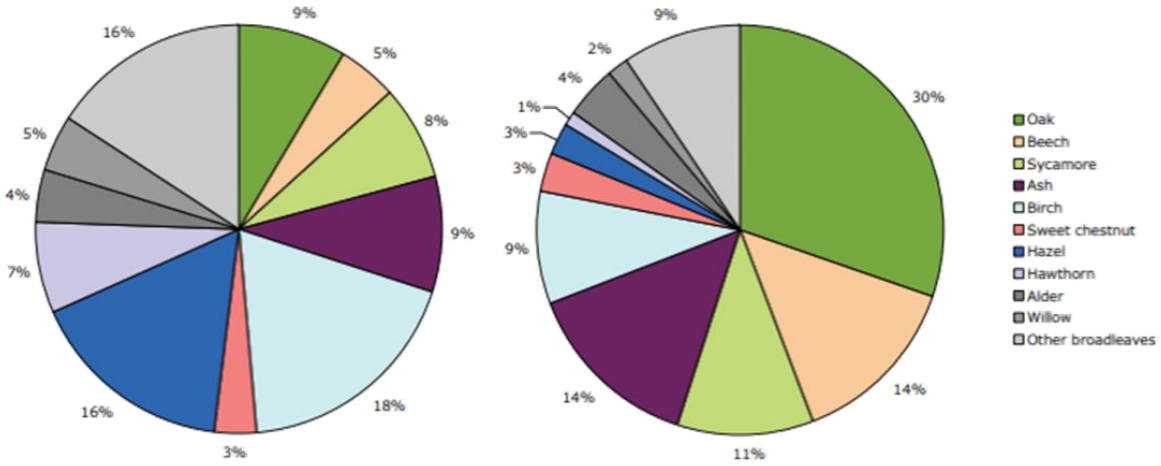

Figure 4: Numerical distribution of broadleaf species (left) and standing volume distribution of broadleaf species (right) as of 2011 [16]**.**

Numerical distribution data from the pollen paper [13] and NFI report [16] seem to correlate regarding oak and ash numbers being similar, with birch numbers being approximately double. Sycamore levels were observed to be similar to oak and ash. This pollen paper data was used as a proxy for tree count estimations due to a lack of available, precise data on deciduous numbers in the UK.

2.2.2 Leaf chemistry

Leaf chemistry refers to the biochemistry of the leaves and more specifically the concentration of biopolymers such as; lignin, pectin, cellulose and other elements (N, Mg, Mn, Ca, Fe, P and K).

The local environment of leaves is also a factor that needs to be considered, for example different soil types, or levels of hydration, will affect both the chemical composition of the leaves as well as the timing of leaf abscission.

Pectin

Pectin is a naturally occurring soluble chemical compound, typically found as either pectin, protopectin or pectic acid [18], [19]. They are functionally and structurally the most complex polysaccharides found in primary and secondary plant cell walls and are commonly used in the food industry as gelling and stabilising agents [20], [21]. A key feature of pectin is that it can be made into a gel [18]. Gelation occurs depending on

a number of factors including pH, heat and concentration of specific metal ions [22], both heat spikes and metal ions are found in the wheel-rail interface.

Pectin has been identified as being abundant in leaf tissue and is possibly an important compound for bonding leaf matter to the railhead [12]. Divalent metal cations such as Ca^{2+}, Cu^{2+} or Fe^{2+} can transform pectin to a gel, due to crosslinking molecules [23], [24]. A 2006 study by Cann [25] on sycamore leaf residue found that it contained esterified[3] pectate and a small amount of cellulose. Additionally, it was found that, due to the high solubility of pectin in water, pectin gel (possibly crosslinked with Fe ions) likely contributes to low adhesion [25].

The characteristic black colouration of leaf films could be caused by chemical reactions between pectin and Fe, producing small particles which appear fibrous as opposed to crystalline. FT-IR analysis of these particles indicated the presence of pectin [25].

The full effect pectin has on adhesion and lowering friction has not yet been fully identified. Further investigation into the formation of the black colouration and bonding of pectin and pectin reacted substances is required.

Cellulose

Cellulose, like starch, is made up of repeating glucose ($C_6H_{12}O_6$) molecules. In starch the glucose is oriented in the same direction, in cellulose each successive glucose unit is rotated 180° around the axis of the polymer backbone chain [26]. It is the most abundant natural polymer and is predominantly found in plant cell walls [27].

It is a main constituent of biomass, a green energy source [28], [29]. Along with lignin and pectin, cellulose is believed to be a binding agent within the leaf film [12], [30]. Cellulose cannot dissolve into water under "normal circumstances" [29], [31]. Under "non-normal circumstances" such as those in the wheel-rail interface, it could be expected that cellulose would break down and react to form a complex with other materials [9].

Applications of cellulose include fibre in the human diet, cotton in clothes manufacturing, paper and much more [29]. However, the most relevant use for cellulose is as an adhesive [18], this implies that it will help to adhere the leaf matter to the railhead, after decomposition under high temperature and pressure [9].

Pendulum friction tests on lignin-cellulose mixtures have found lower adhesion values than a pure lignin film. The conclusion of the tests on lignin and cellulose is that a

[3] When a chemical compound produced by a reaction between an acid and an alcohol, in which the hydrogen of the acid has been replaced by an alkyl group of atoms [182].

lignin-cellulose film is harder than the lignin film and, when wet, has a lower adhesion value than either the cellulose or lignin films [12]. It is, however, not clear if there is a link between a layer's hardness and friction properties, this is yet to be determined.

Lignin

Fourier Transform-Infrared spectroscopy (FT-IR) analysis of laboratory generated leaf layer residue has shown lignin, cellulose and pectin to be the main constituents [12], [32]. Lignin has not been the focus of previous research as it is thought of more as a structural element, as it is water-insoluble [25].

Lignin can be classified into three major groups, dependent upon its origin [33]. Softwood, or guaiacyl lignin, consists of coniferyl alcohol along with trace amounts of sinapyl alcohol-derived units. Hardwood, or guaiacylsyringyl lignin, which contains coniferyl alcohol and sinapyl alcohol in different concentrations. Grass, or guaiacyl-syringyl lignin, contains larger levels of structural elements derived from p-coumaryl alcohol [33]–[35].

Lignin is a complex organic polymer and is found in the cell walls of plants, it makes up between 15 and 25 wt% [36] and about 40% of plant biomass energy content [37]. However, lignin concentration varies greatly between and within plant species [38]. Research has shown that high temperatures and pressures above 25MPa (in supercritical water) can break down the long chain polymer structure [36], [39]–[43], see section 2.6.1. Under such conditions, lignin is known to decompose into various components including phenolic species and other components in a short amount of time (0.5 to 10s) [39]. According to [44], the contact pressure in the wheel-rail interface might be such that lignin does break down as described above, commonly around 800MPa depending upon the vehicle.

When heated to 330-440°C lignin decomposes to produce 50 wt.% charcoals, 10-15 wt.% tar and smaller amount of 2-propanone, ethanoic acid (CH-COOH) and methanol [33], [45], [46]. The charcoal produced coincides with the amorphous carbon found in Raman spectral analysis of laboratory generated leaf residue [9], this supports the theory that lignin breaks down due to high temperatures and pressures in the wheel-rail interface.

Lignin has been reported to have a negative correlation to decomposition rates in leaf litter by some researchers [47], however, other researchers have found no relationship [48]. It has been theorised that the lignin to nitrogen ratio has more of an impact on decomposition rates [49].

As a result, it can be theorised that as the wheels roll or slide over leaves where moisture is present, the lignin in the leaves is transformed into more adhesive substances [9]. This hypothesis also suggests that an interfacial layer of an iron-carbon derivative is formed, using the lignin from the cell wall. Despite lack of reported experimental research, lignin might be a crucial bonding material [9].

Green vs Brown leaves

Deciduous tree leaves, large enough to fall from the tree and be deposited onto the track, are typically in one of two states, green or brown. Green leaves contain high amounts of chlorophyll which is essential for the photosynthesis process. It is noted that chlorophyll molecules are a naturally occurring complex of iron (Fe) within organic components of leaves, confirming the presence of compounds in the leaves that can bind with metals [50]. Brown leaves, however, are undergoing senescence which is the process of deterioration with age, the breakdown of chlorophyll and the loss of the ability of the cells to divide and grow. This leads to abscission, which is natural detachment from the tree.

During the autumn season deciduous tree leaves turn brown, at varying rates and to varying degrees of "brownness". Since the leaves seem to dry out and become more brittle as they turn brown, the chemical components must change, such as chlorophyll and cellulose.

Oak and beech have thick leaves that decompose slowly, and have been documented as being able to retain their leaves until the following spring across northern Europe [51]–[53]. This has been observed in the lower branches of the trees, in order to ensure that when the leaf litter decomposes the nutrients are absorbed by the donor tree in the springtime when they are required. Soluble leaf components are better preserved in leaves retained by the tree than in fallen leaves, partly due to the difference in moisture content [53]. Dryer leaves that remain on the tree do not undergo as much decay by microorganisms [53], [54].

Information from the literature on differences in friction of green and brown leaves is very sparce, as is information on leaf layer formation of green versus brown leaves. One source that compared the friction of green and brown sycamore leaves using a ball on flat contact showed that green and brown leaf friction were very similar for both dry leaf powders and when suspended in water [55].

The literature does not state whether there is a difference between green and brown leaves when forming a well bonded, low adhesion inducing black leaf layer. It is possible that the change in chemical make-up of the leaves as they deteriorate and

turn brown may affect leaf layer formation and/or low adhesion. At this point it is not possible to say whether green or brown leaves are worse for leaf induced low adhesion, however, specific testing could shed light on this.

Research into electrical isolation caused by leaves compared green and brown leaves found that green leaves broke down more easily and had a higher water content and are softer[56]. This same research also suggested that green leaves were also likely to reduce friction however were less likely to lead to layer formation.

2.2.3 Role of iron

Although iron is not a large portion of leaf biochemistry, it is essential to photosynthesis and known to be present in leaves. This is of relevance when discussing how the leaf chemistry affects leaf layer bonding with rail, as this organically bound iron will also be present at the wheel-rail interface. Furthermore, iron oxides are often found on the railhead, as a product of ambient oxidation. It is believed that iron oxide, generated via electrochemical corrosion [57], acts as a catalyst during the bonding reaction between the railhead and leaf matter.

The oxides that will form depend upon conditions such as; pH levels, oxygen levels, pressure, temperature and steel composition [30]. Iron oxide has fifteen different compositions, which differ in Fe valence (number of electrons) and the crystal structures of the various oxides [57]. *In-situ* X-ray Diffraction Crystallography (XRD) analysis found that only five of these compositions form under the environmental conditions of the railhead [58].

These can be split up into two groups, the oxides; magnetite (Fe_3O_4) is known as black oxide and acts as a passivation film which can protect the substrate from further oxidation or corrosion, and hematite (Fe_2O_3), also known as red oxide and is the most common oxide found in nature [30], [59], [60]. The oxyhydroxides include; goethite (α-FeOOH), lepidocrocite (γ-FeOOH) and akaganeite (β-FeOOH or β-FeOCl) [30], [57], [58]. Some properties of the different rust types are shown below in Table 2, it is worth noting that Magnetite, Goethite and Akaganeite are said to reduce friction [61].

Table 2: Properties of iron oxides in the wheel-rail interface [57], [62]**.**

Name	Formula	Colour	Magnetic	Impact on Friction	Catalytic activity
Haematite	Fe_2O_3	Red	No	Increase	Yes [63]
Magnetite	Fe_3O_4	Black	Yes	Decrease	Yes [64]

Goethite	α-FeOOH	Yellow-brown	No	Decrease	Yes [64]
Lepidocrocite	γ-FeOOH	Orange	No	Unknown	Yes [64]
Akaganeite	β-FeOOH-CL	Yellow-brown	No	Decrease	NA
Wustite	FeO	Black	No	Unknown	Yes [65]

Both Haematite and Magnetite are seen on the railhead and are able to create a mechanically mixed layer [66], which could lead to a third layer between the rail substrate and the leaf contamination [67]. Certain environmental conditions can convert oxides due to iron' s nature as a transition metal with variable oxidation states [59], this confirms the railhead to be a 'reactive' surface, as iron oxides are often encountered on mainline track. In the real world, oxide formation occurs across the railhead, while in the running band it is formed between train passes which could range from minutes to hours.

Small scale twin disc laboratory tests have produced black leaf layers within minutes [68] and field testing has generated black layers in approximately 40 axle passes, though this number is highly dependent on the prevailing weather and whether the wheels are rolling or sliding over the leaf matter. This means that the oxide formation occurs in a timescale that could influence the black leaf layer formation.

The effect of iron oxides may be twofold, in that they will either directly cause low adhesion, or bond with leaf matter which will indirectly cause low adhesion. Low friction effects of oxide layers have been researched in multiple cases, such as [57], [59], [62], [66].

2.2.4 Varying leaf conditions

Leaves (deciduous and coniferous) typically grow as either 'sun' or 'shade' leaves depending upon their position on the tree and the average amount of light seen by the tree. They can be differentiated by shape, colour, texture, tissue morphology and physiology [69]. Shade leaves grow lower on the tree and receive less light, as a result they develop larger surface areas and thinner cross sections. Sun leaves, however, receive more sun light and have less surface area yet a thicker cross section [69]–[73].

As discussed above leaves are typically either green or brown (ignoring exotic species with red or yellow leaves).

2.2.5 Soil types

The mineralogy of parent soils is important in determining the general structure and functioning of forest ecosystems [74]. The term soil refers to a layer in the earth usually made up varying levels of organic remains, clay and rock particles according to the online oxford dictionary [75].

Research has been conducted into the variation of the chemical composition of green leaves and leaf litters of three deciduous tree types (English Oak, Beech and Sweet Chestnut) from different soil types [74]. Although the paper does not explicitly state that the leaf litter samples were of brown leaves, it can be assumed that they were brown, due to them being collected from the ground in mid-December, 1996. Soil types from 26 locations were found to be made up of 7 brown earths, 9 gleyed brown earths (a sticky blue/grey/brown soil that is saturated with water and low in oxygen), 5 ochreous brown soils (several variations of mineral rich soil, typically red-brown iron oxide in colour) and 5 podzols (infertile acidic soil, usually white/grey in colour), these were then divided into high fertility (HF) and low fertility (LF) groups. The brown earth and gleyed brown earth, represent high fertility soils while the ochreous brown earth and podzols represent low fertility soils.

Sariyildiz and Anderson [74], [76] found that Beech and Oak growing on three different soil types showed significant variation in the quality and decomposition rates of leaf litters. Data gathered by Clayden and Sariyildiz and Anderson [74], [77] on different soil types in Devon, UK, shows the soil from each site, the mean values with standard deviation are shown below in Table 3.

Table 3: Mean values with standard deviation of the four soil types [74], [77]**.**

Soil type	Mean values			
	pH (H_2O)	**BS (%)**	**CEC (m eqiv $100g^{-1}$)**	**N-mineralization (µg N g/ (soil day))**
Brown earth	5.8 (0.22)	61.0 (10.3)	16.1 (1.28)	12.0 (2.95)
Gleyed brown earth	6.3 (0.28)	69.6 (4.40)	15.4 (0.87)	12.9 (1.87)
Ochreous brown earth	4.7 (0.98)	11.2 (0.80)	12.1 (1.20)	3.61 (0.27)
Podzol	4.48 (0.11)	10.2 (3.22)	7.30 (0.05)	3.39 (0.22)

Table 3 shows the pH levels, base saturation (BS) as a percentage, cation exchange capacity (CEC) in milliequivalents per 100g and nitrogen mineralization (N-mineralization) in micrograms of nitrogen, per gram of soil.

According to a publication by the University of Georgia [78], BS is the percentage of CEC sites occupied by the base (also known as alkaline) cations, Ca^{2+}, Mg^{2+} and K^{+}. Base cations are distinguished from acid cations like H^{+} and Al^{3+}. At soil pH levels of 5.4 or less, toxic Al^{3+} is present in high enough concentrations as to hinder plant growth, as soil pH lowers, Al^{3+} levels rise. Therefore, soils with high BS are generally more fertile.

According to Poole [12] there is a strong indication that the acidity or alkalinity of the system (railhead with leaf matter present) has a large impact on the formation and removal of leaf film. There may be a connection between this and the potential generation of acidic gel polymers.

CEC is a measure of how many cations (positively charged ions) can be retained by a particle of soil, such as calcium (Ca^{2+}), magnesium (Mg^{2+}) and potassium (K^{+}), [78]. According to a Cornell University Cooperative Extension paper [79]; mineralization is the process by which microbes decompose organic nitrogen from manure, as well as organic matter and crop residues to ammonium. Because it is a biological process, rates of mineralization vary with soil temperature, moisture and the amount of oxygen in the soil (aeration). A higher value corresponds to a quicker process. The study found that Oak leaves from HF sites contained higher levels of lignin, cellulose, Ca, Mn, K, and P. However, lower levels of Mg than those from the LF sites were noted. In addition, sugar levels in all leaves tested were lower in those from LF soils than HF soils.

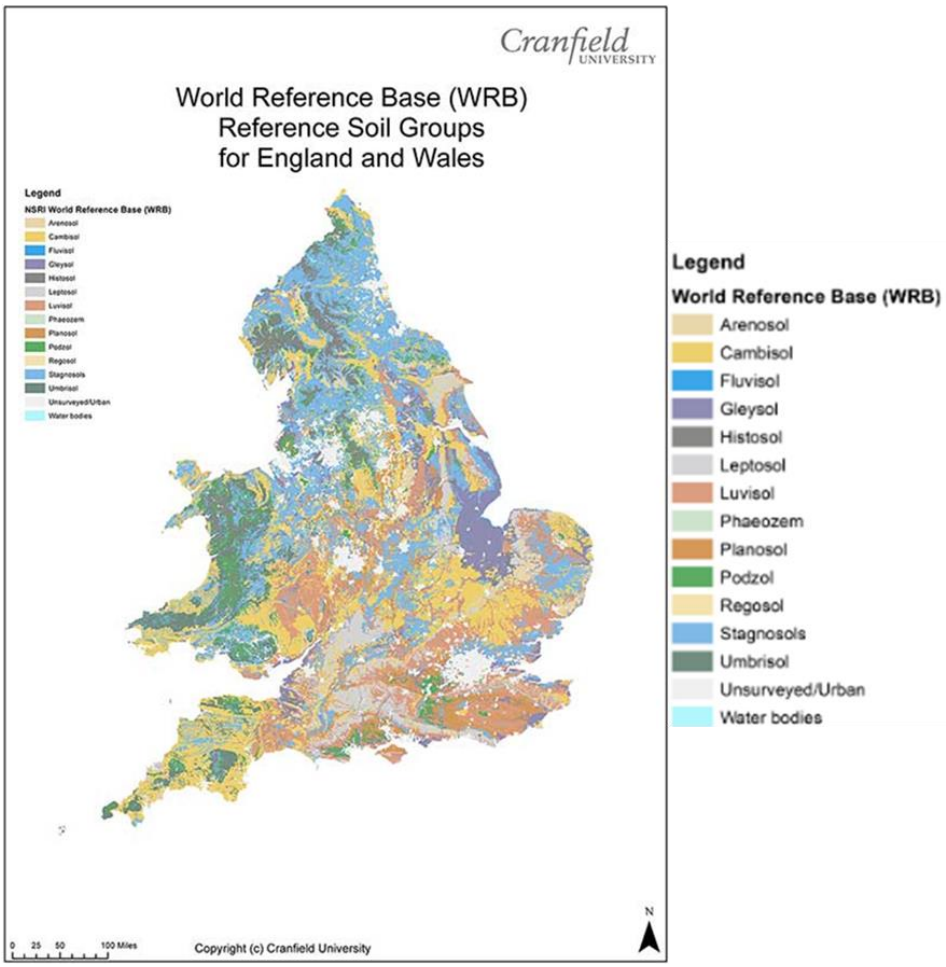

Figure 5: A map of England and Wales showing different soil types with enlarged legend on the right [80]**.**

The diversity of soil types across England and Wales has been recorded [80], see Figure 5. However, most of these soil types have not been investigated to the same extent as the four mentioned above, and as such the characteristics they pass onto the leaves that grow there are largely unknown.

2.3 Chemical analysis techniques

The following analysis techniques have been used by Ishizaka [44] in previous experiments to analyse sycamore leaf matter only. Each method is noted to have its own benefits and drawbacks, hence the use of multiple techniques. Chemical analysis will be conducted to identify the components of the leaf matter, hypotheses can then be formed on what specifically is causing the bonding to the track and low adhesion with the wheels.

Brown leaf Black Precipitate (BBP) and Green leaf Black Precipitate (GBP) (made using brown and green sycamore leaves) are water soluble components of the leaf mulch reacted with steel rail sample to form a black precipitate, which is then evaporated to

isolate the reacted components. They take the form of a dark reddish brown/black powder residue.

An RSSB report titled "Biochemistry of Railhead Leaf Film Contamination", by Somashekara et al. [30], investigated laboratory generated leaf films. The techniques used included; Scanning Electron Microscopy (SEM), Energy Dispersive X-Ray analysis (EDX), Fourier Transform Infra-Red spectroscopy (FT-IR) and X-Ray Diffraction analysis (XRD). The leaf types featured were horse chestnut, sycamore and oak. Information from this report [30] formed part of a larger RSSB report by Poole [12].

Research by Ishizaka [44] on variations of sycamore leaf contamination has involved the use of FT-IR, Laser Raman Spectroscopy (LRS), XPS, XRD, EDX, and others. Some of these analysis techniques will be briefly discussed to outline their advantages and disadvantages, and discuss previous research they have been included in.

2.3.1 X-ray Photoelectron Spectroscopy (XPS)

XPS theory involves the photoemission process, in which a target sample is bombarded with x-ray beams which interact with electrons of a known energy state. If the x-ray photon has enough energy, then it will free an electron. The kinetic energy of the freed electron will depend upon the photon energy and the binding energy of the electron (the energy required to free it from the atom). By measuring the kinetic energy of the emitted electrons, it is possible to determine which elements are near a material's surface, their chemical states and the binding energy of the electron [81].

XPS is also commonly referred to as ESCA (Electron Spectroscopy for Chemical Analysis). As a surface analysis technique, XPS is particularly versatile as it can be used for both compositional and chemical state analysis, and since the XPS technique causes very little electrical charging of samples it is useful for both electrically conductive and non-conductive materials [82].

Advantages of XPS include; it is less-destructive, it is surface sensitive, it can detect all elements (except H, He and Li), it is quantitative (with values in %atomic content), it reveals chemical bonding information, such as the presence of oxides or C-H bonds [83].

The drawbacks of XPS include: the apparatus required is non-mobile, requires a high-vacuum and is expensive as well as being a time-consuming process. Also, the penetration depth into a sample for analysis is limited to ranges from 1 to 10nm.

Table 4: Relative elemental weight amounts of leaf contaminated rail [84]**, where – is below detection limit.**

%atomic concentration	C	O	Fe	N	Si	F	S	Na	Ca	Al	Mn
September	14.0	27.3	50.7	0.5	3.2	0.2	0.2	-	1.3	2.2	0.5
October	48.0	29.3	13.2	1.4	2.9	-	0.8	-	2.8	1.5	-
November	11.4	26.8	54.6	0.6	2.3	0.9	0.3	0.2	1.1	1.3	0.5

The results can be tabulated to indicate the relative elemental weight amounts on the surface, an example is shown above in Table 4, [84]. Leaf contaminated rail samples have been collected in Sweden and examined using XPS, in which the leaf layer was found to consist of higher levels of Ca, C, S and N [84].

2.3.2 Laser Raman Spectroscopy (LRS)

The principle of Raman spectroscopy first involves illuminating the sample with a monochromatic light source, such as a laser, much of the light that scatters off has no change in energy, this is known as Rayleigh scattering. A minute fraction will have lost or gained energy and this is known as Raman scattering. This Raman shift occurs because photons exchange part of their energy with molecular vibrations in the material [85]. Figure 6 shows the Raman spectra for sycamore Brown-leaf Black Precipitate (BBP) from earlier research.

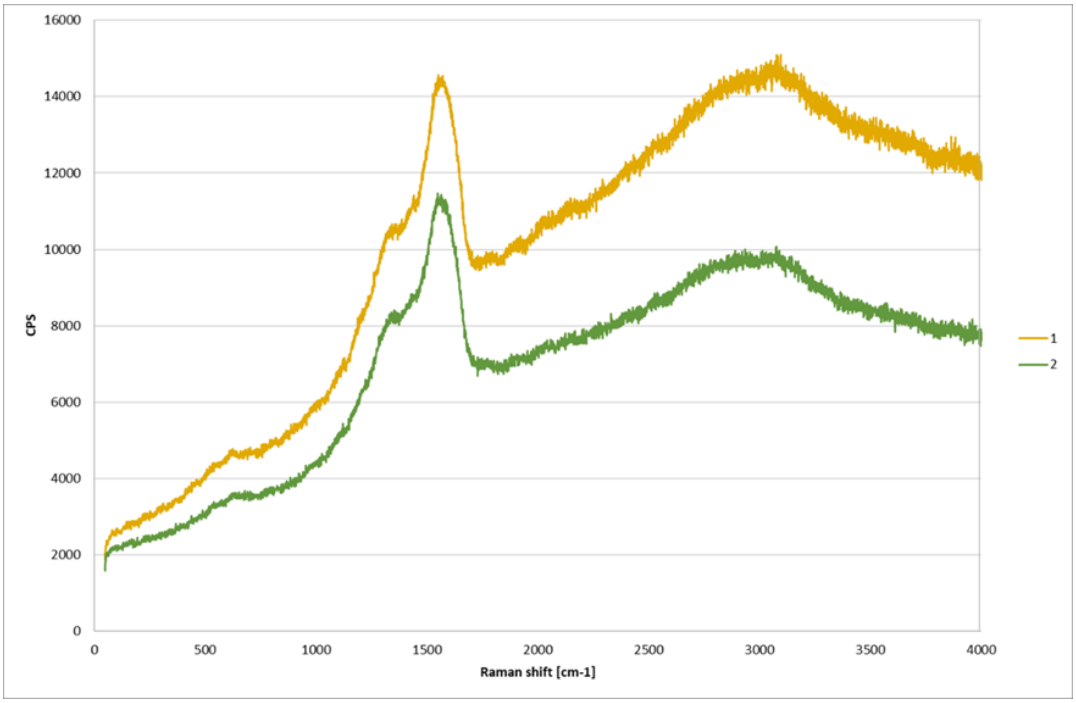

Figure 6: Raman spectra of sycamore – steel reacted leaf black precipitation from previous unpublished work.

Some advantages of Raman spectroscopy are that; it is non-destructive, it is a non-contact technique, there is minimal interference by water, little sample preparation needed and solids, liquids and vapours can be analysed [86].

Some disadvantages of Raman spectroscopy include; metals and alloys cannot be analysed, the Raman effect is very weak which leads to low sensitivity, it can be swamped by fluorescence from some materials [86].

2.3.3 Fourier Transform-Infrared Spectroscopy (FT-IR)

FT-IR spectroscopy is a chemical analysis method used to detect molecular bonds in samples, more specifically organic bonds such as C=O or C-O-H [25]. FT-IR is used to characterise the molecular structure of the leaf film based upon the identification of functional groups present in the leaf material [12].

IR involves the special mathematical treatment (a Fourier Transformation) of spectral data [87]. The spectral data is generated by means of an infrared beam being passed through the sample, then observing what has been absorbed and what has passed through. The resultant signal reaching the detector is a spectrum representing a molecular "fingerprint" of the sample. Different chemical structures/molecules produce different spectral fingerprints [88].

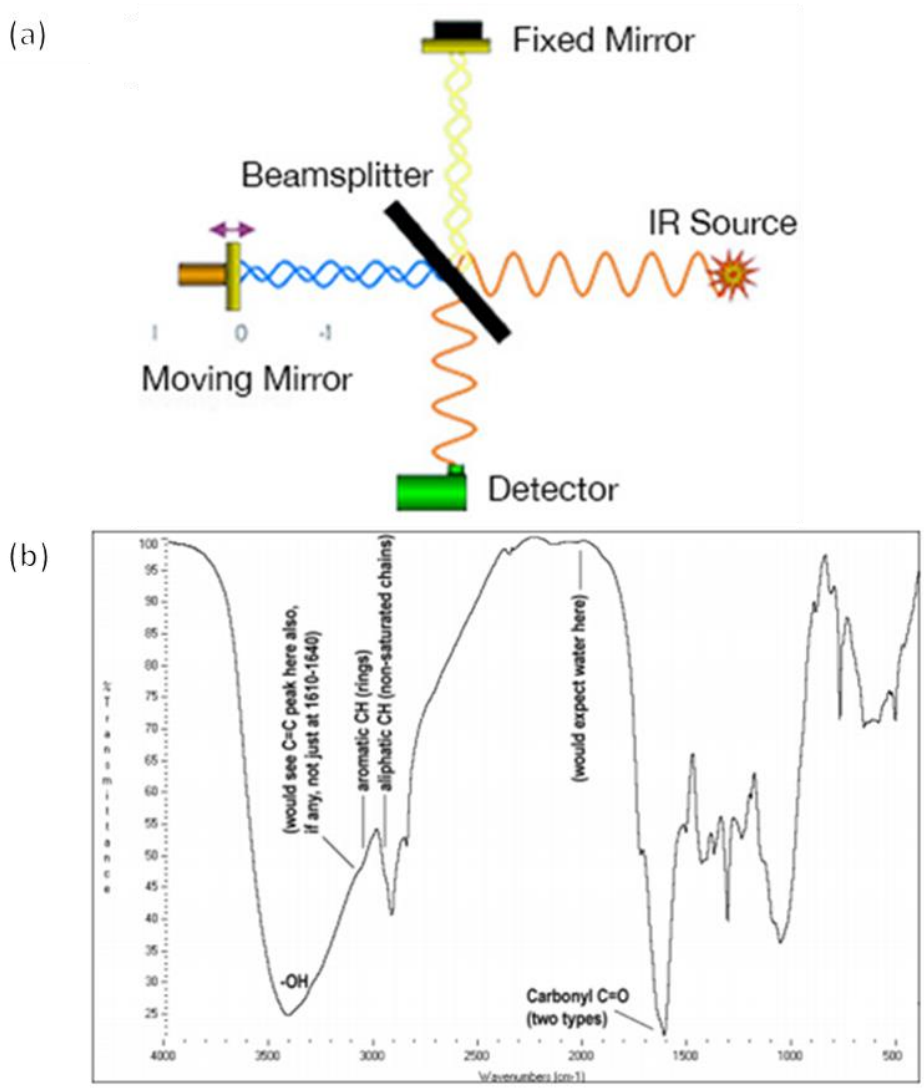

Figure 7: a) a simple diagram of FT-IR apparatus [88]**, b) an FT-IR spectra of a Horse Chestnut leaf sample** [12]**.**

Figure 7 (a) shows a simplistic diagram of the FT-IR apparatus, where the sample would be placed in the IR beam path before the detector. Figure 7 (b) shows an example IR spectral output of a sample of Horse Chestnut leaf, as can be seen the peaks and valleys at different wavelengths are indicative that certain chemical bonds are present. FT-IR has been used to investigate leaf contamination by multiple researchers [12], [30], [44].

Advantages of FT-IR include; quick data acquisition time, relatively high sensitivity, it is non-destructive and in some cases it can be portable. Disadvantages of FT-IR include; aqueous solutions can be difficult to analyse, complex mixtures can give complex (difficult to interpret) spectra, [89]

2.3.4 X-Ray Diffraction (XRD)

XRD (X-Ray Diffraction or X-Ray powder Diffraction) is an analysis technique that has been used to investigate leaf contamination by several researchers [12], [44]. It is used to determine the molecular structure of crystalline substances, by diffracting a beam of monochromatic X-rays through the substance and observing the change in energy.

According to [90], the interaction of the X-rays with the sample will produce constructive interference (plus a diffracted ray) when Bragg' s Law ($n\lambda=2d \sin \theta$) is satisfied. Where λ is the wavelength of the x-ray, θ is the diffraction angle and d is the lattice spacing of the crystalline sample. The diffraction pattern generated by a sample is unique and gives a "fingerprint" that can be checked or compared against a standard reference pattern, this allows identification of the sample crystalline form.

However, XRD analysis cannot analyse organic substances such as oils, grease and plant material, which generally have no crystalline structure, for this FT-IR and LRS are recommended [58].

2.4 Leaf fall

2.4.1 How do leaves arrive on the track?

There is very little information on the different mechanisms that take leaves from the branch to the railhead and hold them there as a train passes over. There are several obvious factors that will contribute, such as; wind, airflow from the train, moisture levels/wetness of the leaves, railhead wetness, railhead contaminants, leaf condition, leaf size and mass, and so on.

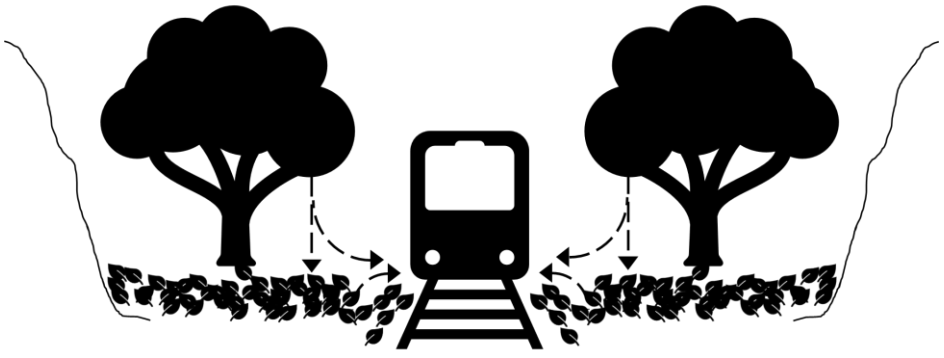

Figure 8: Simplified topography of the leaf corridor (created by author).

The topography of the leaf corridor can incorporate several crucial factors, such as; steep corridor/valley sides, a tunnel, dense woodland, or flat open land,

cuttings/embankments (see Figure 8). These factors influence how leaf litter remains near or on the track.

RSSB have conducted research into "Aerodynamic Influences of Vehicle Design on Wheel/Rail Contamination" (project code T546), due to vehicle aerodynamics being deemed a major contributor to rail leaf contamination [91].

The relevant objectives included identifying the features that influence railhead contamination, ranking vehicles in terms of their low adhesion performance, finding effective and financially viable solutions and guiding future train design.

The approach involved reviewing previous work, wind tunnel tests with train and bogie scale models, CFD (Computational Fluid Dynamics) modelling, theoretical leaf trajectory modelling, a cost benefit analysis of one solution and developing a ranking method for propensity to trap leaves in the wheel-rail interface.

Table 5: Paper leaf parameters [91]**.**

Parameter	**Value**	**Unit**
Length	0.074	m
Width	0.053	m
Area	0.0039	m^2
Mass	0.0014	kg
Moment of inertia	6.4×10^{-7}	$kg.m^2$

The paper leaves that were used in the investigation were made from A4 size 80gsm paper cut into 16 pieces (i.e. A8), see Table 5. It is not stated how the paper leaf sizes were chosen, therefore it is assumed that they were chosen because they are most similar to typical leaf sizes.

The findings of the paper leaf testing suggested that there is "evidence of a weak rotational flow structure alongside the carriage" that is centred around 1m outside the rail and at the same height as the carriage floor [91]. There was found to be no significant difference between flow structures of different train units that have differing leaf contamination statistics. The velocity of the airflows generated by trains was found to be sufficiently large when compared to the leaf threshold velocities as to dominate the smaller scale leaf aerodynamics, meaning that the leaves followed the flow of air more so than their own 'natural' path. Gravity was found to be the main differentiating force between a leaves natural flow and that generated by a passing train.

The conclusion of the investigation stated that the "general magnitude of the transverse and vertical velocities of the global flow field immediately upstream of the wheel are probably the best indicators of the statistical likelihood of contamination" [91]. This suggests that leaves are likely to be picked-up from the rail/ballast area and deposited onto the railhead, but the magnitude and required train design and speeds still remain unclear.Additionally, leaves may arrive on a section of track by means of sticking to the wheel and remaining there before detaching on a different section of track, this is known as carry down and will be discussed later on in the review.

2.4.2 When do the leaves fall?

Arguably one of the most important factors when considering the problem of leaf contamination is the time of year or season, especially since the Autumn period is synonymous with the idea of leaves turning brown and falling off trees. Information on leaf fall times and quantities is collected by observers across the UK rail network.

The Met Office model for leaf fall was first developed in 1995 and contains a record of leaf fall observation and railway experience data. They describe how environmental and meteorological factors influence leaf fall times. These factors vary between and within tree species due to environmental stresses such as wind, temperature pollution etc., and between years due to climatological drivers. They have also found that there is a variation in the forecast due to the species present, the density of trees and the lineside topography (open flat area, small valley, tree corridor etc.).

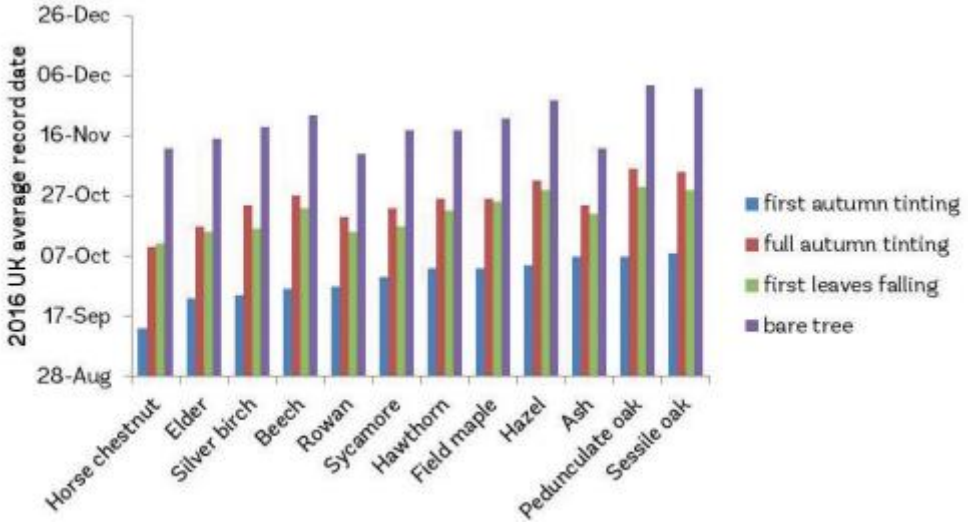

Figure 9: Leaf drop times for popular UK tree species [92]**.**

The main leaf fall season is from September to November with different trees shedding their leaves at different times [92], shown in Figure 9. This graph contradicts other data

on oak trees retaining leaves until springtime, although it does state that the results are averaged.

When leaves fall and what environmental/weather conditions contribute, is known as 'Phenology' . Trends in leaf senescence and phenological stages (typically a wider and later starting autumn season) have been related to temperature increases (due to global warming) over the last 50 years [93]–[95]. Other factors theorised to influence deciduous leaf senescence include; low mean daily temperature, short days, severe drought and mineral deficiencies [94], [96]–[101].

2.4.3 Weather effects

According to research carried out by Nagase [102], when the rails are dry, the adhesion coefficient shows no dependency upon speed. They further go on to state that at the beginning of rainfall the adhesion coefficient lowers sharply, with its value being remarkably dependent upon speed [102].

The time of day is an important factor as it correlates with phenomena such as morning dew, rise and fall of ambient temperature and subsequently wind. Moisture levels are known to play a key role in the adhesion reduction of the leaf layer. In dry weather uncontaminated rails should have an adhesion level between 20% - 40%, or between 10% - 20% for really wet conditions [3].

The wind will have various affects, some of which will counteract others, such as leaves being blown onto the railhead, then being blown off, or helping to evaporate moisture levels and drying the leaf layer out leading to higher adhesion levels. These are currently speculative and would need to be investigated and quantified.

At present there is very little literature stating what factors are most important for leaf layer formation. Leaf size, leaf shape, leaf wetness, ambient temperature and humidity, and wind speed may all play different roles in contributing to this risk however they are all difficult to quantify at this stage and all require investigation to understand better.

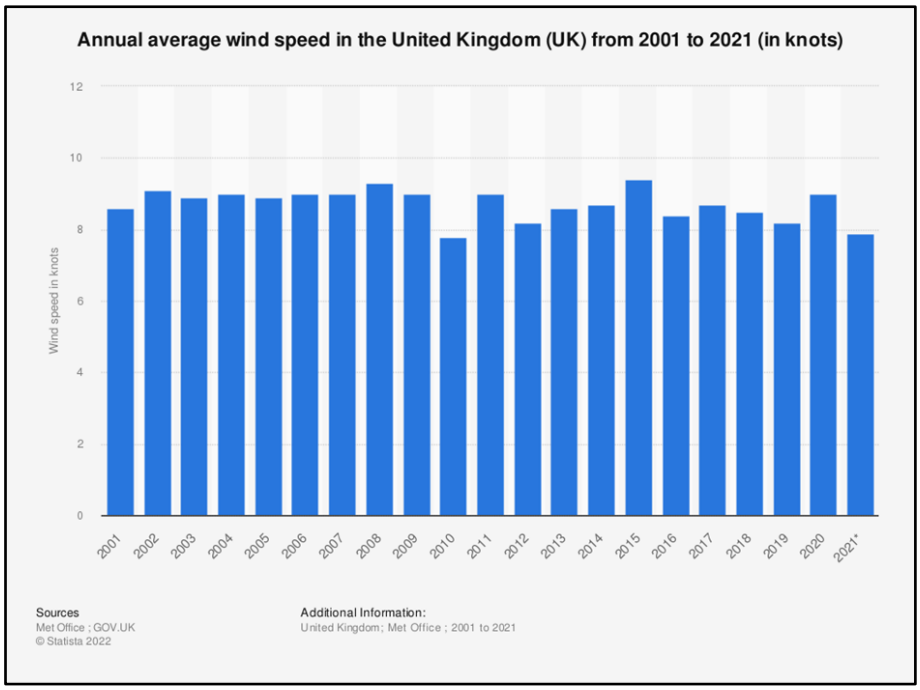

Figure 10: Annual average wind speeds (knots) in the UK from 2001 to 2021 [103]**.**

Average wind speeds in the UK from 2001 to 2021 (see Figure 10) were relatively consistent and varied between 7.8 and 9.4 knots (4.0 and 4.8 m/s respectively). These wind speeds were recorded by the Met Office in the UK and compiled in [103].

2.4.4 Mechanisms of leaf fall

The mechanical properties and characteristics of leaves are key factors when considering how they transition from being attached to a tree branch to arriving on the railhead. Factors such as size, mass and geometry will affect how leaves move during and after they fall from the tree. Hydration in leaves is also an important factor as it alters the mass and stiffness of the leaf. Drier leaves are lighter, stiffer and typically more brittle than wet leaves, which are heavier and more flexible (typically 35-50% when compared to the same dry leaves) [104].

There is widespread speculation on the numerical volume of leaves that are dropped annually. Network Rail report that there are over 13 million trees on and next to the railway in Britain and, every autumn, thousands of tonnes of leaves fall onto the tracks [105].

A viscous water-glycerol mixture was used to dampen and slow down the fall of discs in a study on "Classes of natural leaf fall motion" defined in a lecture presentation from

UNC Chapel Hill [106], [107]. Figure 11 was used at to classify leaf fall during leaf drop tests.

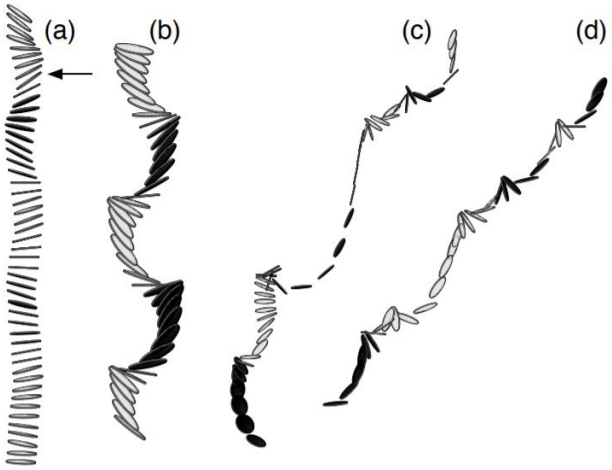

Figure 11: Trajectories of falling disks, obtained using a side mounted video camera [107]**.**

The classes shown above in Figure 11 are described below;

a) Steady falling: any initial orientation settles down quickly to a steady fall.
b) Periodic oscillation: oscillations with well-defined period.
c) Chaotic: oscillations with increasing amplitude until it flips.
d) Tumbling: the disk to turn end-over-end continuously while drifting in one direction.

2.4.5 How are leaves entrained to the wheel-rail interface?

Due to the topology of the railhead, as the wheels roll over and compact, or shear/spread leaf matter, they have a high probability of moving the contamination along the track as opposed to out of the running band. Thickness measurements of UK field and laboratory generated leaf layers have ranged from 10 to 100 μm depending upon the compaction to which the leaves had been subjected [5], [12], [32]. Samples from the Dutch rail network showed a thickness of 20 to 30 μm, and post twin-disk tests layers measured between 3 and 13 μm, the layer thickness is typically larger than the roughness of the materials, as such this prevents wheel and rail contact [28].

Leaf modelling has been researched as part of the RSSB investigation into the aerodynamic properties of train designs [91]. The section findings from the report are summarised as;

- Weak transverse and vertical flow structures from wind tunnel tests and CFD studies are sufficient enough to transport paper leaves across the rail position.

- The low strength of these particular flow structures and impact on leaf trajectories suggest that the detailed flow around the train underbody structures must also be considered to determine the movement of leaves caused by passing trains.
- Leaf trajectories do not seem to follow airflow, especially when on the ground, however once airborne the leaves take notably different paths from the air flow, particularly when there are vortices present.
- When comparing with previous paper leaf test results, the study doubts the existence of leaf vortical structures alongside trains.
- The leaf trajectory model was useful to gain understanding of the relationship between leaf trajectory and underlying air flow.
- Predictions of paper leaf correlated well with observations made during validation and full scale tests.

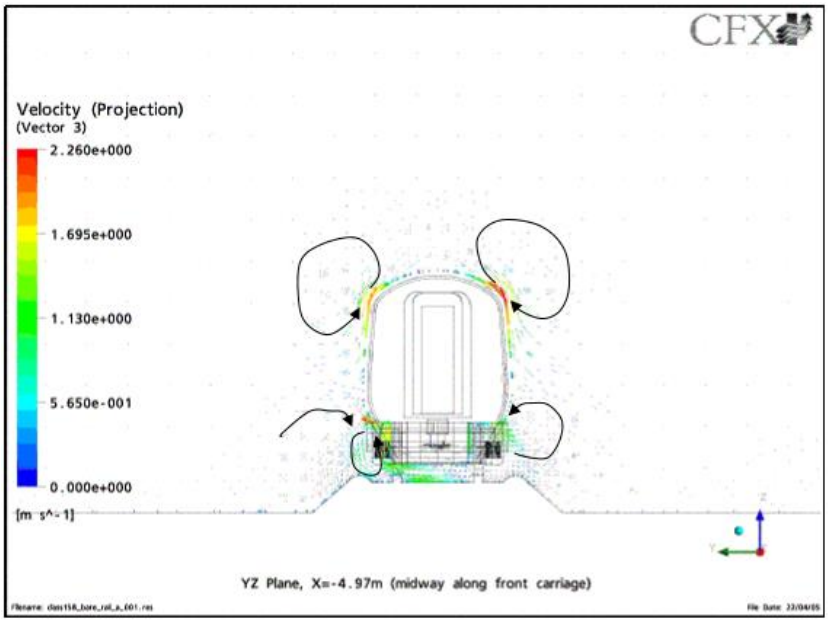

Figure 12: A CFD train airflow simulation indicating vortical structures [91]**.**

For a train travelling at 75 mph the vortical structures or rotational flows of air were short lived, lasting approximately 0.35 seconds and extending roughly halfway down the vehicle for Class 165 and Class 158 trains. The diameter of the rotational flows were between 0.8 m and 1.6 m, and the flow speed was about 1 m/s [91]. It can therefore be estimated that any leaves within 0.8 m to 1.6 m of the train may be picked up and potentially sucked into the wheel-rail contact. A screenshot of the CFD simulation indicating the vortical structures described above is shown in Figure 12.

A low pressure area would be generated behind the last section of a moving train that may suck leaves upwards and deposit them on the track area. However, no formation

in the literature was found to describe or quantify this effect. CFD analysis has been conducted on trains moving through tunnels and experiencing the 'piston effect' where a patch of turbulent air is generated behind a train moving through a tunnel[108]. It is possible that a similar effect occurs when trains are moving on open ground.

2.4.6 Carry down

Carry down describes the movement of contaminants attaching to the wheel and being transported further along the railhead. While this may be ideal for traction enhancing products such as traction gel, it is less than ideal for leaves or oil/grease. Additionally, as contaminants attach to the wheel perimeter, tread braked trains may suffer an increased loss of braking control. Carry down has been widely documented in rail research documents for various contaminants [10], [109].

While there has been research on the distance of carry down of products applied to the railhead, there is a large gap regarding leaf and black layer carry down. Liquid friction modifiers have been measured to travel no more than 100m on wheel tread and up to 2km on wheel flanges and become deposited on the rail at curved sections where the flange makes contact [110]. Under certain conditions it is possible for softened black layer matter to be carried down using the same mechanisms as described above [111].

Carry down can also occur when the wind (natural and train generated) picks the leaves up and moves them further along the rail. This effect is discussed in more detail in the previous sub-section.

2.5 Operational data analysis

2.5.1 Autumn KPI data

The Autumn KPIs reviewed in this section all refer to the rail industry regarding Signals Passed At Danger (SPADs), station overruns, collisions, WSTCFs and delay minutes attributed to weather or leaf contamination throughout the Autumn season (September while December).

The Autumn KPI data shown in Figure 13 was supplied by Network Rail. It shows station overruns and SPADs in the UK rail network between 10/10/2016 and 10/12/2016, the incidents were attributed to either "weather related" (not leaf) or to "leaf fall". This data is shown in Figure 13, with a total of 52 weather and 72 leaf related incidents. The

Office of Rail and Road (ORR) defines a SPAD as "when a train passes a stop signal without authority to do so", every occurrence is reported, with location, date and time, distance overran and suspected source of SPAD recorded.

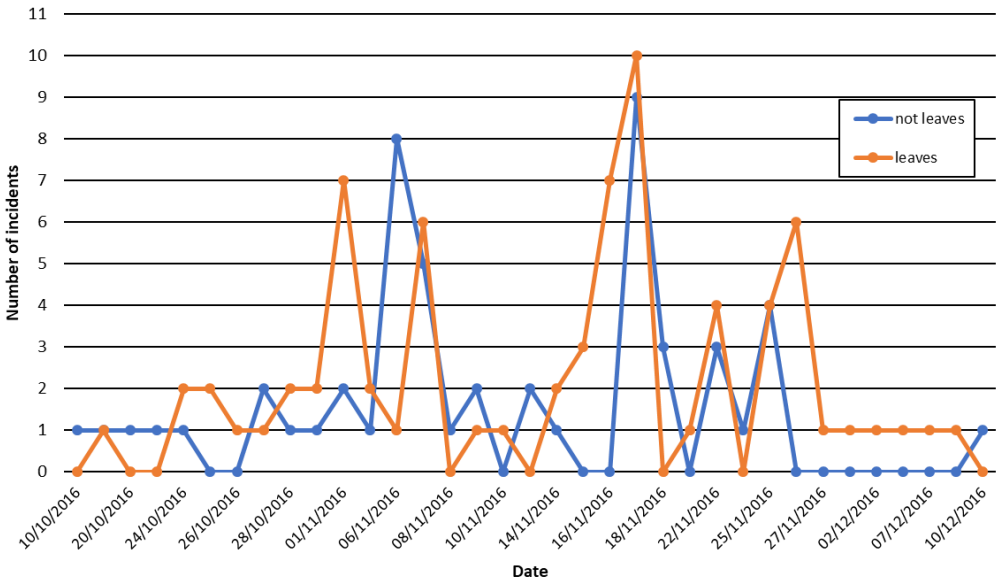

Figure 13: Daily Rail incidents for Autumn of 2016.

It is clear that there is a relationship between occurrence of "leaf" and "not leaf" caused incidents. It is notable that the highest single day occurrences were on the same day (17/11/2016) and that the majority of occurrences were between 27/10/2016 and 27/11/2016. In the UK, the RSSB categorises SPADs on their severity. There are four main categories A to D with A having 8 subcategories, according to the length of the overrun and if any damage or injury occurred [112]. Category A SPADs are particularly concerning.

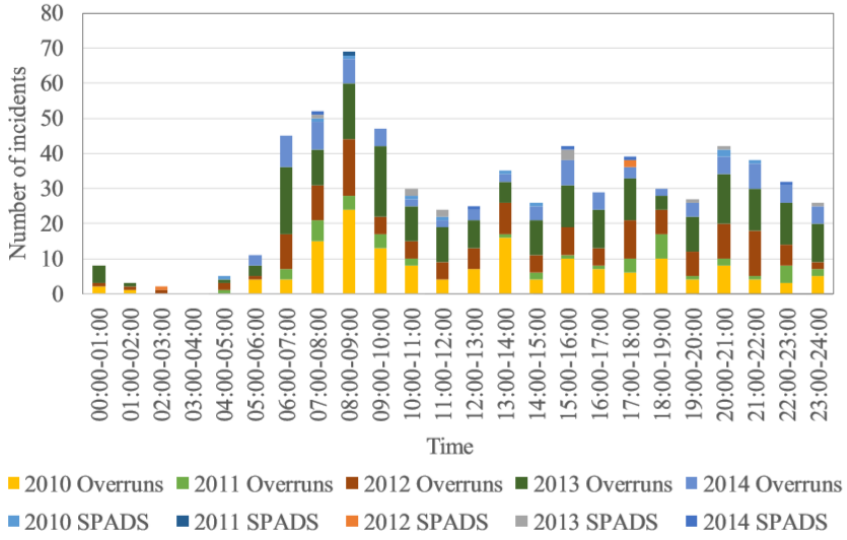

Figure 14: Number of incidents versus time of day of SPADs and station overruns for 2010 to 2014 [9]**.**

Figure 14 shows a chart displaying the number and time of incidents in one hour slots for the 2010 to 2014 autumn seasons. It clearly shows low (10 or less) incidents between 00:00 and 06:00, then a sharp increase to around 45 between 06:00 and 07:00, up to around 69 08:00 and 09:00. This is likely due to a higher volume of train journeys throughout the commuter rush hour(s), although it could be influenced by the morning dew reducing friction. From 10:00 to 24:00 Overruns and SPADs stay between 24 and 43 incidents per hourly slot. The data tends to increase from year to year, with similar trends being shown throughout the day.

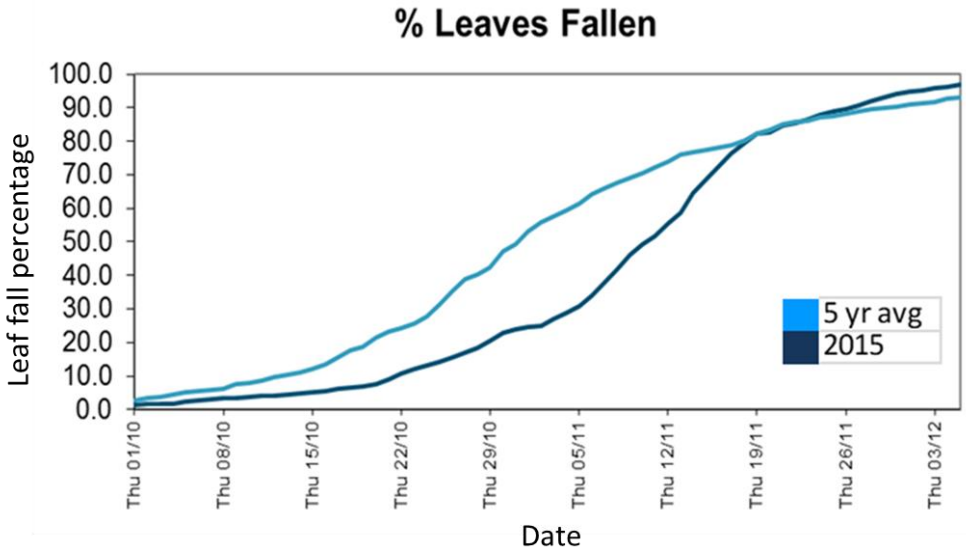

Figure 15: % leaf fall rate for 2015 and a 5 year average [113]**.**

Figure 15 is from a Network Rail presentation titled "2015 National Autumn Review" [114], it shows leaf fall rates for 2015 and for the previous 5 years. The origins and scope of the measurements were not explained in the presentation, this must be kept in mind when analysing the data.

Figure 16 is taken from the same Network Rail presentation and shows the delay minutes for the 2015/16 season, and the mean for the previous 5 seasons (2010/11 to 2015/16). It is interesting that the curves in Figure 15 and Figure 16 are so similar, indicating a positive correlation with leaf fall and rail delay minutes.

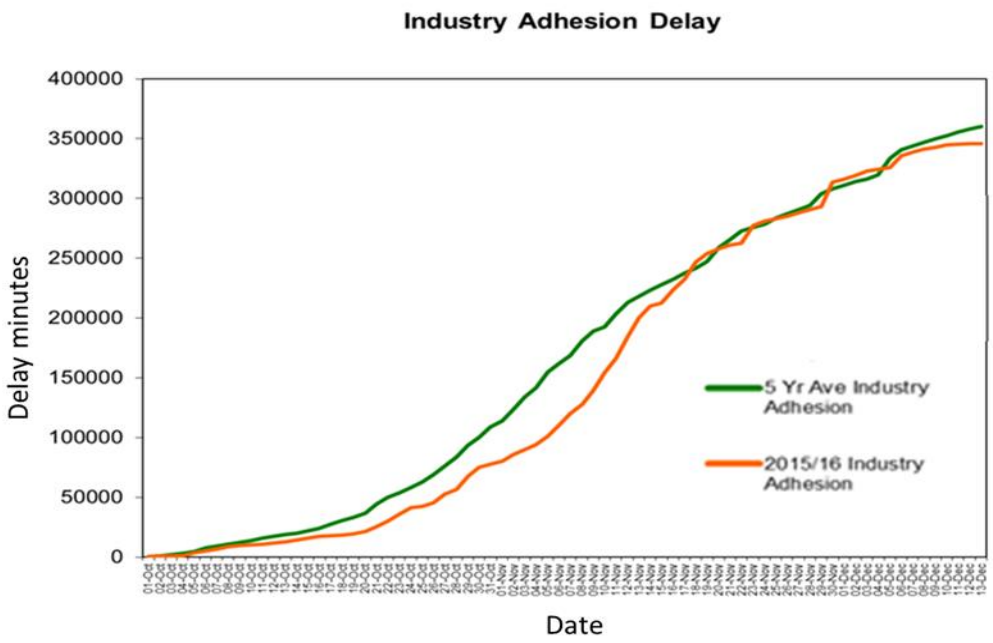

Figure 16: Industry adhesion delay minutes for 2015/16 and 5 previous years [114]**.**

Due to Autumn KPI data being released annually, it will have to be reviewed upon release and compared to other data sources and previous KPI data.

2.5.2 Trib-train data

The Trib-train (also 'Tribotrain' or 'Tribometer Train') [115], was a train run by British Rail. It was equipped with a laboratory carriage, with controlled brakes which measured the amount of force required to initiate wheel slide by the train. It was in use from the early 1970's through to several decades ago, when it was used between the 26th of June and 20th of September along a 180 mile route (Derby, Birmingham, Crewe, Beeston, Derby) which was surveyed 18 times (seven times between 14:00 and 22:00 hours, seven times between 02:00 and 06:00 hours and four times between 0:00 and 14:00 hours). It was noted that the weather was mostly sunny for the majority of the tests with light rain only occurring on two tests and then only for a short period of time. Misty conditions (possibly resulting in condensation on the railhead) were encountered on three occasions.

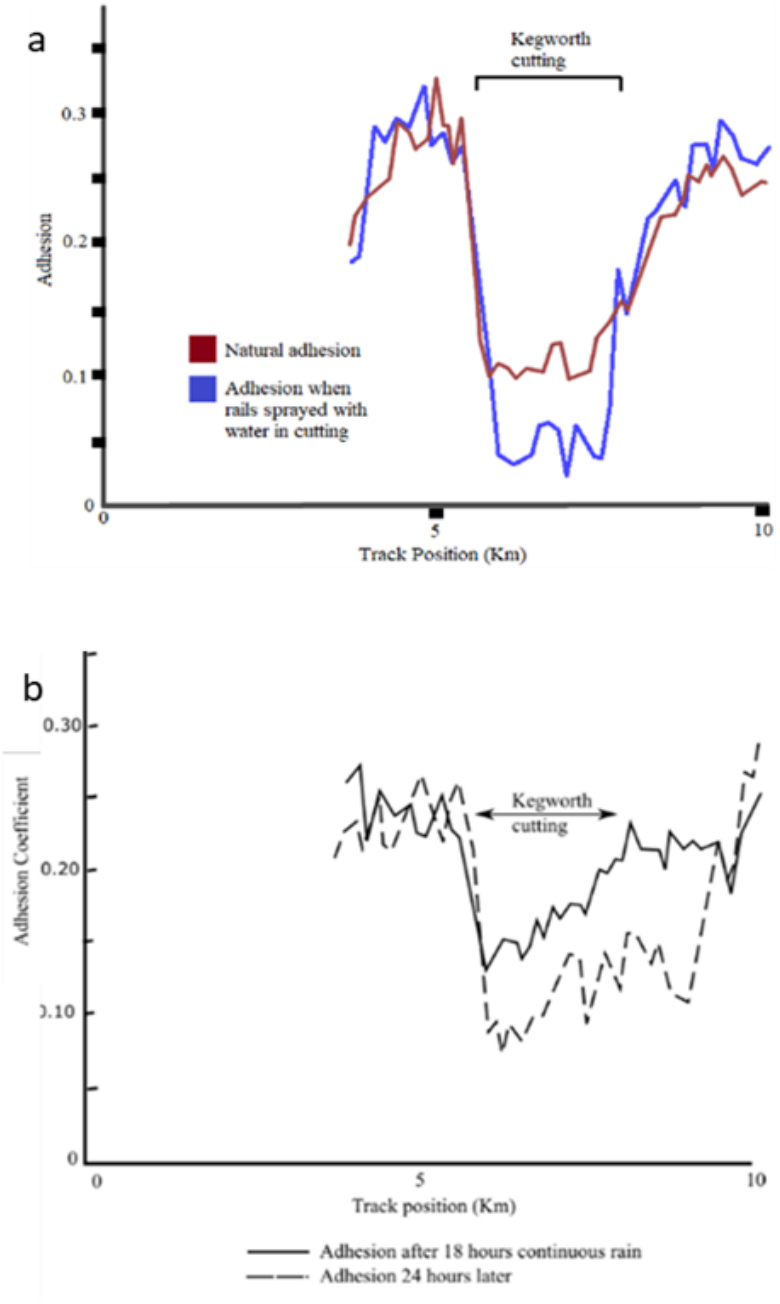

Figure 17: a) Adhesion loss when a train passes through Kegworth cutting, with natural and artificially wetted surfaces [57], [116]**, b) Adhesion loss on Kegworth cutting post rain fall** [57], [116]**.**

Figure 17 a) shows the adhesion levels recorded by the trib-train on a stretch of track that included a cutting, it was originally part of a Trib-train report [116], but has been enhanced by modern software [57]. It shows how the adhesion is reduced to roughly one third when the train enters the Kegworth cutting, an area known for low adhesion. The natural rail shows a drop from around 0.3 to around 0.1, while the wetted rail drops from around 0.3 to around 0.05. The natural rail conditions may have also contained levels of moisture, far lower than the wetted rails though. In contrast, either side of the

cutting the adhesion levels for both natural and wetted rails were very similar and at levels of around 0.25 to 0.3. This sudden drop of adhesion in the cutting could be caused by the presence of organic leaf matter contamination being present on the railhead, this is believed to be the most likely explanation. Other causes were discussed, such as iron oxides formation due to increased atmospheric moisture levels [57].

The same stretch of track was monitored 18 and 24 hours after rainfall, again this was taken from the trib-train report [116] and enhanced by modern software [57], see Figure 17 b). After 18 hours the adhesion had dropped to 0.15, which is higher than the natural level before the rainfall, possibly due to contaminants being washed off the railhead. 24 hours after the rainfall the adhesion level dropped to 0.1, possibly due to recontamination by leaves.

Despite leaf related low adhesion being primarily thought of as an Autumn problem, leaf fall can occur throughout the year. It can be caused by high wind levels, storms or raised or lowered temperatures.

2.5.3 Adhesion index

Adhesion is forecast for the rail network (both UK wide and regional) during the Autumn period and used to advise drivers on what to expect when braking or accelerating, as certain days might require a more conservative braking approach [57]. Forecasts are provided by weather organisations to help the industry plan with safety, mitigation, advice to drivers and scheduling in mind.

If low adhesion is predicted then mitigation methods can be used, such as sanding, traction gel or sending out a railhead cleaning vehicle. The index model uses information on daily leaf fall, wind levels and moisture/rain levels as its main inputs. Figure 18 shows an example of the leaf fall and low adhesion prediction for a location in the UK in 2003 [57], [117].

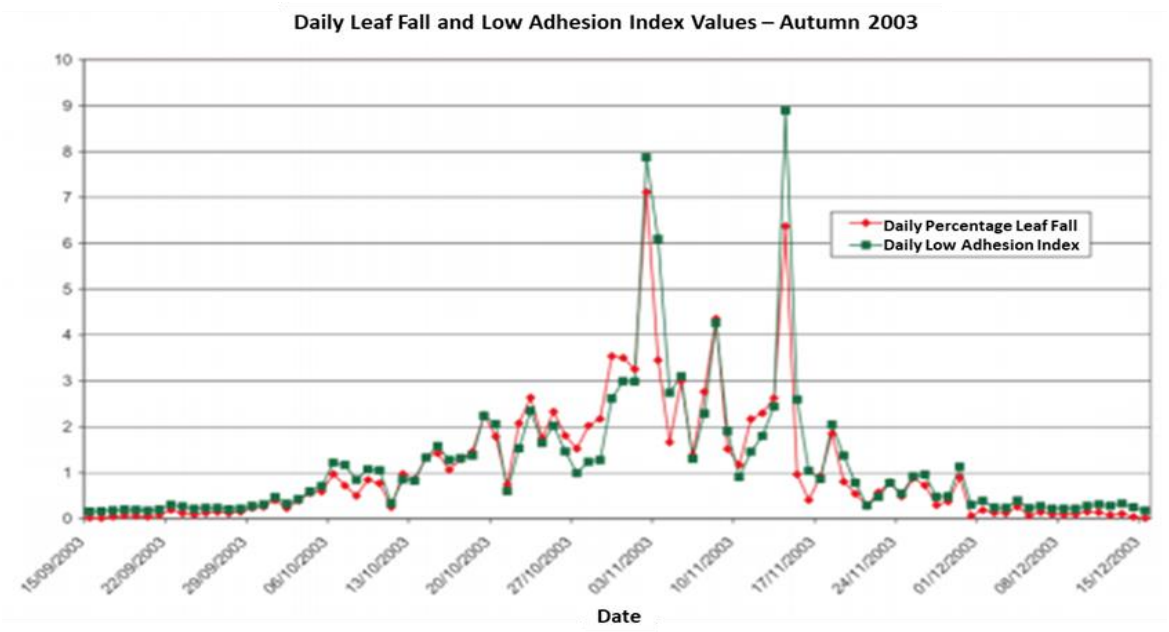

Figure 18: Daily average percentage leaf fall and low adhesion index for autumn 2003 [117]**.**

Figure 18 clearly indicates that the low adhesion index closely matches the daily percentage leaf fall. It is clear that the location of the SPADs are mostly around the greater London area and southeast coast from Hampshire to Norfolk, and in the middle to north around Liverpool and Leeds on this particular day.

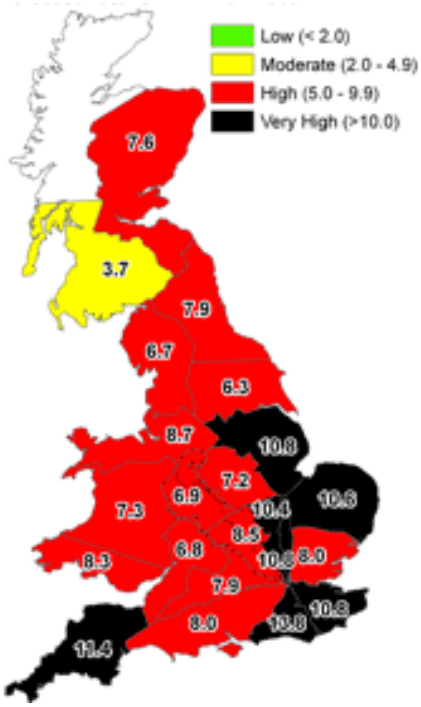

Figure 19: A regionalised map of the UK with adhesion index predictions [118]**.**

Figure 19 shows a regionalised map of the UK with colour coded adhesion prediction values provided by the Met Office [118]. Their forecasts are available at hourly resolutions for up to 48 hours in advance, with 3 hourly, 6 hourly and daily resolutions for longer lead times. The prediction lead time extends to 10 days. Their service also provides percentage leaf-fall that has occurred throughout the season, with dates for 50% and 95% leaf fall, text summaries of the causes of low adhesion and hourly summaries of low adhesion coinciding with peak traffic times.

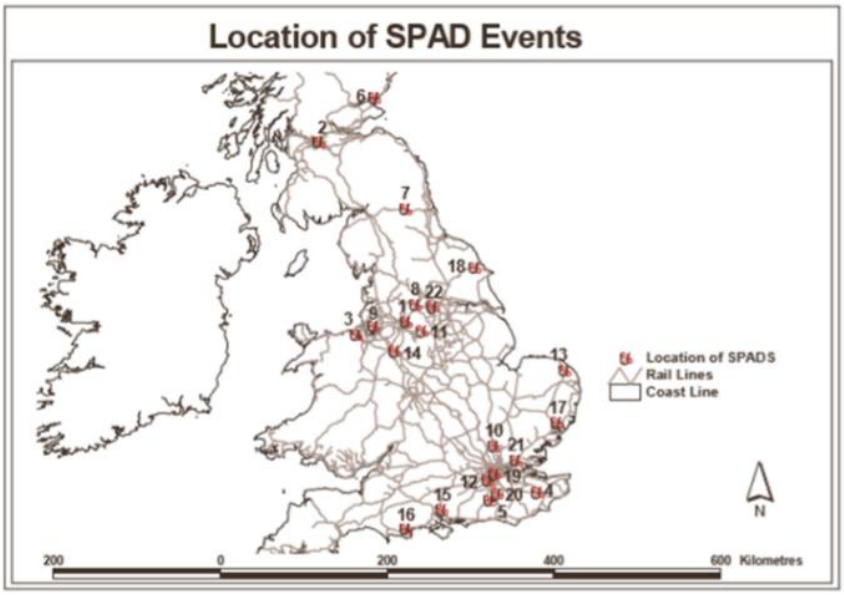

Figure 20: Locations of SPAD events for autumn 2003 [117]**.**

Adhesion index predictions are different for different regions of the UK and for different localised regions [119]. Figure 20 shows the locations of SPAD events in the UK throughout autumn of 2003 [117]. Leaf fall risk and low adhesion prediction are provided separately to allow for different mitigation techniques to be used. They are provided as hourly segments with an adhesion risk rating of between 0 and 10, where 0-2 is good (green), 3-5 is moderate (yellow), 6-8 is poor (red), while 9-10 is very poor (black).

MetDesk provides an adhesion forecast service with both a 24 hour and a 2-5 day range. The 1-5 day range forecast consists of a numerical rating from 0-10 that is grouped into; good (0-2), damp (3), moderate (4-5), poor (6-8) and very poor (9-10). These scores are provided for each hour of the first 2 days and every six hours for days 3-5. A colour coded map is also provided where regions are shown as; green – good, slightly lighter green – damp, yellow – damp, red – poor, black – very poor. The 24 hour forecast consists of a written paragraph detailing specific weather behaviour expected across different regions of mainland UK, the 2-5 day range also receives a detailed written paragraph. The advantages of this service are that; it provides a high level of

detail for the whole 5 day range, hourly predictions for the first 48 hours alongside an easy to interpret colour coded map. The disadvantages are more difficult to comment on from an outside perspective, however it is noted that the forecast does not mention specific track/vegetation features that may be responsible for contributing to the risk.

Factors known to contribute to the forecast include contaminants such as leaves, grease, rust and other pollutants, and low moisture levels caused by morning dew or light rain. With an increase in the lead time of the prediction, there is an increase in associated risk [119].

2.6 Leaves and friction

Three of the most commonly referred to, and easily misunderstood terms used when discussing the wheel-rail interface and tribology in general are friction, traction and adhesion [9]. Friction can be defined as the tangential force transmitted between two objects that slide against one another, traction (often referred to in the rail industry as "adhesion") is defined as the transmitted force between a cylindrical object rolling on a flat plane [120]. The traction/adhesion coefficient covers the region where the contact is in partial slip – friction coefficient where the contact is fully saturated with slip. The relationship between slip, creep and traction is described in section 2.6.1 below.

Leaf contamination is widely known to adhere to the railhead and provide low adhesion to the wheel-rail interface, however the leaf layer does have other properties that need to be considered. These have been taken from a 2007 RSSB report [12] and include;

- Thickness
- Hardness
- Shear strength
- Moisture content
- Adhesion/Skid Resistance
- Electrical properties
- Surface roughness

There is a lack of information on the difference in properties of leaf layers formed using specific leaf species, this current research aimed to investigate this.

2.6.1 The wheel-rail interface

Contaminants such as iron oxides, greases, sycamore leaves, friction modifiers and sand particles have been researched extensively. However, most friction testing on leaf matter is done with clean uncontaminated steel samples. Research on mitigation methods for preventing and/or removing leaf layers has been carried out in multiple

cases. Iron oxides plus leaf matter have been investigated [57], friction modifiers and their effects on leaf layers have also been researched [32]. The effect of sand on leaf layers has been researched by [32], [121], [122] amongst others.

The fundamental tribological and mechanical principles of the wheel-rail interface have been covered in various levels of detail and from various approaches by a vast amount of research. Basic principles will be described here to ensure the reader understands friction, adhesion and traction within the context of this project.

Coefficient of friction is a commonly used term, it is denoted by 'μ', and is usually either a decimal value between 0 and 1 (values above 1 are possible but are unlikely to be found in this instance).

Contact pressure is a crucial parameter, as mentioned in section 2.4.5 wheel-rail interface contact pressures range from 0.6 to 1.2 GPa [123] (typically around 1GPa) [124], this high pressure has been hypothesized to squash the leaves and bond them to the railhead [44]. Creep is highly likely on curved sections due to the nature of train design, the amount of creep varies with the radii of the curve.

Purely rolling contacts within the wheel-rail interface rarely exist and nearly always have some creepage (longitudinal positive when accelerating and negative when braking) component depending on whether the train is accelerating, braking or going round a curve (lateral creepage). The circumferential velocity of the wheel is therefore different to the linear velocity, causing slippage (or creep) to occur. Creep is usually described as the relative velocity compared to the mean velocity of the wheel, and is represented as a percentage, where 0 is purely rolling and 100 is purely sliding [57].

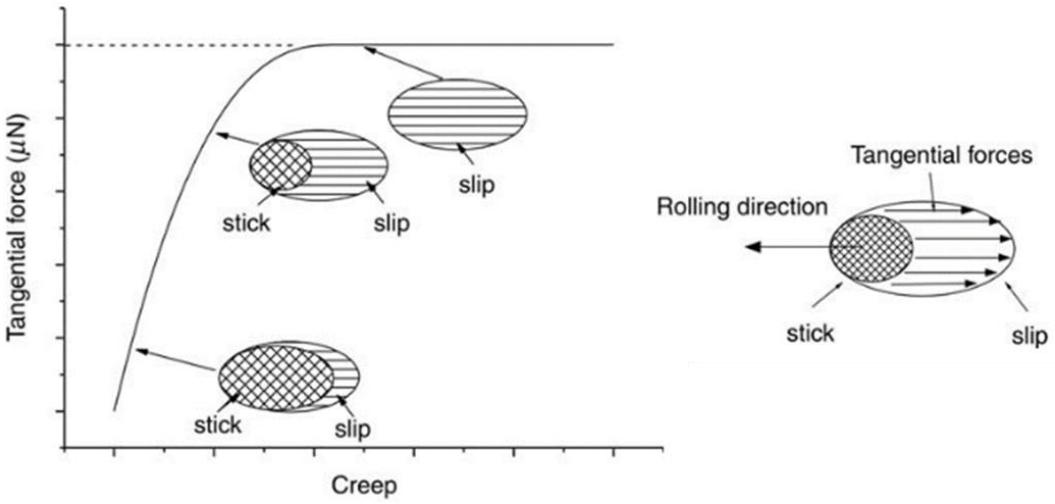

Figure 21: Relationship between tangential force and creep [125]**.**

The relationship between slip and the traction force is described by the creep curve, shown in Figure 21. For a purely rolling contact, creep is 0% and the traction coefficient (μ) is also 0, meaning that there is 100% stick in the contact, with no slip [126].

As traction forces increase, slip is introduced to the contact from the rear (relative to the rolling direction), which grows while moving up the creep curve, until the stick component has been removed and slip dominates the contact. As this happens the traction coefficient (μ) increases. At the plateau of the curve, the traction coefficient and friction coefficient are equal and cannot increase any further, this is known as saturated creep [57].

Mechanical slip in the top of rail/wheel contact can vary from 0 up to 100%, typically twin-disc tests use either 0.5, 1 or 2% slip values as these represent typical values found in the real world [28]. At the flange contact slip values could be much higher, especially when going round a curve.

Contaminants such as iron oxides, greases, sycamore leaves, friction modifiers and sand particles have been researched extensively. However, most friction testing on leaf matter is done with clean uncontaminated steel samples. Research on mitigation methods for preventing and/or removing leaf layers has been carried out in multiple cases. Iron oxides plus leaf matter has been investigated [57], friction modifiers and their effects on leaf layers have also been researched [32]. The effect of sand on leaf layers has been researched by [32], [121], [122] amongst others.

Moisture levels in the interface are also crucial when describing the friction state, most friction modifiers are water based and leaf layers are known to reduce in friction levels when moisture is added. However, research into the specific bonding mechanisms of leaves to the railhead may require more investigation into combinations of leaf matter and other contaminants.

2.6.2 Friction test methods

Current test methods for testing or simulating friction in the wheel-rail interface include; twin disc rigs, Full Scale Rigs (FSRs), mini Traction Machines (MTM), push tribometers, pendulum rigs and Pin-on-disc tribometers. The information shown in Table 6 on different friction test approaches was compiled in previous research [44]. They are discussed in more detail later on in this review.

Table 6: A table showing friction levels recorded using various instruments in various conditions [44]**.**

Ref.	Test Method	Leaf Type	Test Condition	Friction level
[127]	Twin disc	Mix maple and oak	Dry/Wet - 1 m/s with 0.5, 1, 2, 3.5% slip at 1.5 GPa	< 0.05 Dry, for all slip values < 0.02 Wet, for all slip values
[32]	Twin disc	Cut sycamore	Dry - 1 m/s with 0.5, 1, 2 % slip at1.2 GPa	<0.05 *Typical value
[125]	Pin-on-Disc	Crushed elm	Relative Humidity (RH) = 40±5 and 95±5 % 0.1 m/s with 100 % slip 0.8 and 1.1 GPa	0.25 (average) RH = 40 % 0.15 (average) R.H = 95 %
[25]	Ball on disc MTM*	Chopped sycamore	Wet - 0.02-1 m/s with 1, 50 % slip at 1 GPa	0.01-0.07 Soaked brown leaf 0.04-0.14 Leaf extract
[128]	Twin disc	Unknown	Wet - 1 m/s with 1 % slip at 1.5 GPa	< 0.06 - Leaf films
[129]	Twin disc	Cut sycamore	Dry - 1 m/s with 0.5 % slip at 1.2 GPa	0.02 - *Minimum value
[122]	Twin disc	Mix + extract Soaked maple, beech, oak, birch	Wet - 0.8-3 m/s with 1-10 % slip at 1 GPa	< 0.1 Leaf mix ≈0.1 Leaf extract
[130]	Twin disc	Sycamore paste	Wet - 1 m/s with 3 % slip at 1.5 GPa	0.05-0.15
[121]	Field Locomotive	Unknown	Dry/Wet - Axle load 21.5 t	0.06 - Dry, mean value in 1st run 0.04 - Wet, mean value in 1st run
[84]	Field Tribometer	Unknown	Wet (Light rain)	0.15 - *Minimum value

[102]	Field Test bogie	Pine needles	Dry/Wet 20 km/h at maximum	0.05 - Dry, minimum value 0.05 - Wet, minimum value

Several friction measurement techniques have been analysed by Harmon et al. [131] in order to compare them and discuss their applicability to different conditions. They split the different methods into four categories;

- Small-scale laboratory methods. These are most useful for gaining fundamental understanding of friction behaviour due to easily controllable conditions.
- Full-scale laboratory methods. More realistic geometries compared to small-scale tests but often less versatile.
- Field measurement systems. Enable conditions in the field to be measured, but often at unrealistic geometry/contact pressure and climate/contaminants unable to be controlled.
- Instrumented train. Most accurate way of measuring friction due to realistic loads/speeds. However, limited control over climate, contaminants on the rail and often prohibitively expensive.

In summary, six potential testing methods were assessed: twin disc, pin-on-disc, ball on disc (MTM), field locomotive, field tribometer and field test bogie. These were all considered when designing test plans for the bonding and low μ hypotheses in chapters 6 and 7.

2.6.3 Pendulum

Since low adhesion conditions can be transitory, a quick, portable method for recording adhesion levels is required, initial development tests concluded that the pendulum rig is a viable test method for field adhesion levels [132]. The pendulum rig works on an energy loss principle, a pivoted arm is released from a latch and slides a rubber pad over the surface in question, namely a section of rail. The height is adjusted so that the contact length of the rubber pad on the surface being tested is 127 mm or 5 inches. The level of resistance dictates the position the gauge needle is pushed to, more resistance gives a higher PTV (Pendulum Test Value) [131], see below. The PTV can be converted to a coefficient of friction using the equation shown below.

$$\boldsymbol{CoF_{pendulum} = \left(\frac{110}{PTV} - \frac{1}{3}\right)^{-1}} \qquad \textbf{(1)}$$

The above equation **(1)** is the CoF (Coefficient of Friction) equation for Pendulum Test Values [131]. It is common practice to take multiple consecutive measurements, to find

the average and standard deviation. The pendulum rig is portable and can be taken to real rail track to measure friction in real world conditions. It has a plywood stand to keep it level and at the correct height, it additionally has height adjustment on each of its three feet and a spirit level for vertical alignment.

Potential errors when setting up and operating the pendulum rig include; inconsistent calibration before use, inconsistent height setting after moving the rig or inconsistent reading of the PTV. Additionally, it is difficult to ensure that the rubber pad slides over the running band.

The pendulum rig offers the highest cost advantage of the friction test methods discussed, and it can be used both in the lab and in the field [133], [134]. Pendulum rigs have been used in previous research [9], [12], [57], [84], [133].

2.6.4 Twin disc

The SUROS (Sheffield University ROlling Sliding) rig is a twin disc rig that consists of a lathe and an electric motor, each of which turn a 47mm disc of rail and wheel steel respectively. The speeds of the discs are set to induce a specific amount of slip, and the load applied to compact them is controlled by a hydraulic press and load cell under the wheel disc shaft. A torque transducer on the drive shaft for the rail disc measures the friction from the contact. Typically, the load is set to give a contact pressure of either 0.9, 1.2 or 1.5 GPa. A load of 4.7kN applied to the discs with a 10mm line contact produces a maximum Hertzian contact pressure of 1.2GPa, which is representative of that of passenger trains [32]. Slip if typically set to a value of either 0.5%, 1%, 2%, 3% or 5%, although higher values can be used if necessary.

$$\boldsymbol{Slip} = \frac{\boldsymbol{\omega_{wheel} \cdot r_{wheel} - \omega_{rail} \cdot r_{rail}}}{\boldsymbol{\omega_{wheel} \cdot r_{wheel} + \omega_{rail} \cdot r_{rail}}} \cdot \mathbf{200}\% \qquad \textbf{(2)}$$

$$\boldsymbol{\mu_{adhesion}} \frac{\boldsymbol{T}}{\boldsymbol{F_N \cdot r_{rail}}} \qquad \textbf{(3)}$$

Slip is calculated using the slip equation **(2)**, where ω represents the rotational speed and r represents the rolling radii of the disc. Adhesion coefficient is calculated using equation **(3)**, where T is the reading from the torque transducer and F is the reading from the load cell.

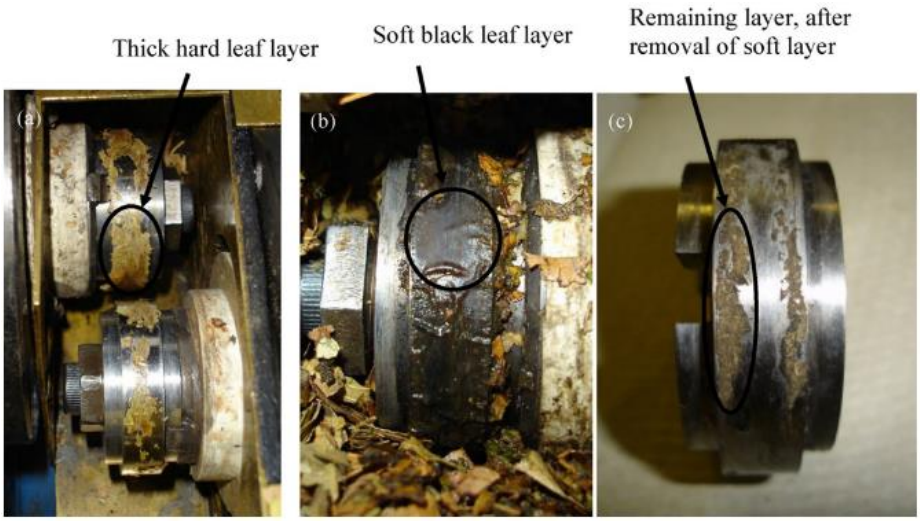

Figure 22: Leaf layers generated on the SUROS twin disc rig [127]**.**

Figure 22 shows leaf layers generated under wet and dry conditions [127]. Twin disc test rigs have been used for assessing the low μ of leaf matter, as well as generating leaf layers for chemical analysis, scratch testing mitigation methods etc. Example leaf friction testing data using the SUROS twin disc rig is shown in Figure 28. Twin disc rigs have been used extensively in rail research projects, such as [9], [10], [32], [44], [57], [109], [122], [127], [128], [130], [131], [135].

2.6.5 Full Scale Rigs

The University of Sheffield has a linear Full Scale Rig (FSR), which is a large scale laboratory rig that involves a full scale wheel that is free to rotate, its vertical travel and loading are controlled by a hydraulic actuator. A section of track is fixed to a slide-bed and moved using another hydraulic actuator. Creep is controlled by a chain attached to the wheel. Media such as water, friction modifiers or leaf matter can be introduced into the interface to observe the effect on friction and how they react with the wheel and rail.

Figure 23: Leaf contamination generated on railhead samples using a full scale rig [12]**.**

Figure 23 shows the cut away rail specimens from the full scale rig with leaf contamination present, the black layer is clearly present and was generated as part of an RSSB investigation [12]. These cut away specimens can then undergo chemical analysis or scratch tests to determine the properties of the leaf layer. It has been used in multiple rail research projects, including but not limited to [12], [57], [109], [131], [135], [136].

Other FSRs include the HAROLD rig at the University of Huddersfield [137], which has a full scale bogie assembly rolling on 2m diameter rotating rail drums. The rig is capable of applying a maximum axle load of 25t and a maximum running speed of 200kph.

2.6.6 Pin on disc

Pin on disc rigs are small scale laboratory rigs, the set-up involves a pin (or ball) contacting a rotating disc face. The load, rotational speed, contact radius and contact geometry can all be varied to represent different contact/wear regimes. The contact is purely sliding and the torque transducer on the disc drive shaft is used to calculate the coefficient of friction.

Figure 24: A pin on disc machine testing Elm leaves [125]**.**

Figure 24 shows a pin on disc set-up testing the friction of Elm leaves. Pin on disc test rigs have been used in multiple rail research projects, such as [25], [125].

2.6.7 High Pressure Torsion (HPT)

High Pressure Torsion (HPT) rigs are a small scale laboratory test method involving compression and torsion. The set-up involves two dies with the sample material compressed in between, while one die is rotated. The compression load and rotational speed are controlled. Torque is measured to give a coefficient of friction. The rig can

apply a normal load of up to 400kN and up to 1000Nm of torque. This is enough to simulate contact stresses of 900MPa and according to Zhou et al [138] is roughly equivalent to the 60kN load of a single rail wheel.

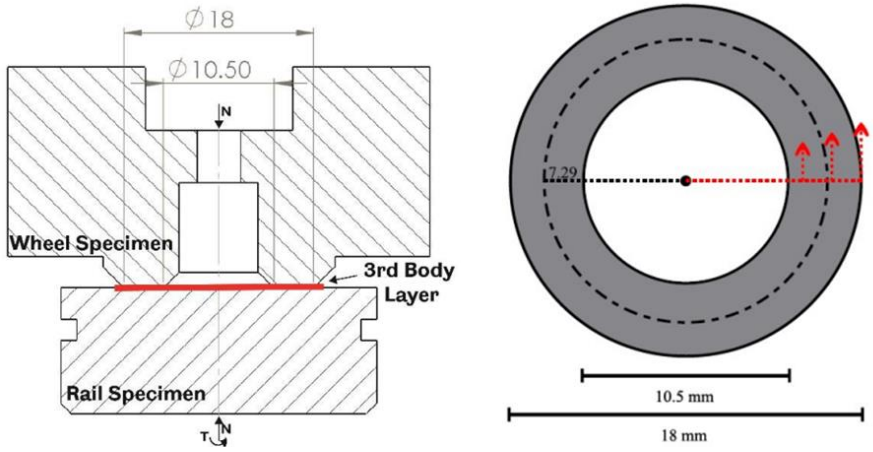

Figure 25: Schematic of HPT specimens (left) and contact dimensions (right) [139], [140]**.**

A simplified principles diagram of the HPT set-up is shown in Figure 25. Due to their relative sparsity, HPT rigs like the one described here are not extensively used in rail research, although they are an established tribological test method [141].

2.6.8 Test method discussion

Several friction measurement techniques have been analysed by Harmon et al. [131] in order to compare them and discuss their applicability to different conditions. They split the different methods into four categories;

- Small-scale laboratory methods. These are most useful for gaining fundamental understanding of friction behaviour due to easily controllable conditions
- Full-scale laboratory methods. More realistic geometries compared to small-scale tests, but often less versatile.
- Field measurement systems. Enable conditions in the field to be measured, but often at unrealistic geometry/contact pressure and climate/contaminants unable to be controlled.
- Instrumented train. Most accurate way of measuring friction due to realistic loads/speeds. However, limited control over climate, contaminants on the rail and often prohibitively expensive.

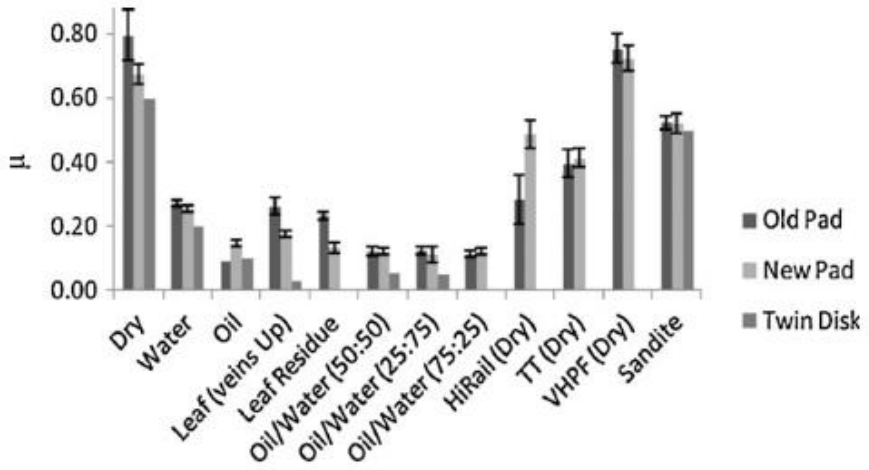

Figure 26: A comparison between friction values of a pendulum and twin disc rig [133]**.**

Research comparing a pendulum rig and a twin disc rig for rail friction testing [133] is displayed in Figure 26. It found that there is good agreement across a range of contaminants including oil, water and oil/water mixes, but not with leaves which were an order of magnitude lower with the twin disc rig. It was noted that with the pendulum testing the sliding rubber pad would just sweep the leaves out of the way, only the twin disc method provided a high enough pressure to crush leaves [133]. However, for existing leaf layers it is believed that the pendulum rig has potential to be a quick check method for friction levels in the field.

2.6.9 Low friction data

As mentioned previously (see section 2.6.1), there is a complicated relationship between friction, stick, slip and creep within the wheel-rail interface. Creep curves for various test scenarios are shown below in Figure 27, where wet and dry leaf friction is compared to a dry and wet contact and oil for reference. Typical leaf friction has been measured as below that of oil and well below 0.1.

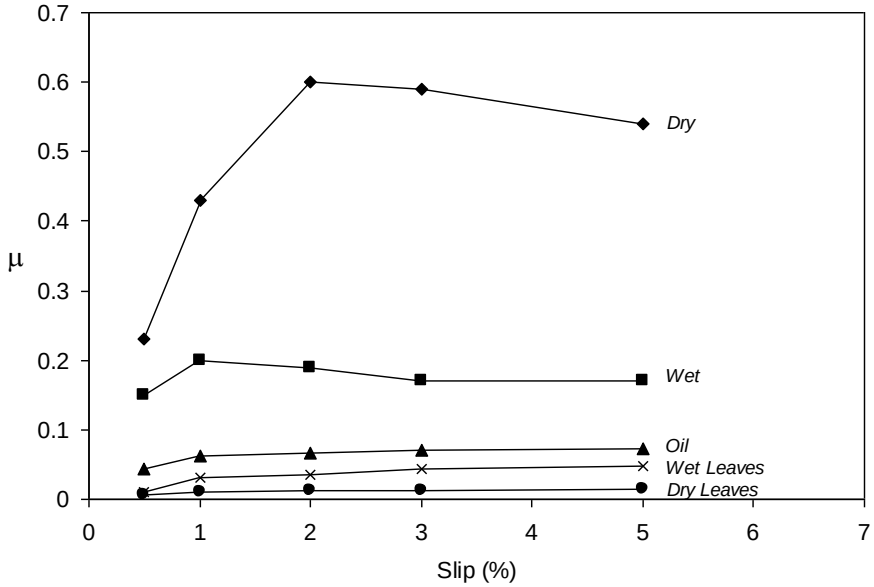

Figure 27: Creep curves for various test conditions [127]**.**

Different contaminants have been tested in laboratory conditions using the SUROS twin disc rig, Figure 28 [127] shows the drop in traction coefficient when leaves are applied. Figure 28 (b) shows that for dry leaves the traction coefficient drops from about 0.15 to around 0.02, while (a) shows that for wet leaves the value drops from about 0.06 to around 0.01. It has been stated that leaf lubrication also reduces the variability of the coefficient of friction [125].

Recent work [44] has been carried out involving generating a black leaf layer in laboratory conditions with the SUROS twin disc rig. The conditions for the test involved a slip ratio of 1% (rail speed of 400rpm), contact pressure of 1.2 GPa, with Sycamore leaf BLP (<150μm) and with varying disc temperatures.

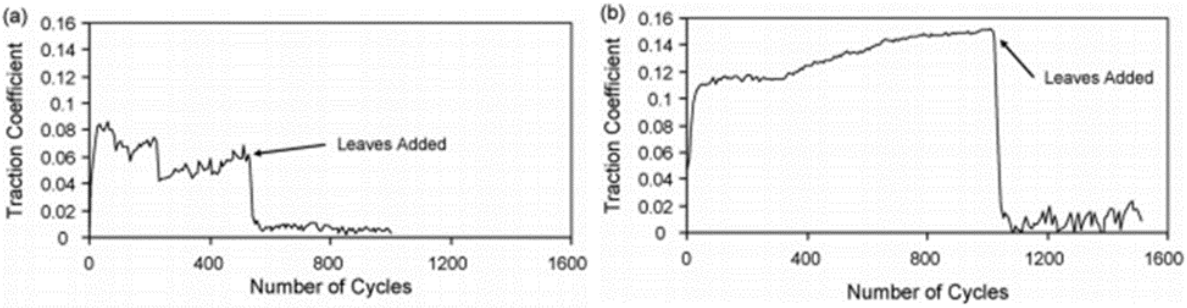

Figure 28: Traction coefficient against number of cycles for (a) wet leaves and (b) dry leaves [127]**.**

Low adhesion in the wheel-rail contact is typically categorised as shown below [128].

- Medium low: $0.1 < \mu < 0.15$
- Low: $0.05 < \mu < 0.1$
- Exceptionally low: $0.02 < \mu < 0.05$

Leaf layers are known to have two major properties: electrical isolation and a low shear strength [12], [32]. According to Nagase [102], when the rails are dry, the adhesion coefficient shows no dependency upon speed. Dry or water saturated leaf layers do not reduce friction nearly as much as they do when there is a small amount of moisture, which can cause exceptionally low friction levels [127], [131].

Data on friction levels of specific leaf species is sparse in the literature, however, recent work conducted in Japan has tested maple, cherry, zelkova, ginkgo and cedar leaves using a twin disc rig [142]. They found that in a when introducing dry leaves, the friction coefficient dropped to an average of 0.225 which was 65% lower than prior to leaves being fed into the contact. Wet leaves reduced the average to 0.053 (almost exceptionally low) which was 75% lower than the pre leaf conditions. They attributed differences in species friction to the oil content of the leaves and also noted that there was no oxide film was formed during the tests.

2.7 Low friction and layer formation/bonding mechanisms and hypotheses

2.7.1 Layer formation/bonding mechanism hypotheses

Laboratory and field tests involving high pressure and leaf matter have produced the black leaf layer. Contact pressures in the wheel-rail interface typically range from 0.6 to 2.7 GPa [124], this high pressure has been hypothesized to squash the leaves to form the leaf layer and bond it to the railhead [44].

Pressures in the wheel-rail interface are sufficiently high as to produce sub or supercritical water. Subcritical water is water that has been pressurised and is able to reach temperatures above its natural boiling point (100°C). Supercritical water is water that has been heated to over 374°C and pressurised to over 22 MPa, at this point the liquid and gas phases of water are indistinguishable. These conditions, with the presence of supercritical water may play a role in the breakdown and reformation of cellulose and/or lignin based adhesives which may be responsible for bonding leaf layers to the railhead [44].

Although research into how the leaf material bonds to the railhead while causing low adhesion to the wheels has been carried out, the exact mechanisms still remain somewhat unclear [44].

The main interacting groups present in leaf matter are hydroxyl (-OH) and/or carboxyl (-COO), which easily bond to iron (Fe) as well as iron oxides (FeO, Fe_2O_3, Fe_3O_4 etc.) and

pyrite (FeS_2) [12], [30]. The same research also hypothesized that biomolecules such as cellulose, lignin, pectin, cutin, free fatty acids and other complex compounds present in the leaf structure are responsible for binding the underside of the leaf and providing low adhesion to the wheel, in damp conditions [30].

Lignin also possesses adhesive potential due to polymer crosslinking, to other organic compounds such as furfural and phenol [143], [144]. When used as an adhesive lignin is known to be relatively strong, displaying 90% of the tensile strength of phenol-formaldehyde resin [144], which is used to make fibreglass, some billiard balls and as an adhesive in the wood industry. However the crosslinking capabilities of lignin would, to a certain extent, repair the decomposition [36], [39]–[43]. The high temperature and pressure break the lignin molecule apart, which is subsequently re-polymerised via crosslinking [40]–[43]. As water (morning dew, rain etc.) is present in the wheel-rail interface, it can act as a solvent and when evaporated, the re-polymerised substance left behind is a hard solid residue [41].

The summary of an investigation by Poole [12] into the biochemistry of leaves and the surface chemistry of rail steel has suggested four bonding hypotheses, in order of likelihood;

- Railhead bonding caused by Fatty Acids from Cutin or Cuticular Wax.
- Railhead bonding caused by cell wall Lignin.
- Railhead bonding caused by cell wall Carbohydrates like Pectin and Cellulose.
- Railhead bonding caused by Pyrite (a combination of iron and sulphur) formation and its degradation.

Temperature is expected to play a major role in the bonding of leaf material and the railhead [9]. The railhead would only reach elevated temperatures in cases of; prolonged exposure to sunlight, hysteresis due to continuing wheel passes, friction generated by wheels undergoing slip (partial and full), electrical conduction caused by a fault, lightning strike or some other heat source due to cleaning of track. The most consistent cause of increased temperature is likely to come from prolonged exposure to sunlight in the summer months, however, this is not as much of an issue in the autumn months. Hysteresis due to continuous wheel passes may increase the temperature on the surface of the rail, however, this is very difficult to measure and is highly dependent on external factors such as ambient temperature, rail bulk temperature and ambient humidity. Friction generated by wheels undergoing full slip is likely the most probable cause for significant increase in railhead temperature, where more slip would give a higher temperature increase.

In a physical sense, the bond strength of the black leaf layer is believed to be high. Bonded leaf layers have been shown to be durable, black sycamore leaf layer remained present after 3000 cycles in a twin disc rig at baseline conditions and 0.5% slip [32]. The hardness of the leaf layer remaining after the tests was measured by Vickers micro-indentation and found to be between 47 HV_{10g} and 68 HV_{10g} [32], and is in accordance with similar results by [127]. In contrast, particles of stainless steel and sand were found to have values of 320 HV_{10g} and 1500 HV_{10g} [32]. Bond strength testing is difficult as the leaf layer is so thin and soft, scratch testing has been used although there are limitations to this method. A new method will have to be developed to better understand the force required to remove the leaf layer.

Moisture levels in the interface are also crucial when describing the friction state, most friction modifiers are water based and leaf layers are known to reduce in friction levels when moisture is added. However, research into the specific bonding mechanisms of leaves to the railhead may require more investigation into combinations of leaf matter and other contaminants.

The current identified leaf layer bonding hypotheses are; Iron oxide catalyst, Cellulose/Lignin based adhesive, metallic substrate effects (possibly via mechanical interlocking) and supercritical water + high temperature and pressure.

Iron oxide driven

This hypothesis also involves high temperature and pressure, but with the presence of iron oxides to act as a driver in the decomposition of the leaf components and the formation of the third body layer. Iron oxides at the surface (e.g. Fe_2O_3 and Fe_3O_4) react with the leaf material and bond with the iron in the rail. These oxides are deemed to form a mechanically mixing layer, presumably leading to third body layer formation, see Figure 29 below.

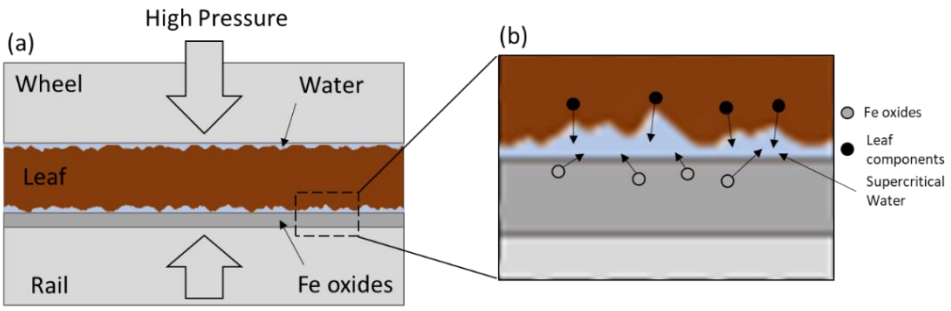

Figure 29: (a) The leaf, water and thin oxide layer on the rail are rolled over by the wheel with high pressure (b) Leaf components are dissolved into the supercritical water along with Fe oxides from the oxide layer (image created by author).

The first step in this hypothesis involves high temperature and pressure being applied to a leaf film with water present. The second step involves the leaf components (cellulose, lignin, pectin) dissolving into the supercritical water present. Iron oxides immediately assist the breaking down of the polymers into fragmented components. The components then react (possibly via polymer chain cross-linking) and form a bonded layer (third layer). Lignin decomposition can occur in under 5s at supercritical conditions [39]. Despite the wheel passage time being considerably shorter than 5s it is worth noting that the pressure can range from 0.6 and 2.7 GPa, which is considerably higher than the requirement for supercritical water. Additionally, multiple consecutive wheel passes will occur and may have a cumulative effect on the polymer decomposition.

Metallic substrate effects

This hypothesis focuses more on the bonding mechanism as opposed to the formation process of the bonding layer, building upon the previous bonding hypothesis regarding an adhesive cellulose/lignin based third body layer. It is assumed that the adhesive material fills the asperities in the surface of the rail and mechanically locks the two materials together.

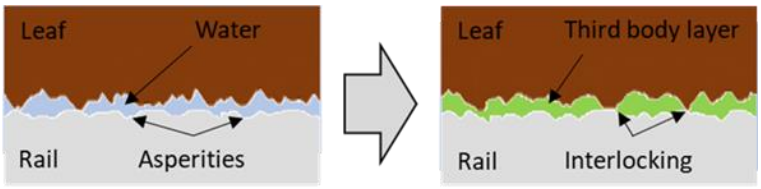

Figure 30: The leaf layer conforms to the surface of the railhead to fill all asperities and mechanically lock to the surface, possibly alongside other hypotheses such as lignin/cellulose based adhesives (image created by author).

It is established that a smoother surface finish with a lower Ra (roughness average) value aids in slowing down the growth of rust (oxides) on steel, as well as increasing corrosion resistance when compared to a rougher surface [145]. The size of the asperities should have an effect on the strength of the bond with the adhesive. There should be an extremely high amount of true surface contact area between the railhead and the leaf layer, see Figure 30 above, due to the leaf matter filling in all of the asperities and interacting with the entirety of the surface as opposed to just the tips of the peaks. This increase in surface contact should increase the total bond strength.

2.7.2 Low μ hypotheses

Laboratory testing has proven that leaves can reduce friction in a simulated wheel-rail contact to low ($0.05 < \mu < 0.1$) and exceptionally low levels ($0.02 < \mu < 0.05$) [127], [131]. The exact mechanisms for how this occurs are still somewhat unclear and a number of hypotheses have been identified from the literature, which include bulk leaves on the line, compressed leaf solid lubricant layer, viscous acid gel formation and thin surface layers. It is also plausible that there is some crossover between the bonding and low μ hypotheses. Iron oxides are one example as they may be required to bond leaf layers to the railhead yet are also known to reduce friction. Cellulose and lignin are another example as they may be responsible for forming a shear thinning gel, whilst also undergoing crosslinking and repolymerisation to bond the layer to the railhead.

Bulk leaves on the line

This hypothesis regards the bulk leaf theory in which it is assumed that a "large" number of leaves has been dumped on the line and multiple wheel passes have compacted the leaves and formed a layer that has bonded to the rail. A large number of leaves present in the wheel-rail interface may have a greater friction reducing impact as opposed to a single leaf.

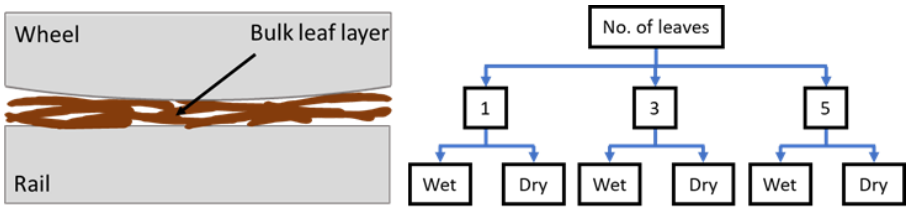

Figure 31: The volume and type of leaf are assumed to be driving factors of low adhesion for this hypothesis (image created by author).

Differences in friction between wet and dry sycamore leaves was investigated for this hypothesis (see Figure 31), as leaf hydration may have an effect on the friction reducing of leaves. Both wet and dry leaves are known to produce low friction levels, and train operators can and do suspend/delay trains immediately after heavy leaf fall [9].

Compressed leaf solid lubricant layer

This hypothesis regards the leaf solid lubricant theory in which the leaf layers prevent wheel rail contact and act as a solid lubricant made only of leaf matter (see Figure 32), lowering the coefficient of friction.

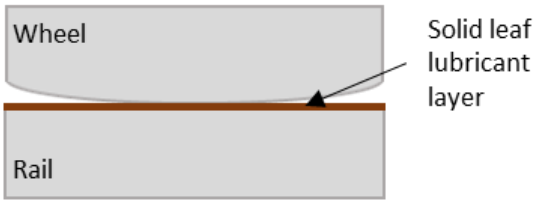

Figure 32: The leaf layer completely prevents any wheel to rail contact, acting as a solid lubricant layer (image created by author).

Both laboratory experiments and experiences from train operators support this theory [9]. Solid lubricants such as graphite powder are widely used and are known to reduce friction greatly.

Viscous acid gel formation

This hypothesis involves a viscous pectin gel being formed within the leaf layer, then released on the surface allowing the wheel to pass over and shear it (see Figure 33) [25].

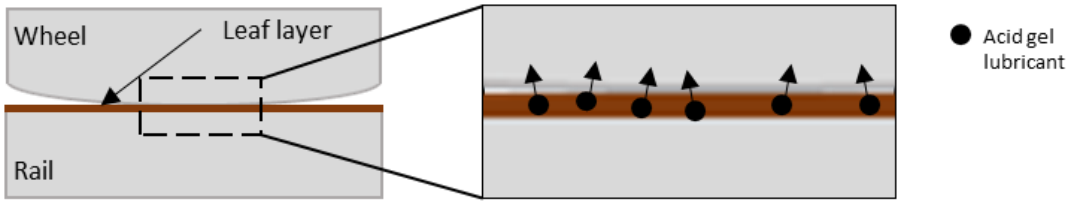

Figure 33: Viscous acids such as pectin or cellulose are released from the leaf layer which are easily sheared by the tangential force at the wheel-rail contact (image created by author).

FT-IR analysis has shown the presence of pectin and cellulose in leaves, both of which are water soluble and would be expected to be released in light rain or morning dew [9]. It has been presumed that the Fe ions assist the pectin transformation into pectin gel [25], thus preventing wheel rail contact and lowering friction via EHL (elastrohydrodynamic lubrication) under the right conditions.

Supercritical water plus high temperature and pressures

Water present in the leaf material and contact is elevated to supercritical conditions in the contact where temperature and pressure are greater than 374 °C and 22.1 MPa respectively. In the wheel-rail contact pressure can be between 0.6 and 2.7 GPa [139], and temperature has been estimated to reach over 727°C [9], [146]. Under these conditions the material microstructure could be changed [147] leading to the creation of a third body layer. If this hypothesis is true then it is assumed that the reaction should occur in the short time period (>1s) in which the wheel passes over a given location, though it is worth considering that a high number of wheel passes from a larger train may have a compounding effect. This third body layer has a fine structure, sometimes nanocrystalline [148]. Figure 34 below shows a simplified diagram where leaf components and Fe ions may react with supercritical water to produce a third body layer that is bonded to the railhead.

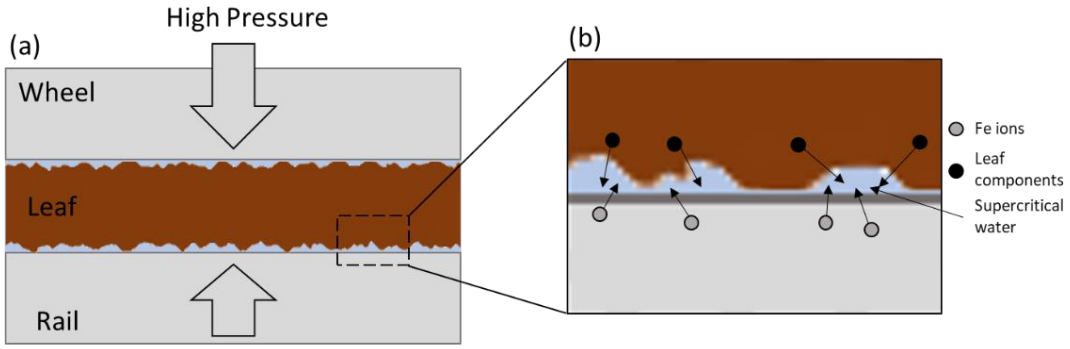

Figure 34: The breakdown of leaf components (a) Asperities/gaps contain water between leaf and rail, with high pressure (b) Leaf components and Fe ions dissolve into water under high temperature (>374°C) and pressure (>22.1MPa) (image created by author).

Investigations [147], [148] have shown that high contact pressures can impact leaf layer formation with severe deformation of the rail surface, also influencing oxide formation [9]. The change seems to be dependent on specific material combinations, the wheel-rail contact meets these requirements so as to reduce the surface grain size from an average of 200 nm to 20 nm [149]. This might contribute to the mechanically mixed layer, assisting the strong bond between the leaf material and the railhead [9], and an ability to reduce friction to safety critical levels.

Thin surface layers

This hypothesis regards the leaf solid lubricant theory in which the leaf matter reacts with the metallic substrate and generate a thin organometallic compound layer

(organic compounds reacted with iron oxides/ions) that prevent wheel-rail contact and act as a solid lubricant (see Figure 35), lowering the coefficient of friction.

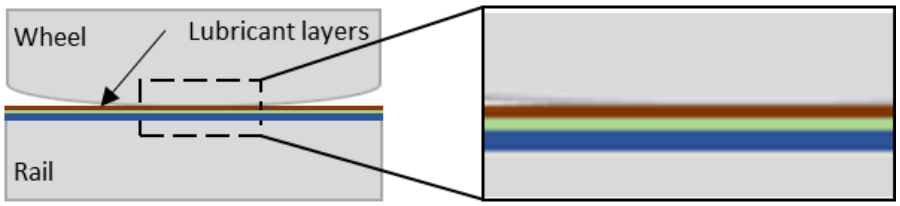

Figure 35: The leaf layer reacts with the rail steel to form a thin organometallic layer that acts as a solid lubricant (image created by author).

It is possible that these layers could comprise of a compressed leaf solid lubricant layer and viscous acid gel layer.

Tribofilm complexes

Surfactants on the railhead and wheel affect the surface tension and therefore the bonding and low adhesion of leaves that have landed on the surface. It is not clear whether certain surfactants (such as oils, alcohols emulsifying agents etc.) will have a positive or negative effect on the bond strength and low adhesion of the leaf layer.

2.8 Paper grading

The purpose of paper grading was to quantitatively analyse the currently available knowledge on topics that are relevant to this project. The outcome was then used to validate and make small adjustments to the scope of the project so that the aims and objectives were reached efficiently.

Almost all of the literature and citations included in this review have been graded in order to visualise the amount of work that has already been carried out and to isolate areas that require more attention. This was achieved by generating a knowledge-map, in which referenced papers are initially divided into five primary categories; Bond strength testing, Mechanisms, Chemistry, Leaf fall mechanics and Friction testing. Each primary category is then split into either two or three secondary categories, see Figure 36. Citations may belong to more than one category, in this case they will be listed multiple times e.g. 1A and 1B, in these cases citations will be graded for each aspect.

The seven criteria to which all references have been analysed by are;

1. Is the source peer reviewed?
2. Does the source contain theory supported by testing?

3. Is the test small scale?
4. Is the test full scale?
5. Does the source contain real world measurements?
6. Are the conclusions in the source evidenced within the data?
7. Are the conclusions validated by operational experience?

All the criteria are objective "yes or no" questions such that a yes answer gives one point, and a no answer gives zero points. The score a citation receives will place it in one of three categories, C (0-2), B (3-4) and A (5-7). This paper grading method originally comes from the literature [9], [10].

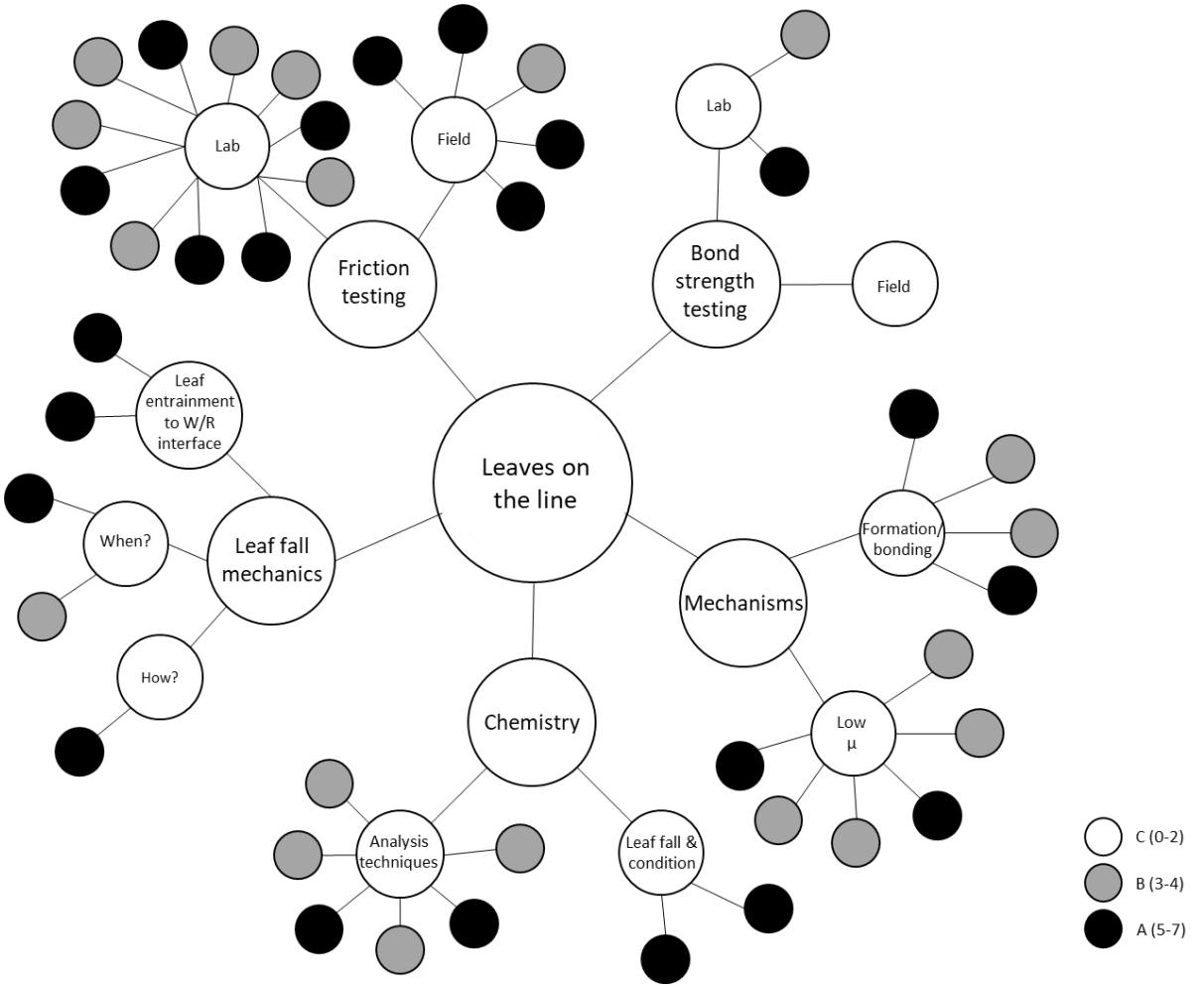

Figure 36: Paper grading map.

The diagram in Figure 36 visually indicates areas that are lacking in "quality" and relevant peer reviewed research literature. The paper grading will have to be reviewed periodically as some sources progress from conference proceedings to journal papers and gain peer reviewed status. This will increase their score by one and could move them up by one classification. A table containing references and their scores is shown in Table 35 in the Appendix.

2.9 Summary

This chapter completes Work Package 1 and parts of Work Package 2 from the project flow chart (Figure 2). The aims of the review were to assess the current literature on the topics of leaf fall mechanics, bond strength testing, friction testing, mechanisms for bonding and low μ and chemistry/chemical analysis of leaf layers, then find gaps in the current understanding in order to steer the research goals of this project.

The objectives were to;

- Read through published papers and associated published documents.
- Organise papers into subject categories.
- Grade papers based on quality.
- Identify gaps in the literature
- Set out research aims for this project.

Gaps in the current understanding

The paper grading found gaps in the following areas;

- Bond strength testing (both lab and field).
- Leaf fall mechanics.
    - How?
    - When?
    - Leaf entrainment to the wheel-rail interface
- Mechanisms.
    - Bonding
    - Low μ
- Chemistry (leaf fall and condition).

One of the research aims of this project was to widen the understanding of leaf induced low adhesion within the wheel-rail interface, specifically how and when leaves arrive on the railhead, how leaves become bonded to the railhead to form the black leaf layer and how they reduce friction to passing trains. This is in line with the outcomes of the paper grading, which highlighted that these areas lacked quality research/publications. These aims address the work outlined in Work Packages 2, 3 and 4 (see Figure 2).

Data gathering

To fully understand the physical effect of leaf induced low adhesion on the UK rail industry, data was first gathered on leaf fall mechanics and leaf layer properties. This was completed by monitoring leaf fall rates and taking friction measurements from the field, covering most of Work Package 2.

Bond strength testing (both lab and field)

In parallel with the paper grading, hypotheses for bonding and low μ were discovered, and are described in more detail along with appropriate testing methods in chapters 6 and 7. The testing and analysis of these hypotheses should fill gaps in mechanisms (bonding and low μ), chemistry (leaf fall and condition) and bond strength testing (lab).

Table 7: Hypotheses testing and/or analysis summary.

	Hypothesis	**Testing and/or analysis**
Formation/bonding	Iron oxide driven	SUROS tests, comparing the friction of leaf and water, and leaf in water with a chelating agent present should indicate whether metallic ions are involved in the bonding process, as well as their effects on low adhesion.
	Metallic substrate effects	Leaf layer formation tests were carried out on rail steel specimens of varying surface roughness (e.g., surface ground, sand blasted) and the bond strength of the resulting layers will be analysed.
Low μ	Bulk leaves on the line	Friction tests are to be carried out using the pendulum skid resistance tester on varying numbers of leaves (e.g., 1, 3, 5 etc.) on a section of rail.
	Compressed leaf solid lubricant layer	Leaf powder/mulch was tested using the HPT rig, alongside Oak Bark Powder (OBP) and graphite powder (an established solid lubricant).
	Viscous acid gel formation	Use the SUROS rig to test leaf friction with the presence of a with buffer to control acidity (pH).
	Supercritical water + high temperature and pressure	HPT testing of leaves/potentially water as the pressure is high enough for this [9], [150], [151].
	Thin surface layers	XPS analysis of leaf layer samples collected from the field should indicate whether thin layers are present.

In summary, a breakdown of the hypotheses and testing/analysis methods are shown above in Table 7, covering the majority of Work Package 3.

Leaf fall mechanics

Due to the wheel-rail interface being part of an open system, a wide range of contaminants can make their way onto the railhead and get run over by train wheels.

Different contaminants have different effects on traction between the wheel and rail, leaves for example are a major cause of low adhesion in the autumn season. The journey of these leaves to the railhead needs to be investigated to address gaps in leaf fall mechanics (how, and leaf entrainment to the wheel-rail interface), this will cover Work Package 4.

Mechanisms (bonding and low μ)

The literature review found gaps in the understanding of the mechanisms of bonding and low μ, while hypotheses were identified they were not fully understood and had not all been tested. This research addresses this by planning specific mechanical and/or chemical analysis for each hypothesis to assess their validity. When possible, hypotheses were quantified, however, this was not always possible.

Chemistry

There is a lacking in the understanding of the chemical differences between leaf layers of different species. To address this, leaf layers were generated at full scale test track testing facilities and swabs were taken for chemical analysis (XPS and/or FT-IR). These artificially generated layers were then compared to naturally occurring layers taken from known low adhesion hotspots.

Low adhesion risk assessment model

Another outcome of the literature review was the lack of a freely available, open source model for assessing the risk of low adhesion occurring due to leaf layer presence on the railhead. Therefore, a model was developed using historical data on low adhesion incidents provided by industry, as well as drawing on the outcomes of the data gathering and hypotheses testing stages. The model development covers the majority of Work Package 5.

3. APPROACH TO PROJECT

3.1 Introduction

To ensure the success of this project, it was important to carefully plan out the approach for each of the 6 work packages. These work packages followed a clear path from start to completion with different deliverables that had to be achieved. This chapter maps out these work packages and deliverables, explaining how and why they were chosen as well as why certain parameters have been investigated and not others.

Figure 2 shows the project plan flow chart. It divides the project into 5 work packages, each with several deliverables within them.

3.2 Work packages

WP1 - Literature review

A comprehensive literature review is key for any research project as it establishes the current understanding of the topic as well as contextualising the work. The conclusion of the literature review should highlight any areas that are lacking in quality research. These gaps are then used to steer the project to ensure that the work done is novel and contributes to the current knowledge base.

One of the most important outcomes of the literature review was the formation of hypotheses for the bonding mechanisms between the railhead and the black leaf layer and the low friction mechanisms between the black leaf layer and passing wheels. Once the hypotheses were identified, the project moved to the data gathering and test planning stage.

WP2 - Data gathering

A plan was made to collect data on railhead friction, leaf layer generation characteristics, longer scale weather behaviour, leaf fall times and associated weather conditions. Unfortunately, it was not possible to collect all data sets regularly and safely on one particular line, therefore, periodic visits to locations on Sheffield' s Supertram network, various heritage railway lines and the Quinton Rail Technology Centre (QRTC) test track at Long Marston were chosen instead. In addition, a weather sensor was attached to a section of dummy rail and left in one location to collect humidity and temperature data over a much longer period with a finer resolution.

The Sheffield Supertram visits allowed leaf fall and weather tracking at locations known for low adhesion. Heritage railway visits allowed friction and weather data to be collected, however, due to the logistical issues it was not possible to collect data as regularly as on the Supertram network, so leaf fall tracking was not possible. Additionally, due to the low train operating frequency of the heritage lines, vegetation coverage, speed limits and railhead conditions were found to be not entirely representative of those found on mainlines.

Visits to Long Marston allowed for field testing, with much higher control over test conditions, meaning that leaf layers could be generated on "clean" railheads, with trains passing at representative speeds while all necessary friction and weather data was recorded.

WP3 - Leaf layer tribology

A thorough test plan was needed to investigate the hypotheses (shown in Table 6) found in the literature review. It was important to have the project deliverables defined by this point as it would have been easy for the scope of the work to expand as more parameters were discovered. The hypotheses gave a clear outline, to which a plan for mechanical testing and chemical analysis was incorporated into a matrix.

WP4 - Leaf to railhead

In order to bridge the gap between the environmental and weather data and the leaf layer low μ and bonding data, it was crucial to investigate the leaf fall characteristics of different leaf species. A test plan was made to assess the horizontal distances covered by leaves dropped from the same height, with and without artificial wind present. Leaf removal wind speeds were also tested for wet and dry leaves on ballast. The outcomes of this work feed into the development of the adhesion model.

WP5 - Adhesion index development

Due to the lack of freely available information on how leaf layer formation/ leaf induced low adhesion risk is calculated, a model was required for assessing particular rail locations. The model must be static (opposed to dynamic, meaning it provides a risk rating for a specific location as opposed to a stretch of line or over a time period), open source and simple enough to be utilised by someone with minimal training.

Following a dissemination presentation to the ARG group in May of 2020, an opportunity for collaboration with industry arose with Chiltern Railways. Through this partnership, KPI data was provided on WSP activation on Chiltern Railways services between January 2018 to October 2020. This formed the basis of a case study to identify locations with a history of low adhesion incidents. These locations were then investigated in order to identify possible characteristics that may contribute to a higher risk of leaf induced low adhesion occurring.

The findings from the Chiltern Railway case study formed the basis of the development for a model for predicting low adhesion hotspots where leaves are believed to be a key factor.

4. AUTUMN DATA COLLECTION

4.1 Introduction

This chapter concerns Work Package 2 – 'Data gathering' , from the project specification (shown in Figure 2). To achieve this, the timing and rate of leaf fall in the autumn/winter seasons, associated weather conditions and rail friction levels were investigated. Ideally, railhead friction data would have been collected in parallel with the other data, however, this was not always possible due to logistical and safety issues. Therefore, the autumn data gathering set was split into three different groups, those being the Sheffield Supertram multiple location set, the single location weather set, and the heritage, test track and live rail locations, for example Ecclesbourne Valley Railway (EVR) in Derbyshire.

The Sheffield Supertram data collection plan was designed for:

- Tracking of leaf fall progression throughout the season.
- Tracking of weather trends throughout the season.
- Comparing the leaf fall and weather data to identify any potential correlations.

The single location data plan was designed for:

- Tracking of weather trends throughout the season more consistently and with a higher time resolution (15 minute increments).
- Comparing the data collected to that from other data sets.

The friction and weather data measurement/analysis was designed to:

- Measure railhead friction alongside weather and contamination layer thickness data at heritage, test track and other live rail locations.
- Compare this data to that from the other data sets.

Information gathered from the three data sets outlined above was compiled and used to;

- Aid the design of efficient and appropriate laboratory tests.
- Expand the understanding of when and why leaves fall, and the role weather plays.
- Design a more comprehensive adhesion index risk level calculator regarding leaves on the line.

4.2 Sheffield Supertram data

Sheffield appeared to be an ideal location for leaf related rail research due to the high number of trees present throughout the city and the city wide tram network.

The data was gathered along Sheffield Supertram routes at both "problem hotspots" and other areas. The problem hotspots were investigated to assess the extent of the low adhesion due to leaf contamination, while the other less problematic areas should give good contrasting data. The location, track layout and local tree populations was recorded, as well as any other obvious forms of contamination.

The 2018 and 2019 Sheffield Supertram data collection ran between the 5th of September and the 20th of December with 18 data collection dates in 2018 and 27 data collection dates in 2019. All data was collected safely and rapidly between approximately 7:00 am and 10:30 am. The reason the data was collected in the morning was to give a better representation of the state of the network going into each new day, ideally before the effects of road and rail traffic could influence the number of leaves on trees or their position on the ground (via airflow generated by passing cars and trams) too much.

The data collection plan involved; leaf fall observations, as well as recording ambient weather conditions (humidity, temperature and pressure). However, it was not possible to record railhead friction due to the high traffic nature of the tram network (including road vehicles).

Key issue investigated

How do ambient weather conditions and railhead temperature change throughout autumn and do either correlate with leaf fall rates?

What data was recorded?

Initial location information required from each location included:

- Where it was located and what are the nearest stops?
- Is the track embedded into the road or raised/separated from road traffic?
- Is there direct coverage by trees?
- What type of trees are nearby?
- Any other means of contamination?
- Is the track on an incline/decline, if so, how steep is it?
- Was there visible leaf contamination on the track?
- Can pendulum tribometer tests be conducted at this spot?
- Could a weather box be left here safely?

After consideration it was decided that it was not possible to leave a weather box alone at any location near the tram network as it could be easily stolen/vandalised. It was also not possible to conduct any pendulum tests due to safety and logistical concerns.

Therefore, it was decided that the Supertram network should be used to collect autumn wide data, that is, data recorded periodically throughout the season. These included images of trees showing the number of leaves that were still present as well as approximations of how many had fallen onto the floor and surrounding area, ambient temperature, pressure and humidity as well as railhead temperature, but no friction data.

How was the data recorded?

Weather data was recorded using the weather box developed at the University of Sheffield, which measures ambient humidity, pressure, temperature and moisture. The railhead surface temperature was measured using a non-contact Infra-Red (IR) thermometer, with three readings taken 5 seconds apart on the running band, these were then averaged. The data was taken from the weather box via a mobile messenger app, sending the data to a PC, where they can then be transferred into a spreadsheet for further analysis.

Photographs of the trees, leaf canopies and track were taken using a mobile phone. Table 8 summarises the data collection methods.

Table 8: Supertram autumn measurement plan

Variable	Means of Measurement
Leaf fall state	Specific trees images
Railhead state	Railhead images
Environmental conditions -temperature, humidity, dew point -weather conditions	Weather box - temperature, humidity, pressure
Railhead temperature	Non-contact Infra-Red (IR) thermometer

When and where was the data recorded?

Data recordings took place at each of the twelve Sheffield Supertram "problem hotspot" locations described below throughout the autumn of 2018 and 2019, from early September through mid-December. Information regarding whether the track is embedded, and local tree species remained the same, but the condition of the leaf coverage, visible contamination present and weather conditions changed. Data was collected two to three times per week on varying, but never concurrent days or weekends. Concurrent data collection dates were avoided in order to give a better spread of data, allowing at least one non data collection day in between.

Locations were selected because they all had 10 or more low adhesion reports from tram drivers in 2017. The track on approach or departure from these stops, where either braking or traction is required, and low adhesion can occur are of particular interest. Additionally, these locations represented a mixture of embedded and raised track with varying degrees of inclination.

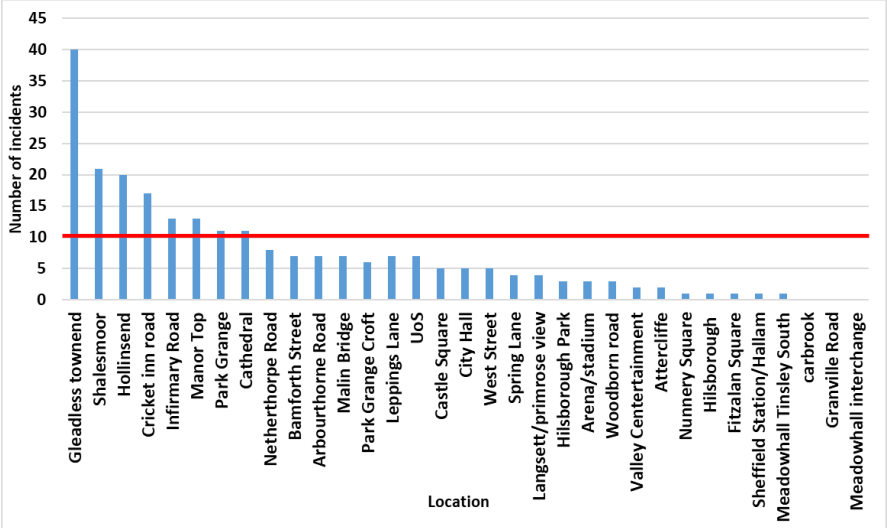

Figure 37: Number of low adhesion incidents reported at each stop by Supertram in 2017.

Figure 37 shows the number of driver-reported low adhesion incidents recorded at each stop throughout 2017. This information was used to select the low adhesion hotspots that will be investigated for this project, as those with more than ten incidents were selected. The cut off value of 10 incidents (shown by the horizontal red line) was chosen as it provided a manageable number of locations to investigate.

Despite mid-November being typically known as the time of year most associated with low adhesion incidents, the whole autumn season was measured in order to gain a larger understanding of other potential trends in weather or leaf fall.

Although it would have been ideal to correlate low adhesion incident data to leaf fall observations, unfortunately Supertram stopped collecting wheel slip incident data in 2017 so newer information was unavailable.

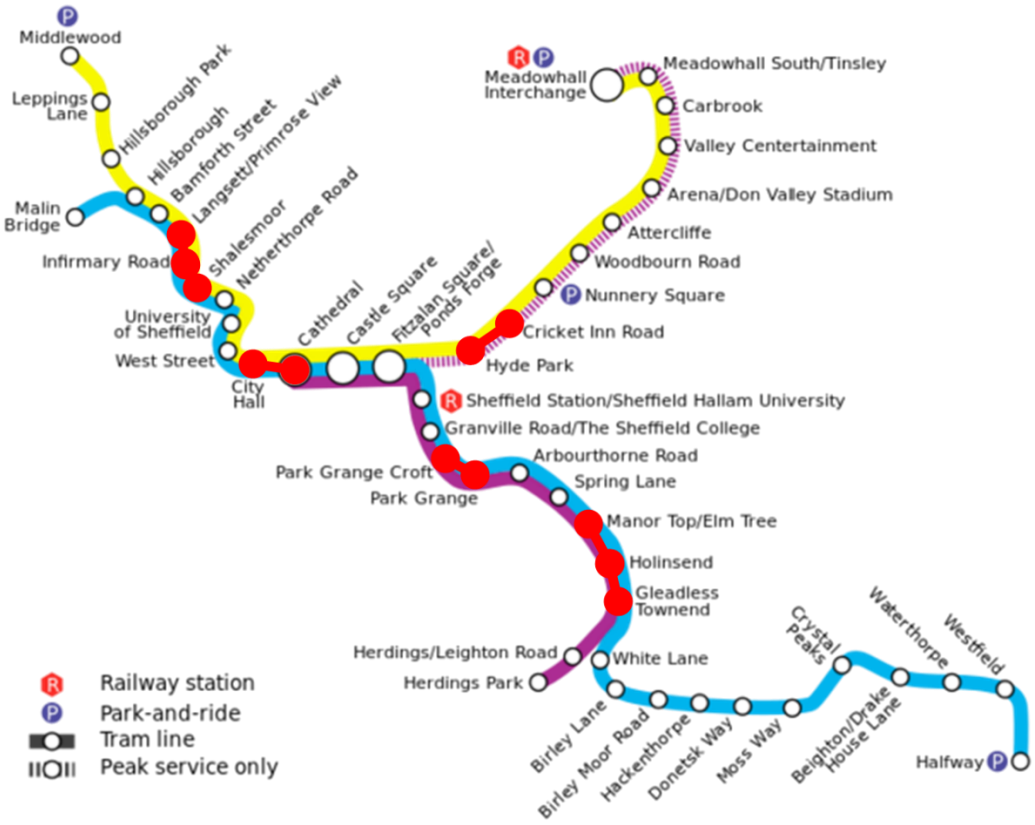

Figure 38: Locations of the twelve hotspots across the Supertram network shown by red dots [152]**.**

The chosen locations highlighted by red dots in Figure 38 were:

- Hollinsend - Gleadless Townend
- Gleadless Townend - Manor Top
- Park Grange - Park Grange Croft
- Cathedral - City Hall
- Shalesmoor - Infirmary Road
- Infirmary Road - Langsett/Primrose View
- Cricket Inn - Hyde Park

How was the data used?

After a large dataset was compiled, any trends were identified and compared against railhead friction levels recorded in other datasets. This data was then used to predict when trees might "dump" (substantial amounts of abscission in a short time period) their leaves in the future, and whether it would occur in a short space of time or more spread out throughout the season. Following this, railhead friction regarding leaves on the line could be predicted and mitigated.

Strengths and weaknesses

The strengths of this method include; data was collected over two autumn seasons (2018 and 2019), covered a wide range of collection dates (every 2-3 days), included ambient temperature, ambient humidity, railhead temperature and leaf retention/fall state.

Disadvantages include; no friction values could be measured alongside other measurements, also no railhead contamination swabs could be taken (due to safety and logistics).

4.3 Single location data

Autumn Supertram data was collected twice a week, however it was not clear how representative the weather data was. Therefore, it was necessary to record and map the environmental data with a higher time resolution and over a longer overall timespan. This gave a more complete, larger scale picture of daily, weekly or monthly trends in weather conditions.

Key issue investigated

How do ambient weather conditions and railhead temperature change throughout autumn for one location? Are there any shared patterns or correlations with the multiple location data?

What data was recorded?

Ambient temperature, pressure and humidity as well as railhead temperature and railhead moisture level, at frequent intervals (every 15 minutes).

How was the data recorded?

The ambient temperature, pressure and humidity as well as railhead temperature and moisture was recorded using a weather sensor (Wintersense) developed by the University of Birmingham. The data was stored and displayed on the Wintersense network website.

When and where was the data recorded?

A weather sensor (see Figure 39 below) developed by The University of Birmingham and designed to be attached to an unused section of rail near the live track was used to collect data over a longer time span. The sensor was placed outside the home of the researcher due to logistical reasons and partially as a result of the COVID-19 pandemic. Every 15 minutes the sensor recorded parameters (railhead temperature, air

temperature, railhead moisture) and uploaded them to an online network operating until the battery ran flat in March of 2020.

Figure 39: Section of rail with the Wintersense weather sensor attached

The sensor was attached to a section of dummy rail, approximately 30cm in length. The sensor was designed to either be left at one location for a long period of time or be placed in a specific location for a shorter amount of time i.e. a week.

Strengths and weaknesses

The strengths of this method include; a high granularity and consistency (every 15 minutes) when compared to other measurements, the automated data collection and uploading ensured data was logged securely.

Disadvantages include; the location for the measurements was not directly near any railway line (due to logistical concerns), the railhead surface moisture sensor did not yield any usable results so railhead wetness could not be commented on, and data was only collected in 2019.

4.4 Friction and weather data

Data collected and described above does not represent a complete dataset (e.g., photos of railhead accompanied by data quantifying friction and weather conditions), so a more complete dataset was designed. Data collection was permitted at Ecclesbourne Valley Railway (EVR), Peak rail, QRTC at Long Marston and Monk Bretton (a rarely used freight line running between Sheffield and a glass factory that is a known low adhesion hotspot by Northern). These lines offered test opportunities with no charge for access, infrequent traffic and many were conveniently near the Sheffield area.

Key issue investigated

What ambient weather conditions and friction levels can be found on sections of heritage railway? And how do these conditions and friction levels change over distances?

What data was recorded?

The data recorded for this dataset includes;

- Railhead condition images (oxide layer, leaf layer, visually clean etc.)
- Friction level at each location using the Pendulum skid resistance tester
- Railhead temperature values
- Thickness of any railhead surface layers, assessed using an eddy current probe
- Ambient weather conditions (% humidity, temperature)

How was the data recorded?

The pendulum skid resistance tester was used for the friction level tests, a total of eight readings were taken at each location. Images of the railhead were recorded using a 'GoPro' camera mounted on the pendulum rig to ensure consistent images in the dataset. Ambient temperature, pressure and humidity were recorded using the weather box made by the University of Sheffield, the railhead temperature and dewpoint were recorded using an infrared pyrometer measuring device. The thickness of any surface layer was measured using an eddy current probe. Swabs were taken at each location directly adjacent to the location of the friction tests to calculate the railhead moisture level. These are all detailed below in Table 9.

Table 9: Variables and means of measurement used on heritage railways

Variable	**Means of Measurement**
Terrain (trees, industrial etc.)	Written description + images
Railhead state	Railhead photos
Railhead coefficient of friction	Pendulum skid resistance rig, 8 recordings per location
Environmental conditions: Air and railhead temperature, humidity and dew point	Non-contact temperature probe (infrared pyrometer)
Low adhesion layer thickness	Eddy current thickness gauge

When and where was the data recorded?

Multiple sections of line from the locations described above were available for data collection from 14/08/19 through to 12/02/20. Access points for EVR and Peak Rail are shown in Figure 40 below. Typically, one measurement can be made in the station followed by others further along the line, spaced approximately 20m apart. EVR operate services along 8 miles of track between Wirksworth and Duffield in Derbyshire, with access for measurements at Wirksworth station, Idridgehay station, and Shottle station.

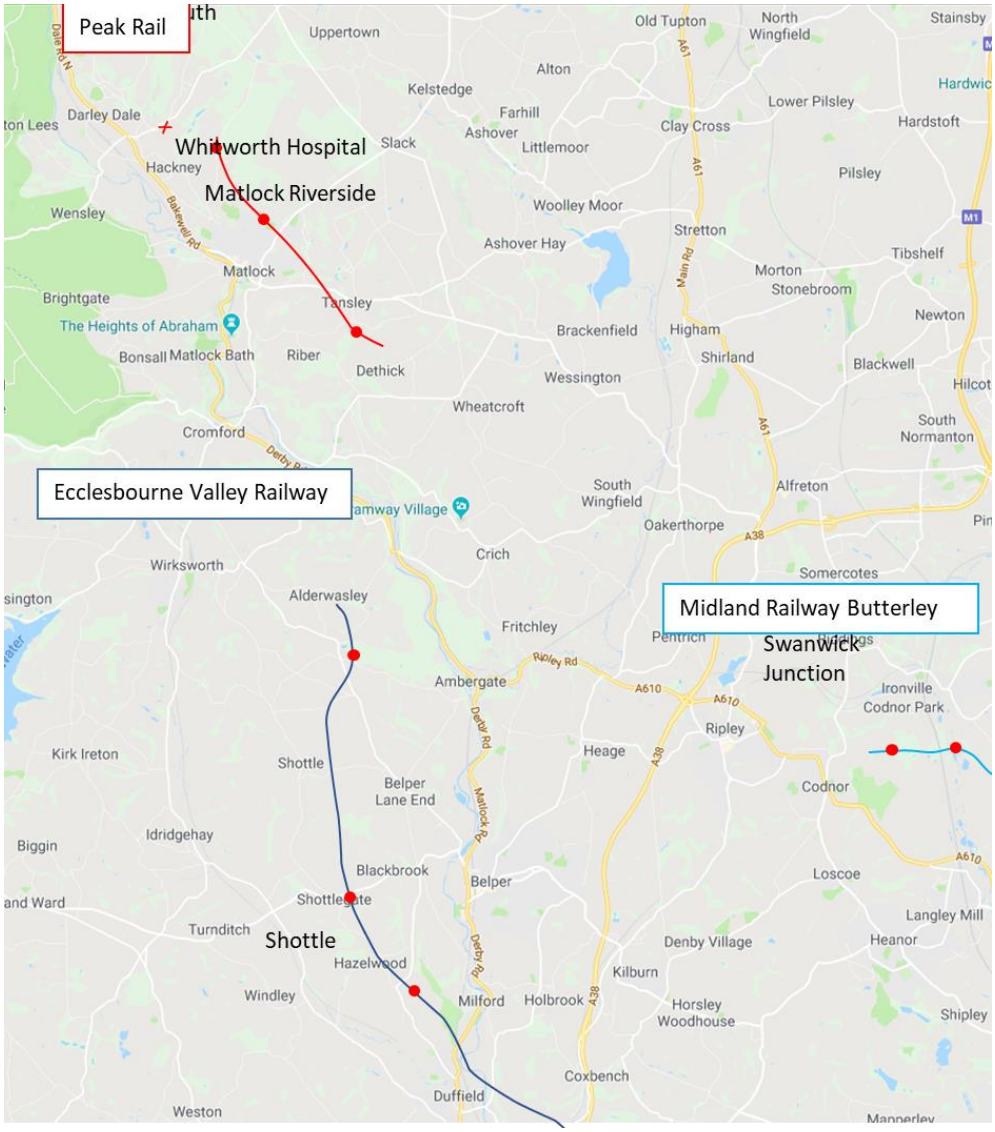

Figure 40: Heritage lines with stations and access points marked as red circles [153]**.**

Datasets were collected on each of the 22 visit days, the access points are shown as red circles in Figure 40. Data collection usually ran from just before 12 am to around 3 pm. The data collection dates are shown below in Table 10.

Table 10: Heritage line testing dates.

Testing dates		
14/08/2019	08/10/2019	28/11/2019
22/08/2019	16/10/2019	30/11/2019
28/08/2019	22/10/2019	11/12/2019
05/09/2019	13/11/2019	12/12/2019
12/09/2019	14/11/2019	14/12/2019
13/09/2019	21/11/2019	12/02/2020
01/10/2019	26/11/2019	
02/10/2019	27/11/2019	

How was the data used?

Friction and weather data, as well as the experience of data gathering was used in the development stage of the risk assessment model.

Strengths and weaknesses

The strength of this method includes the fact that friction data was collected alongside railhead swabs and environmental data (ambient temperature, pressure, humidity etc.).

Disadvantages include; due to the lines being on heritage railways, the contamination conditions and railhead wear state are not entirely representative of a "real" live line (leading to potentially different railhead friction and contamination) due to lower speed limits, frequency of use and loads on the railhead, due to logistical factors the frequency of data collection dates was not as high as with other tests.

4.5 Results

Sheffield Supertram leaf fall observations

Figure 41 shows leaf fall tracking images for location 2 (Langsett/Primrose View) through 2018, where the start and end of the majority of leaf fall is represented by the images and dates in red boxes.

Figure 41: Location 2 showing images from 2018 with a sycamore tree (left), with outlined silhouette of tree in question (right)

Figure 42 shows the Sheffield Supertram location leaf fall spans as horizontal lines, the lower line for each location represents 2018 values while the upper represents 2019 values. The locations numbers are shown on the vertical axis, while dates are shown on the horizontal axis with the years removed as the graph contains data from two years.

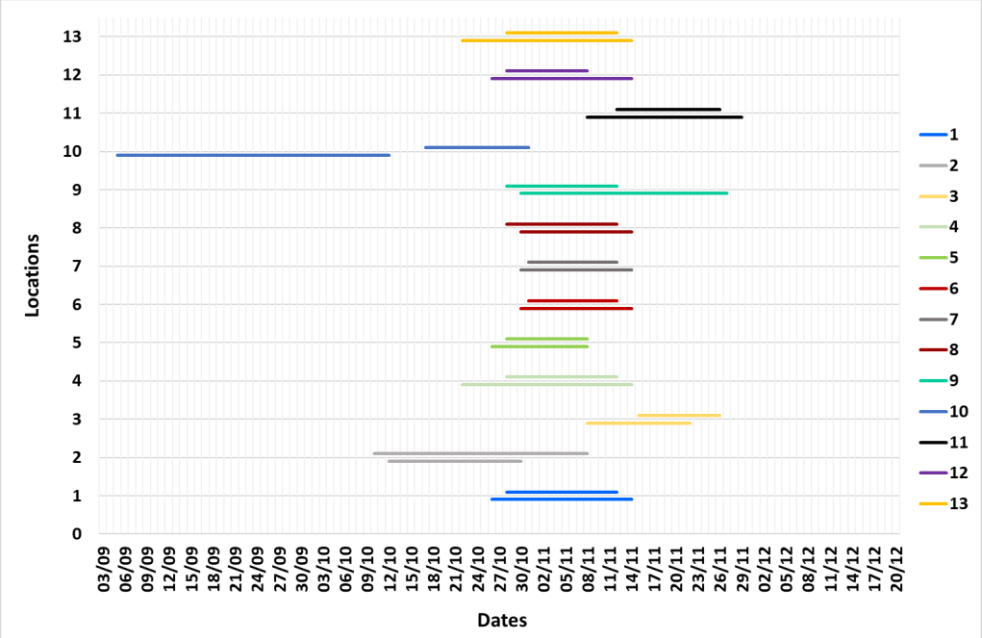

Figure 42: Drop spans for Supertram locations in 2018 and 2019.

For all locations (except location 10) the leaf fall spans overlapped each other for 2018 and 2019, and in most cases started and ended within 3-5 days of each other. Another trend identified is that locations 1, 4, 5, 6, 7, 8, 12 and 13 all fell within the same 19 day window, with the locations 2, 3, 9, 10 and 11 partially dropping within this window.

It is possible that the early leaf drop for location 10 (sycamore) in 2019 was due to the fact that the tree in at one of the highest points that were measured on the Supertram network and that it is next to a dual carriageway road with a 40mph speed limit. Other than the reasons stated, no other causes were apparent.

Due to changes in light conditions at the time of the measurements (caused by the reduction in daylight hours throughout the season) the images recorded were not sufficient that meaningful leaf drop percentages could be calculated/assessed. Therefore, it was not possible to say whether the leaf drop was linear, though, notable events (such as storms with high winds) may have caused leaves to be 'dumped' in larger amounts. This was not noted though.

Table 11: Table of locations, species and drop spans for 2018 and 2019 in days

Location	Species	2018 drop span	2019 drop span
1	Sycamore	19	15
2	Sycamore	18	29
3	Sycamore	14	20
4	Sycamore	23	15
5	Copper Beech	13	11

6	Sweet Chestnut	15	13
7	Sycamore	15	13
8	Sycamore	15	15
9	Sycamore	28	15
10	Sycamore	37	14
11	Common Lime	21	14
12	Silver Birch	19	11
13	Sycamore	23	15
Avg.	Sycamore	20	15.4
St. Dev.	-	6.4	4.5

Table 11 shows the tree species and drop span (days) for 2018 and 2019 for each location. Nine locations contained sycamore trees, with one location showing copper beech, sweet chestnut, common lime and silver birch each.

Single location data

Despite the sensor being fitted with a surface moisture sensor fitted to the railhead, the data recorded was found to be unusable (possibly due to a malfunction with the sensor), leaving the surface and air temperatures.

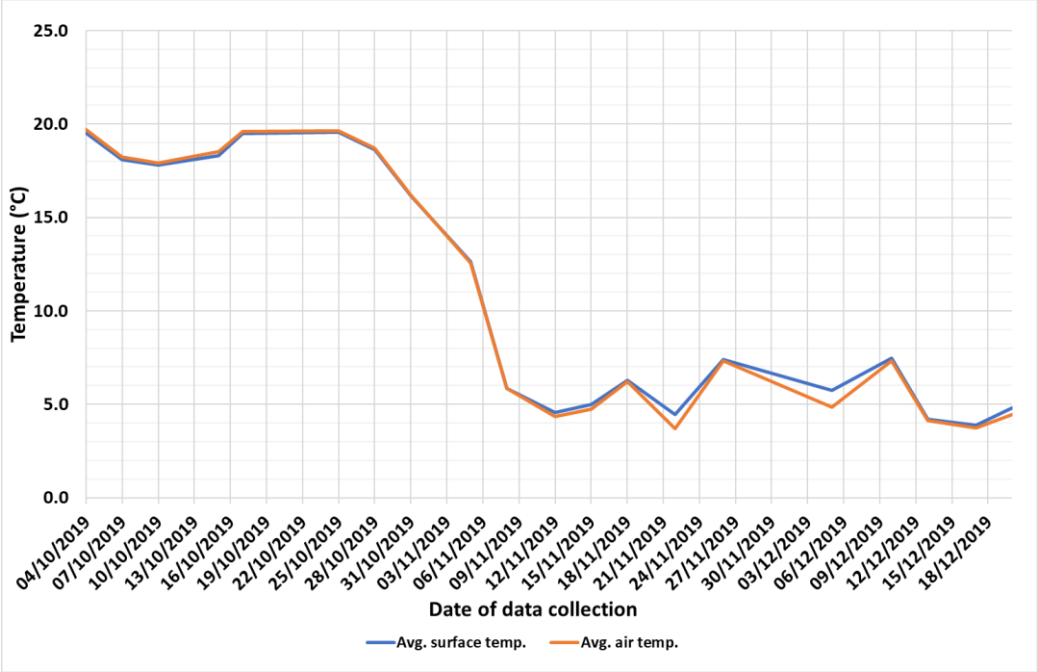

Figure 43: Daily average air and surface temperatures

As shown in Figure 43, the 'Wintersense' data recorder consists of a railhead surface and ambient air temperature, both of which follow each other very closely. Data was recorded at 15 minute intervals. The daily averages are shown in the graph above. The

start date was the 1st of October 2019, when the device was received, the final data record date was the 22nd of January 2020. However, the data in Figure 43 has been cropped to align with other datasets.

One significant trend in the data can be observed, that is the drop from just below 20 °C at around the 25th of October 2019 to between 3°C and 8°C by around the 12th of November 2019, see Figures 43 and 45. This average drop of around 14°C occurs within an 18 day window.

Friction and weather data

Averages for all parameters were calculated in order to identify any trends and compare against other datasets, these are shown below in Table 12. The dates for data collection occurred an average of 9 days apart and was due to logistical reasons.

Table 12: Daily averages for parameters at the heritage railway locations including ambient weather, layer thickness and friction levels (both pendulum and British Rail Research converted values).

Date	Temp. (°C)		Humidity (%)	Layer Thickness (µm)		CoF		
	Air	Railhead		Avg.	St. dev.	Pendulum	BRR	St. dev.
14/08/19	15.3	17.4	97	2.60	3.0	26	0.13	0.03
22/08/19	12.8	11.3	74	5.20	4.1	57	0.29	0.00
28/08/19	18.1	19.6	86	1.16	2.3	38	0.19	0.08
05/09/19	21.4	21.1	46	0.30	0.7	55	0.28	0.02
12/09/19	13.4	12.6	80	0.00	0.0	60	0.31	0.00
13/09/19	12.8	11.3	74	0.00	0.0	57	0.29	0.01
01/10/19	14.8	14.1	85	0.10	0.4	31	0.16	0.03
02/10/19	14.9	11.8	51	0.00	4.1	56	0.28	0.06
08/10/19	17.5	12.6	60	0.25	0.7	62	0.32	0.04
16/10/19	16.2	13.7	61	6.63	5.9	59	0.30	0.02
22/10/19	13.5	10.4	64	0.95	1.6	47	0.24	0.07
13/11/19	11.1	1.0	58	4.50	4.5	35	0.18	0.00
14/11/19	6.4	6.4	80	1.24	1.4	37	0.19	0.01
21/11/19	7.0	3.9	71	3.05	4.7	54	0.27	0.08
26/11/19	14.5	9.2	72	13.40	2.6	31	0.16	0.01
27/11/19	11.9	12.1	83	2.79	3.5	36	0.18	0.05
28/11/19	9.2	9.0	89	19.20	27.3	29	0.15	0.03
30/11/19	2.6	-0.8	85	33.19	35.1	24	0.12	0.03
11/12/19	8.6	-0.5	63	22.80	0.2	31	0.16	0.02
12/12/19	4.9	2.0	84	12.89	8.0	33	0.17	0.02
14/12/19	5.0	1.3	77	0.76	1.6	34	0.17	0.02
12/02/20	12.0	4.4	52	11.76	9.6	26	0.13	0.01

The weather for conditions observed ranged from dry and relatively sunny, to cloudy and dry, to light and heavy rain, even small amounts of snow and ice. Each dataset included a description of the conditions and when split into "wet" and "dry" categories. The average BRR dry friction value was 0.29, whereas the average wet was 0.16.

Notable low friction occurred on 14/08/19, 30/11/19 and 12/02/20 and there do not appear to be any obvious links with air or railhead temperature, air humidity or layer thickness. It is likely that any leaf layers present on the railhead are responsible for the variation in friction measured and are responsible for the low measurements.

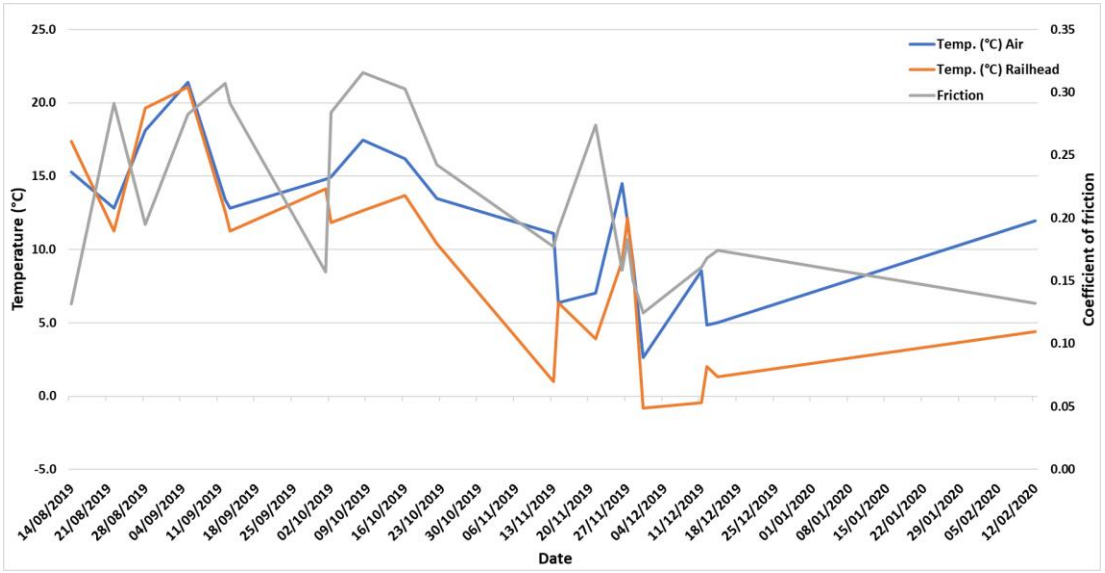

Figure 44: Daily average air and railhead temperature with BRR coefficient of friction.

Figure 44 shows the average daily railhead and air temperatures (left axis) along with BRR friction values (right axis) from the data shown in Table 12.

Comparison of data

Figure 45 shows a graph of average temperatures against data collection dates for the single location and Sheffield Supertram network data.

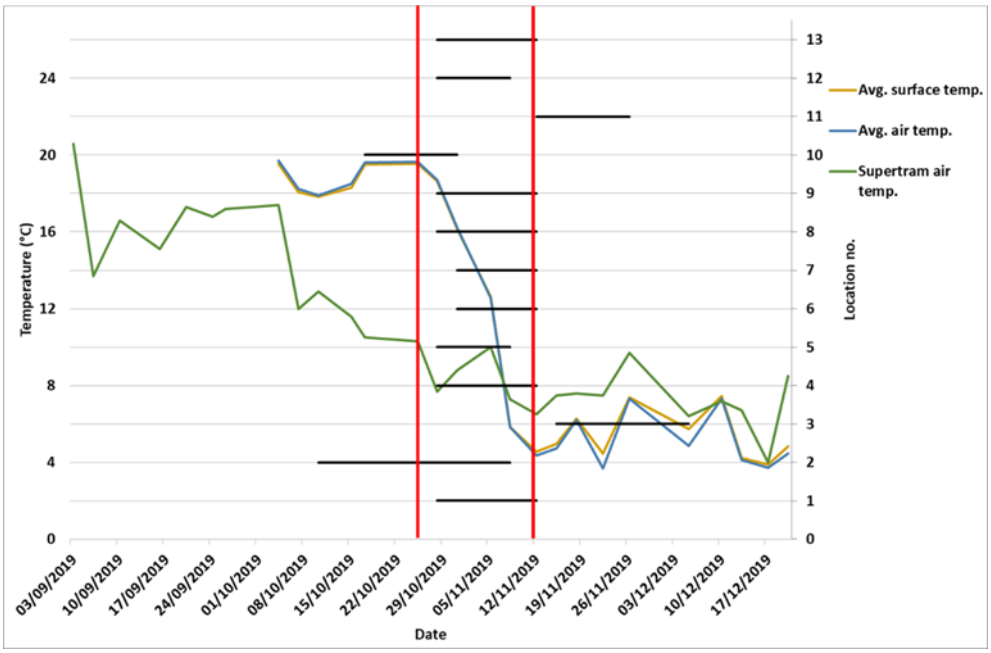

Figure 45: Temperature (°C) against date with 2019 Supertram location drop spans.

The vertical red lines indicate the start and finish of the "significant temperature drop window" (from just below 20° C to between 3° C and 8° C) recorded by the single location data recorder, at 25/10/2019 and 12/11/2019 respectively. The horizontal lines show the start and end of the leaf fall for specific trees at certain locations, where approximately 95% and 5% of leaves are shown on the trees respectively.

Table 13: Average parameter values for before 25/10/2019 and after 12/11/2019.

	Temp. (°C)		Humidity (%)	Layer thickness		Friction	
	Air	Railhead		Thickness (µm)	St. dev.	Pendulum	BRR
Before 25/10/19	15.5	14.2	70.7	1.6	2.1	49.8	0.25
After 12/11/19	8.5	4.4	74.1	11.4	9.0	33.7	0.17
% Change	-45	-69	4.8	613	-	-32	-32

Table 13 shows average parameter values measured on the infrequently used heritage lines before the left vertical red line and after the right red vertical line in Figure 45, described as the "significant temperature drop window". After this period the average air and railhead temperatures drop by 7°C (45%) and 9.8°C (69%) respectively,

while the humidity increases by 3.4%. The contamination layer thickness increases by over 600% from 1.6 µm to 11.4 µm, with a visibly thicker layer being observed. Friction levels drop by approximately 32%, from 0.25 to 0.17.

4.6 Discussion

Analysis of the leaf fall study provided useful information regarding timing, this is especially interesting when compared to the air and railhead surface temperature data. A correlation can be observed in Figure 45, between the significant temperature drop from the single location data and the majority of the leaf drop spans from the Sheffield Supertram leaf fall tracking. Both of these occur within the same 19 day span. The data collected suggests that leaf fall is initiated by the drop in temperature, which agrees with the current scientific understanding [154]. It is also noteworthy that the drop spans from 2018 and 2019 are very similar, indicating year-on-year consistency regarding the calendar dates at which leaves fall. It is also probable that wind played a large role in leaf abscission, though wind speeds were not measured in this work.

Sycamore was by far the most common species seen near the Supertram network, out of the thirteen trees monitored, nine of them were sycamore, with one copper beech, sweet chestnut, silver birch and common lime each. Sycamore had the highest average drop span, at 19 days, followed by common lime with 18, silver birch with 15, sweet chestnut with 14 and copper beech with 12. In 2019, the copper beech, sweet chestnut, silver birch and six of the sycamore dropped their leaves within the significant temperature drop window. This left the common lime, and three sycamore with drop spans straying out (both before and after) of the significant temperature drop window.

Initial analysis of the environmental data shows inconsistencies between the measurements of the different stops on the same days, more so than would be expected under normal circumstances. No trends in the environmental data leading up to and during the 19 day period were observed. Initial improvements for data collection in autumn 2019 could have included; more measurement locations, image tracking starting earlier in the year and finishing early the following year, including more of the ground under the trees to show if leaves remained near the parent tree or were being moved and/or spread. It could also be worth more accurately finding any quantifying other contaminants such as that generated from road traffic (oil, pollution etc).

When looking at Figure 44, trends in friction values appear to loosely follow trends in the temperature (both air and railhead) data, in that they all follow a downward trajectory moving through autumn and winter. At times there does appear to be a

delay where the friction follows a very similar pattern to the temperature(s) but a week or so later, as shown on the left side of Figure 44. On the right side of the graph, the temperatures start to rise as spring is approaching, meanwhile the friction continues to fall, this could be due to changing levels of surface moisture. Data trends from Table 13 support the noted drop in temperature shown in Figure 43 and Figure 45.

Suggestions for leaf corridor design

When considering suggestions for leaf corridor design, the findings from the autumn data collection would suggest that any work on vegetation management should be more effective if conducted before the significant leaf fall occurs in mid-October. A sudden drop in ambient temperature should be considered as a marker indicating imminent leaf fall, from this point on leaves should be expected on or near vegetated sections of the railway.

Limitations

Images of leaf fall from the Supertram network did not consistently include enough of the ground around the base of the trees and the surrounding area, as a result it was not possible to assess whether leaves remained in the area or were dispersed.

Measurement times for the Supertram weather data were varied throughout the mid to late morning due to the time taken to travel between locations, though this was somewhat limited due to the fact that all temperature measurements each day were averaged.

The single location ambient weather data relied on a sensor fitted to a small section of rail (approximately 25cm in length) and would not represent as much of a heat sink as a full length section of rail. However, the dummy section should still reach the same ultimate temperatures as a full length section of track, albeit possibly more quickly. Attaching a sensor to a section of live or heritage rail was not possible though due to safety reasons.

Weather data from only two years was analysed, with four named storms (Ali, Bronagh, Callum and Deirdre) occurring during the autumn period of 2018 and only one (Atiyah) in the autumn period of 2019. This is compared to 4 in autumn of 2020, and 2 in autumn of 2021. It was not possible to quantify the effect of these storms as the majority occurred within the 5% to 95% leaf fall window, where specific differences in leaf fall percentage were very difficult to assess and attribute. When comparing the dates of the storms, no notable differences were observed. In the future, daily leaf measurements could make it possible to notice smaller differences in the remaining

leaf coverage. Due to the effects of climate change it is possible that notable storms in the UK will increase in both frequency and severity, meaning that more attention may be needed when assessing the risk of leaf fall and leaf layer formation. Additionally, dramatic changes in temperature must be watched out for, as they are known to coincide with leaf dumping.

Access to a local weather station data that would have provided more information than what was collected by the researcher was unfortunately not found to be available.

4.7 Conclusions

- In 2018, 95% of leaves dropped between 05/09/2018 and 29/11/2018 (85 days), with the majority falling between 26/10/2018 and 14/11/2018 (19 days).
- In 2019, 95% of leaves dropped between 10/10/2019 and 26/11/2019 (47 days), with the majority falling between 28/10/2019 and 12/11/2019 (15 days).
- Temperature was observed to be a driving factor for leaf fall as the significant temperature drop preceded the significant leaf fall by 3 days, which agrees with the literature [154].
- Between the leaf fall dates, the leaf layer on heritage lines was observed to have grown by over 600%.
- The majority of sycamore as well as copper beech, sweet chestnut, silver birch dropped their leaves within the significant temperature drop, while 33% of the sycamore and common lime dropped their leaves at least partially out of the window.

5. LEAF FALL STUDY

5.1 Introduction

A study of leaf fall behaviour and dynamics is described in this chapter. In this work the term 'dynamics' is used to describe the classes of leaf fall motion (chaotic, periodic, steady tumbling), as described in section 2.4.4. The term 'characteristics' is used in this work to encompass both dynamics and horizontal distance covered by the leaves as they fall. This forms the majority of Work Package 4 - Leaf to Railhead.

5.2 Aims, objectives and outcomes

The aims of this work are to:

- Investigate leaf drop characteristics for different tree species.
- Investigate the sizes and masses of different leaves.
- Propose suggestions for leaf corridor[4] design (section 10.3.1).
- Investigate the relocation behaviour of leaves on ballast under different wind speeds.

The methods by which leaves fall from the branch to the ground appears to differ between tree species, as they fall and land in a seemingly unpredictable and random manner. Certain leaves appear to drift or glide as they fall and disperse from the tree, which is of particular concern for trees directly adjacent to rail lines.

The purpose of this experiment was to investigate the path of different leaf types as they fall from trees to the railhead and/or ballast, and then assess the differences between leaf types for relocation once on the ground. These outcomes were then used to input into the low adhesion prediction model that amongst other things takes tree species into account when assessing risk of leaf induced low adhesion occurring.

5.3 Methodology

Leaf fall and mobility tests were conducted under laboratory conditions, using seven ash, common lime (abbreviated to c. lime) and sycamore leaves. These species were chosen as they represent a range of average sizes, masses and shapes, with the c. Lime being typically smaller in size and mass, with ash being intermediate and sycamore being relatively large. All three of these species were classified as "troublesome as far as low adhesion is concerned" in the AWG's Adhesion Manual 6.0 from 2018 [3].

[4] Vegetation immediately surrounding railway line.

An attempt was made to choose leaves with a range of sizes (see Table 14 below) and masses (see Table 15) from each species.

From the literature review, it was found that there wasn't an established method for assessing leaf fall characteristics beyond just fall dynamics, therefore, a new method was developed to consider fall dynamics and relocation of leaves on the ground (ballast/rail). Leaf fall classes were defined using the results of the investigation by UNC Chapel Hill [106], [107], described in section 2.4.4.

Equipment required

The following equipment was needed for the leaf fall and mobility tests:

- Step ladder
- Fan (with at least 3 speed settings)
- The available ballast covered a 30x30cm area)
- Leaves (7 sycamore, ash and c. lime each)
- Spray bottle and water
- Air velocity meter/anemometer (RS Pro IM-740 air velocity meter)
- Scales with a high degree of accuracy (0.001g or higher to precisely measure leaf – water absorption)

Figure 46: Generic spray bottle used (left), and fan used (right).

The spray bottle (Figure 46, left) produced an average 0.677g of water per spray, with a standard deviation of 0.051g. At 1m, the fan used (Figure 46, right) produced wind that varied between 1.6 to 1.8m/s (3.5 to 4mph) at speed setting one, 2.9 to 3.3m/s (6.4 to 7.3mph) for speed setting two and 3.1 to 3.3m/s (6.9 to 7.4mph) for speed setting three. At 1.5m the fan produced wind of 1.6 to 1.7m/s (3.5 to 3.8mph) when set to the first speed setting. In section 2.4.3 annual average UK wind speeds were found to range between 4.0 and 4.8m/s, and since gusts of wind are much harder to account for and quantify the average wind speeds were chosen to test. Additionally, to test higher wind speeds, a more powerful fan would be required.

5.3.1 Leaf fall

To investigate the characteristics displayed by different leaf species when falling, the leaves were firstly all dropped from a height of 2m above a specific position. A drop height of 2m was chosen partly due to it being easily reachable by a step ladder and partly due to it being a realistic height for a low level branch on a tree, it also means the tests could be repeated without the use of specialist equipment. This was done under still and artificially windy conditions where wind was simulated by a fan.

All tests were performed in a large, empty laboratory, which allowed for control of simulated wind plus a flat, level floor enabling accurate distance measurements. A fan with a centre height of 1m and blade diameter of 40cm was used, with the intention of preventing leaves that had landed on the ground from being re-distributed and thus invalidating the results. The lowest speed setting on the fan was used, the wind speed over the origin point was measured at 1.6 to 1.7m/s using the anemometer.

Vortex wind speeds from the CFD based analysis described in section 2.4.5 [91] found that for a train travelling at 75mph, vortexes were produced with a diameter of between 0.8 and 1.6m, lasting only 0.35 seconds and with a flow speed of around 1m/s. Meanwhile, annual average wind speeds in the UK typically range between 4 and 4.8m/s [103]. From this, it was decided that the wind speed (1.6 to 1.7m/s) produced by the fan was representative as it fell between the CFD and annual wind speeds from the literature. Additionally, rail lines are frequently lined with trees meaning that the wind experienced could possibly be lower than the national average, or higher than the national average when flowing in line with the railway.

Procedure

Seven leaves were collected from each species, with an attempt made to choose leaves of assorted sizes and masses to give a more representative sample group. The leaves were left to air dry for a minimum of 24 hours to reach the same humidity level, before being photographed and weighed. Figure 47 shows an example from each species.

Figure 47: Sycamore (left), ash (middle) and c. lime (right) leaves.

The laboratory space was set-up, tape was placed on the floor with an "X" marked on it to give a centre position above which the leaves would be dropped. Then tape was placed and marked at 50cm in the y-axis, as well as 50, 100 and 150cm in the x-axis. This was done to provide a scale for image analysis, see Figure 48.

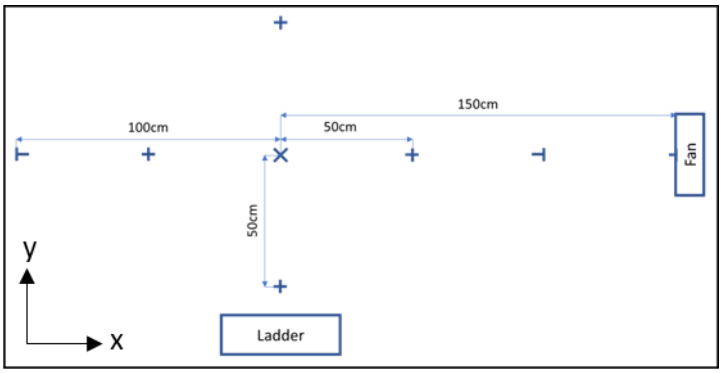

Figure 48: Overhead schematic diagram of leaf drop test.

Using a ladder and tape measure, the drop position was found. Video recordings were then taken of each of the drop sets per species and with fan vs no-fan conditions. After this, photographs of the spread were taken from as close to the drop position as possible, making sure to include every leaf. This was done for a total of 8 times per leaf species.

For simulated wind tests, the fan was set up at 1.5m in the positive x direction pointing directly in the negative x direction at the centre mark. The fan was set to the lowest speed setting and the test procedure described above was repeated for all leaf types and repeats.

Image analysis

The image analysis was conducted using Microsoft PowerPoint to store and organise the photographs taken of the leaf spread. One image was shown per slide, see Figure 49. Horizontal and vertical lines were added and adjusted to line up with the markings on the masking tape on the floor.

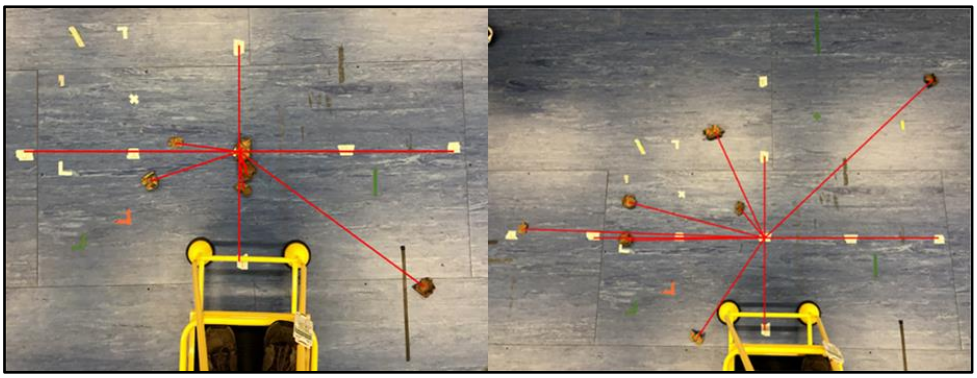

Figure 49: Sycamore leaf spread with no-fan (left) and fan (right).

X and Y coordinates were recorded in a Microsoft Excel spreadsheet where the scaling, as well as total and average distance were calculated.

5.3.2 Leaf on ballast mobility

To better understand how wind moves and relocates leaves that have landed on ballast near rail track a leaf mobility study was carried out. This study involved the same leaves used in the leaf drop tests and was conducted immediately after. The conditions for mobility tests included "dry", "semi wet" and "fully wet". "Semi wet" leaves were each sprayed 3 times on each side 1-2 minutes before testing to ensure the surfaces of the leaves were fully wet, but there was minimal absorption at the time of testing. "Fully wetted" leaves were each sprayed 15 times, then left in a sealed plastic container for at least 24 hours to allow them to fully hydrate with a slight excess of water to ensure full absorption. The "semi wet" leaves should retain most of their structural properties (shape, stiffness etc.) while having potentially altered surface friction properties. The "fully wet" leaves became softer and more pliable, again with potentially altered surface and friction properties. Each spray produced an average of 0.677g of water.

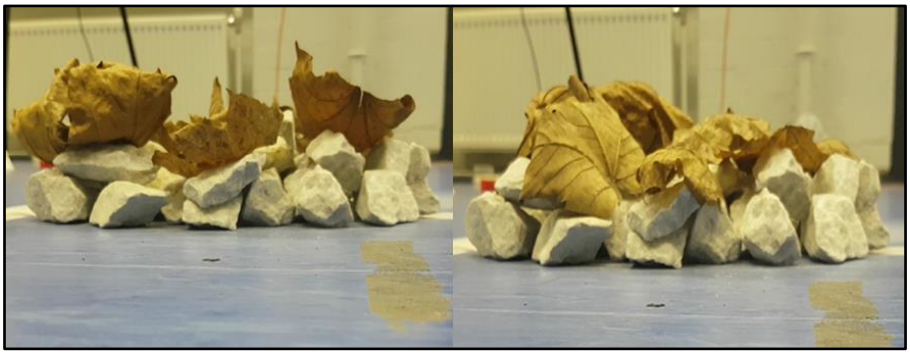

Figure 50: Leaves in "upward orientation" (left), and "downward orientation" (right).

Leaf orientation was another variable observed in all leaf types, though it appeared more obviously in sycamore and ash and less so in c. lime. As the leaves dried, some appeared to curl up like fingers on a semi-closed hand. This was of interest when setting up for the leaf on ballast mobility tests as those in a "downward orientation" (Figure 50 – right) seemed to almost grip the ballast whereas those in the "upward orientation" seemed to do the opposite and appear to be more vulnerable to the effects of the simulated wind. As a result, each test was performed three times with leaves in each orientation.

The variables for this study were the "wetness" of the leaves and ballast, speed of the fan (simulated wind speed), leaf species and leaf orientation.

Procedure

Loose ballast was spread evenly across a 30cm by 30cm area (available ballast only sufficiently covering a 30x30cm area) of the laboratory floor, with the fan (same as used in the leaf fall tests) set up at ground level, 1m away (as a more consistent wind speed was measured 1m away from the fan when placed on the floor). Place the anemometer at the leading edge of the ballast to give precise, real time wind speed readings, as shown below in Figure 51.

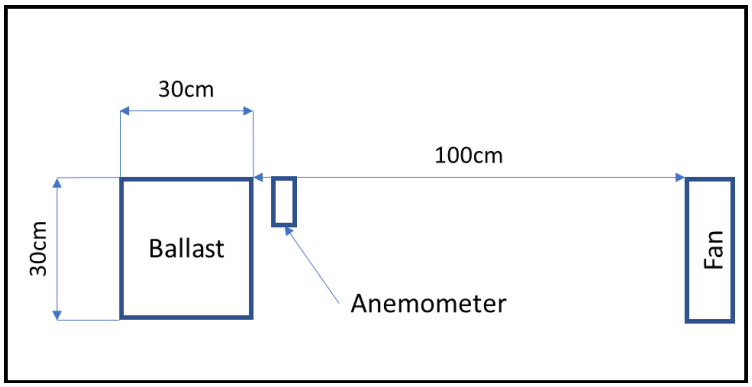

Figure 51: Overhead schematic diagram of leaf mobility test.

Seven leaves were placed on the ballast (in either upward or downward orientation) as shown below in Figure 52, the fan was then turned on at its lowest speed setting. 10 seconds were allowed while observing whether any leaves were blown away, then the next speed setting was selected. Again, 10 seconds were allowed for observation before increasing to the highest speed setting. Meanwhile, a video was recorded showing the leaves and anemometer using a mobile device so that accurate wind speed values for when the leaves are blown off the ballast were recorded.

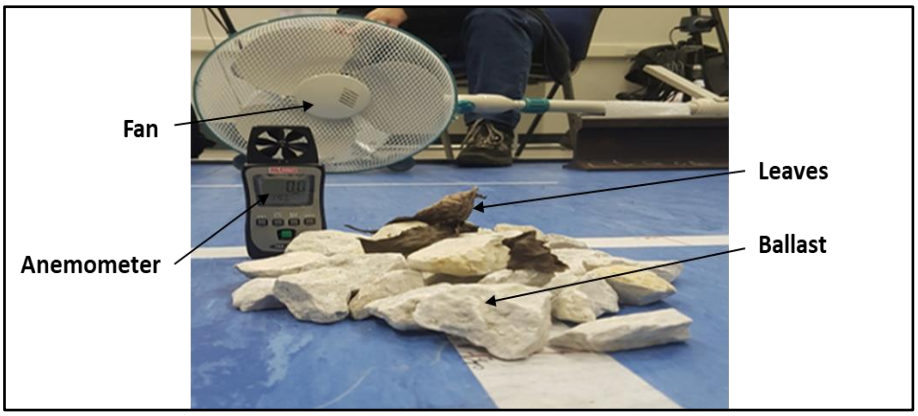

Figure 52: Mobility test setup with Ash leaves on ballast.

The test was repeated for the other orientation and remaining two leaf species with a total of 6 tests per species (18 tests in total).

For the "semi wetted" tests, the spray bottle was used to spray each leaf 3 times on each side as well as 3 sprays onto the ballast. The same procedure was repeated from the dry tests, while periodically spraying the ballast with water as it dries out from the simulated wind.

For "fully wetted" leaves, the same procedure as "semi wetted" tests was used except the leaves were fully hydrated as described in 5.4.2.

5.4 Results

Averages and standard deviations for lengths and widths of the leaves used are shown in Table 14. The column on the right shows an approximated area for each leaf species and is equal to the average length multiplied by the average width (in the future image processing software might be a better choice for measuring the surface area of the leaves) and does not consider the intricate shapes of any of the leaves.

Table 14: Average and standard deviation of leaf lengths and widths.

		Length (cm)	Width (cm)	Approximated area (cm²)	Dry mass (g)
Sycamore	**Average**	10.44	14.18	148.0	0.868
	St. dev.	2.70	4.05		0.522
C. Lime	**Average**	5.89	5.07	29.9	0.185
	St. dev.	0.79	0.78		0.047
Ash	**Average**	4.70	2.04	9.6	0.249
	St. dev.	0.47	0.35		0.136

The purpose of the approximated area is to compare the effective size of each leaf species, that is, the potential reach of the leaf in any orientation. Sycamore leaves have the largest area by far, almost 5 times larger more than C. Lime and over 15 times more than Ash.

5.4.1 Leaf fall

Dry and fully wetted leaf masses prior to testing are shown in Table 15, while falling classes are shown in Table 16. Classes were assigned by an undergraduate researcher as part of their final year project [155].

The classes were defined using the outcome of a study on "Classes of natural leaf fall motion" [106], [107] that was described in section 2.4.4 of the Literature Review chapter. Figure 11 shows a simplified diagram of leaf/disk fall classes that were observed in the study and was used to classify falling behaviour in this study.

Table 15: Dry and fully wetted leaf masses with % increase.

	Dry mass (g)			Fully wetted mass (g)			% Increase		
	Syc.	**C. Lime**	**Ash**	**Syc.**	**C. Lime**	**Ash**	**Syc.**	**C. Lime**	**Ash**
Mean	0.868	0.185	0.249	1.711	0.365	0.918	99	93	269
St. dev.	0.522	0.047	0.136	1.048	0.125	0.446	24	23	46

Table 15 shows the fully wetted leaf masses, where sycamore, c. lime and ash increased by an average of 99%, 93% and 269% respectively. The increase in mass is due to the absorption of water into the leaves.

Table 16: Leaf fall classes.

	Sycamore		C. lime		Ash	
	No-fan	**Fan**	**No-fan**	**Fan**	**No-fan**	**Fan**
1	Chaotic	Tumbling	Chaotic	Tumbling	Chaotic	Tumbling
2	Periodic	Chaotic	Periodic	Chaotic	Periodic	Periodic
3	Periodic	Periodic	Periodic	Chaotic	Steady	Chaotic
4	Periodic	Periodic	Tumbling	Tumbling	Periodic	Periodic
5	Chaotic	Tumbling	Chaotic	Tumbling	Chaotic	Chaotic
6	Steady	Chaotic	Periodic	Chaotic	Steady	Chaotic
7	Steady	Steady	Periodic	Periodic	Steady	Chaotic

Table 15 shows the classes assigned to each leaf during one drop test for each condition. It was observed that leaf species does not define the fall class for fan and

no fan conditions, however, a larger test group would give a better overall picture and more definitive answer.

Figure 53, Figure 54 and Figure 55 show plots of leaf fall locations for sycamore, c. lime and ash respectively both with and without the simulated wind.

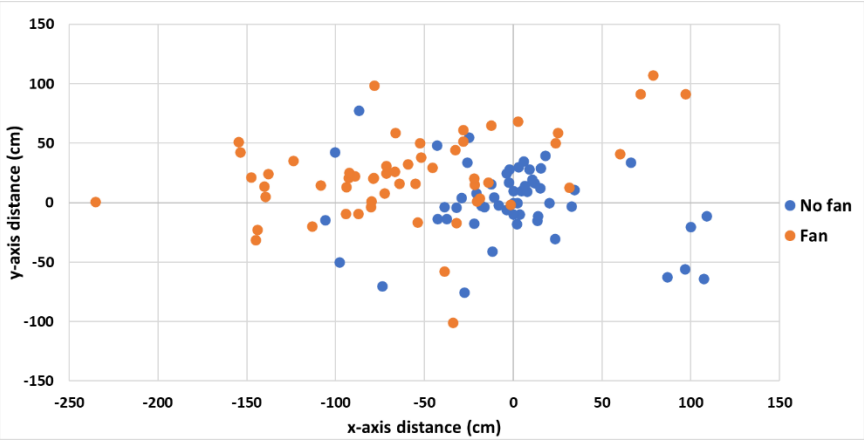

Figure 53: Leaf spread for sycamore.

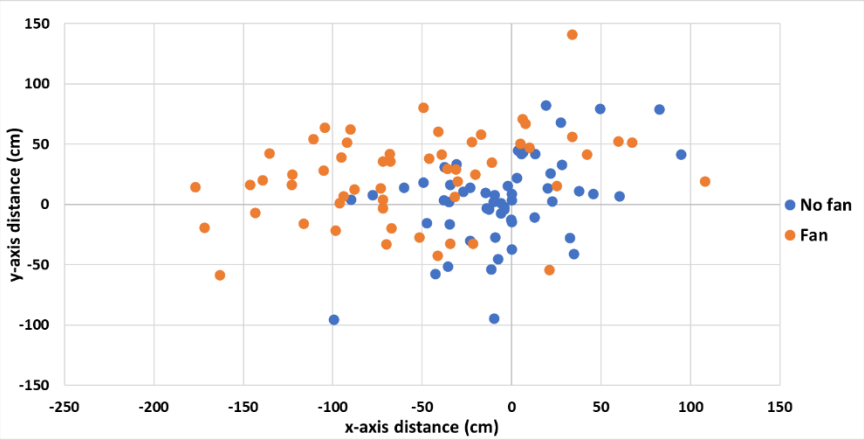

Figure 54: Leaf spread for c. lime.

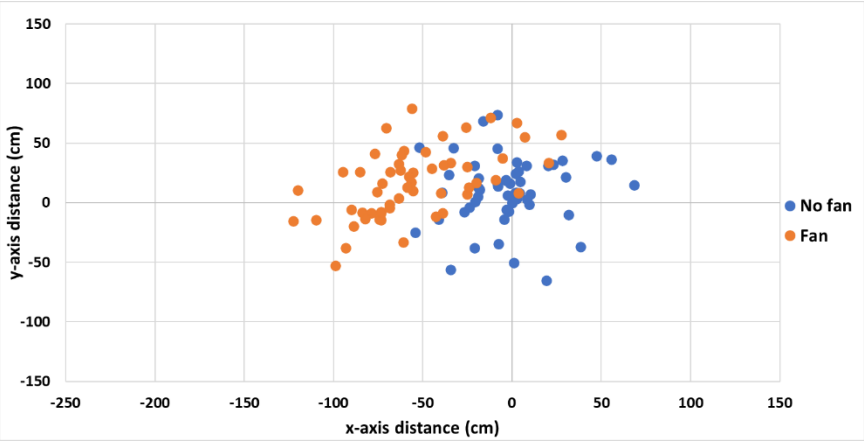

Figure 55: Leaf spread for ash.

Figure 53, Figure 54 and Figure 55 show plots of all drop tests with and simulated wind for sycamore, c. lime and ash respectively. Table 17 below shows the mean and standard deviation of distances from each drop test condition.

Table 17: Mean and standard deviation of distances from drop tests.

	No-fan distance			Fan distance		
	Sycamore	**C. Lime**	**Ash**	**Sycamore**	**C. Lime**	**Ash**
Mean (cm)	0.42	0.43	0.31	0.87	0.86	0.68
St. dev.	0.35	0.30	0.21	0.43	0.38	0.24

Figure 56 shows a box and whisker plot of leaf fall distances in no-fan and simulated wind conditions. The top and bottom of the of the upper and lower lines represent the maximum and minimum values observed respectively. The top and bottom of the boxes show the 3rd and 1st quartile respectively, while the line inside the box shows the median of the distances measured.

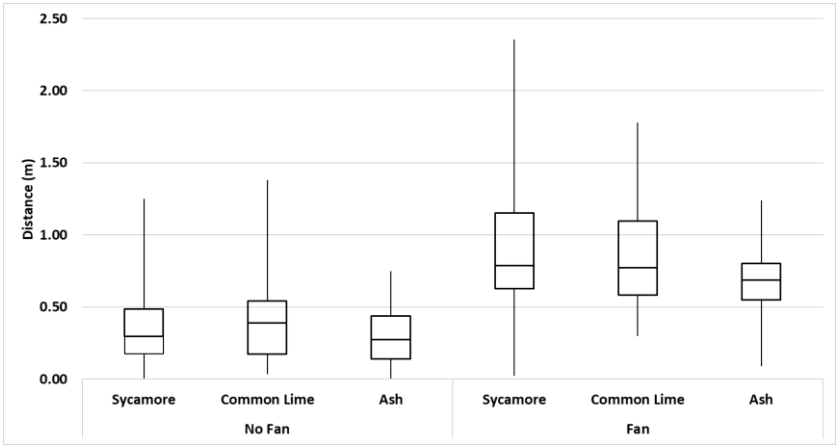

Figure 56: Average leaf distances for fan and no-fan.

Figure 57 shows the mean masses of the seven leaves of each species against the mean horizontal distance covered in both wind and no-fan conditions.

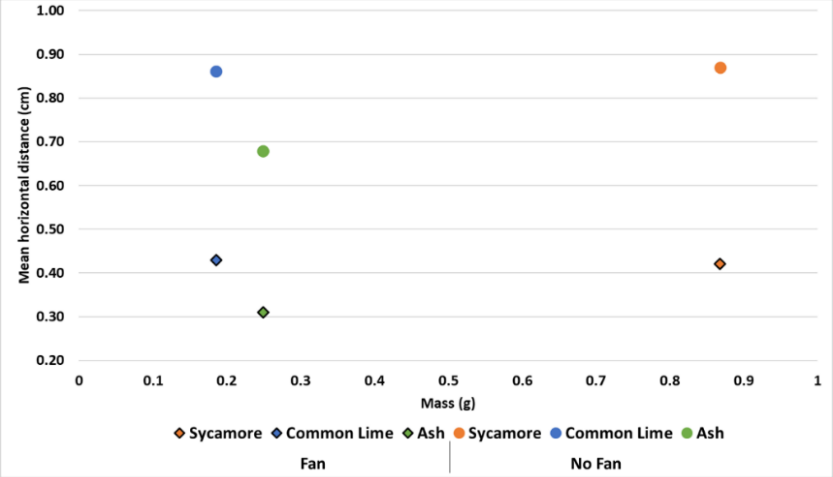

Figure 57: Leaf mass versus mean horizontal drift distances without and with fan.

Due to the outcome of this graph (showing no clear link between leaf mass and distance covered), an additional small test was conducted where leaf masses were compared directly against lateral drop distances. This involved recording the mass of each leaf, then dropping them from the same 2m high position (with no simulated wind) and recording the direct distance between the landing position and the origin point.

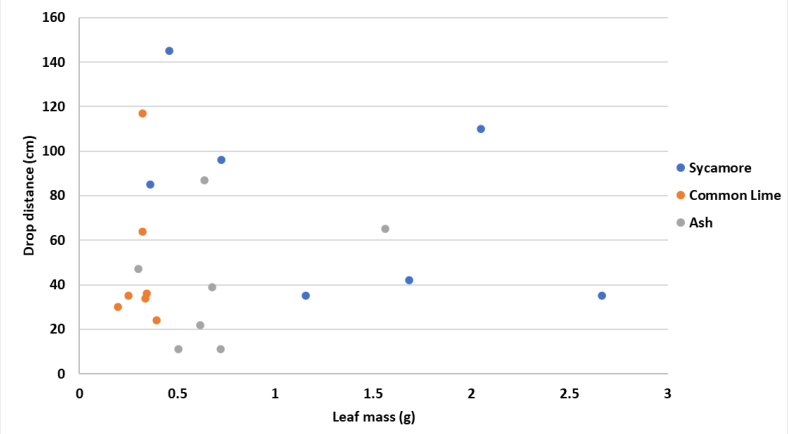

Figure 58: Single set mass-distance drop test.

Figure 58 shows the single set leaf drop distance versus mass with no-fan for sycamore, c. lime and ash.

5.4.2 Leaf on ballast mobility

Leaf orientation proved to be influential on the wind speed required to move leaves off the ballast. As shown in Figure 50, sycamore leaves exhibited either "upward" or "downward" positions where the natural curl of the leaf either curled away from the ballast or "clung" onto it respectively. It was assumed that when in the downward

position the leaves would be able to withstand a higher wind speed before moving, when compared to those in the upward position.

To avoid a bias due to this factor the first test was done with leaves in the upward position, the second with the leaves in the downward position and the third with them in a combination. It is noted that this phenomenon was far more prominent with dry sycamore and ash leaves, as c. lime leaves largely remained flat.

Figure 59 through to Figure 64 show the air speed and number of leaves removed for dry, semi wetted and fully wetted leaves where in some cases not all leaves were removed. Leaves were not replaced once they had initially moved during each test as it would not be possible to replace them with the fan running.

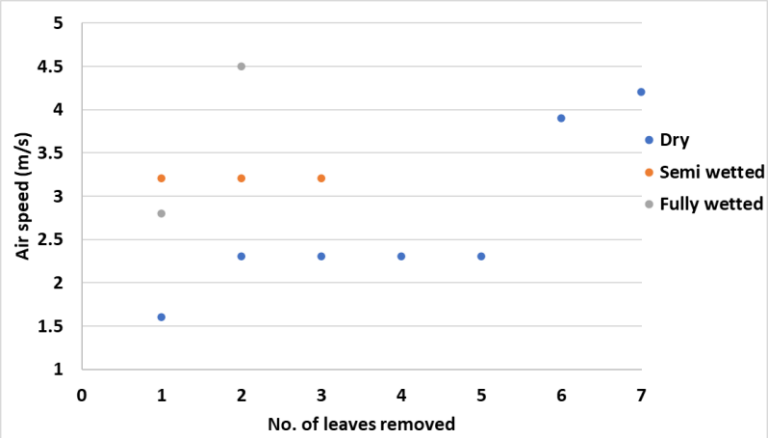

Figure 59: Upward orientation sycamore leaf removal air speeds.

Most dry leaves were moved by wind at 2.3m/s and by 4.2m/s all seven leaves had been moved. Only three semi wetted leaves were moved, all at 3.2m/s, while only two fully wetted leaves were moved, one at 2.8m/s and one at 4.5m/s.

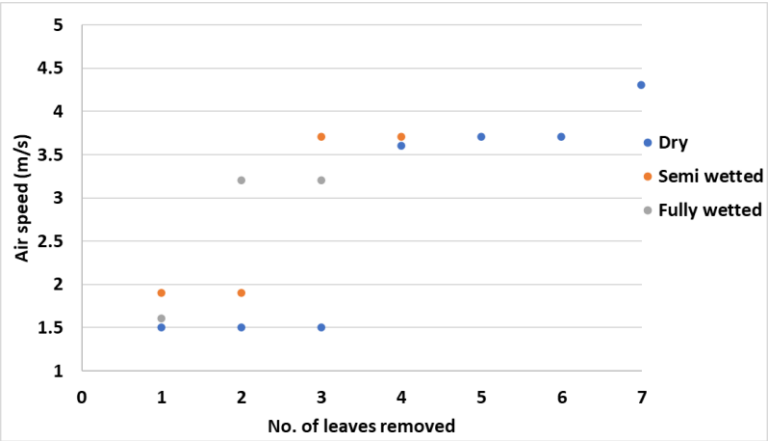

Figure 60: Downward orientation sycamore leaf removal air speeds.

All seven dry leaves were moved, three at 1.5m/s, one at 3.6m/s, two at 3.7m/s, and one at 4.3m/s. Four semi wetted leaves were moved, two at 1.9m/s and two at 3.7m/s. Three fully wet leaves were moved, one at 1.6m/s and two at 3.2m/s.

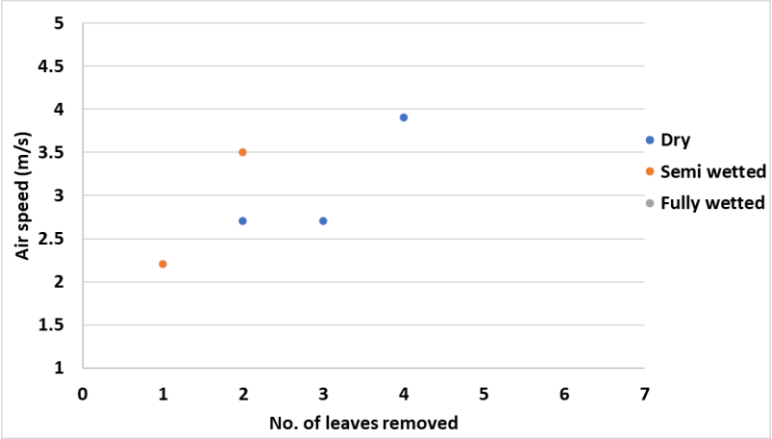

Figure 61: Upward orientation C. Lime leaf removal air speeds.

Four dry leaves were moved, one at 2.2m/s, two at 2.7m/s and one at 3.9m/s. Only two semi wetted leaves were moved, at 2.2m/s and 3.5m/s. No fully wetted leaves were removed.

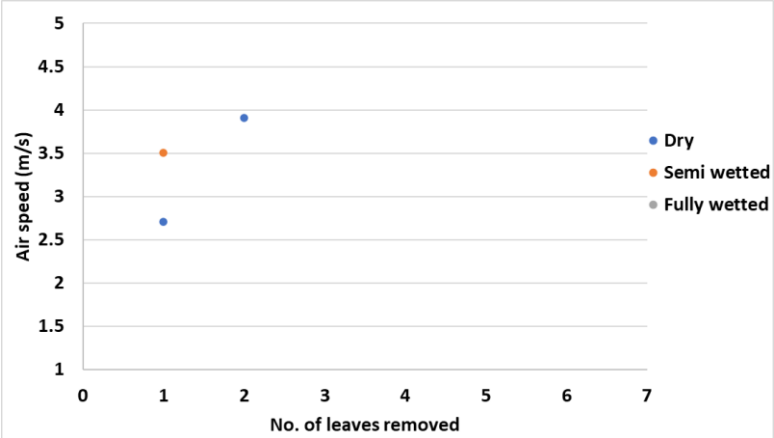

Figure 62: Downward orientation C. Lime leaf removal air speeds.

Two dry leaves were moved, one at 2.7m/s, the other at 3.9m/s. Only one semi wetted leaf was moved, at 3.5m/s. No fully wetted leaves were removed.

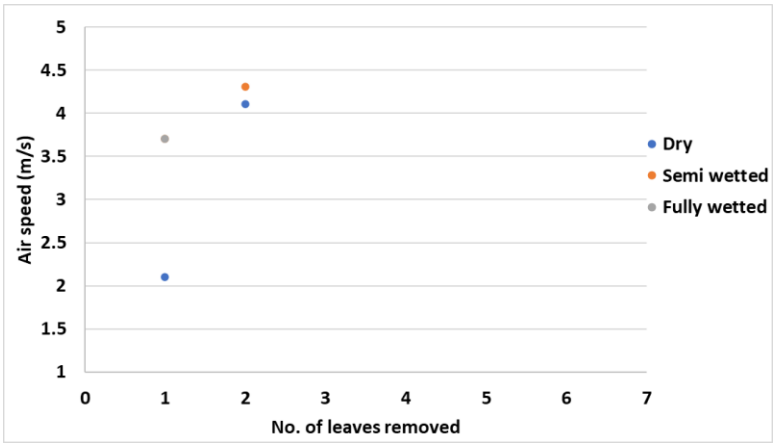

Figure 63: Upward orientation Ash leaf removal air speeds.

Two dry leaves were moved, one at 2.1m/s, the other at 4.1m/s. Two semi wetted leaves were moved, one at 2.1m/s and one at 4.3m/s. Only one fully wetted leaf was moved, at 3.7m/s.

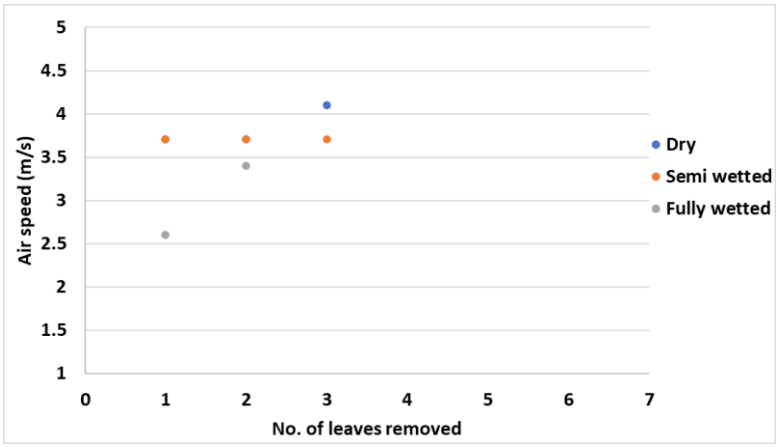

Figure 64: Downward orientation Ash leaf removal air speeds.

Three dry leaves were moved, one at 2.7m/s, another at 3.4m/s and the last at 4.1m/s. Three semi wetted leaves were moved, all at 3.7m/s. Two fully wetted leaves were moved, one at 2.6m/s and the other at 3.4m/s.

Table 18: Leaves moved by species.

	Leaves moved (total/42)
Sycamore	26 – (62%)
Ash	13 – (31%)
C. Lime	9 – (21%)

Table 18 shows a comparison of percentage of leaves moved, out of a possible 42 (7 leaves in 2 orientations, with 3 levels of dry/wetness). 26 of 42 (62%) of sycamore, 13 of 42 (31%) of ash leaves and 9 out of 42 (21%) c. lime leaves were moved.

Table 19: Leaves moved by dry/wetness.

	Leaves moved (total/42)
Dry	25 – (60%)
Semi wetted	15 – (36%)
Fully wetted	8 – (19%)

Table 19 shows a comparison of percentage of dry, semi and fully wetted leaves moved, out of a possible 42 (7 leaves of 3 species and 2 orientations). 25 of 42 (60%) dry leaves, 15 of 42 (36%) of semi wetted leaves and 8 out of 42 (19%) fully wetted leaves were moved.

Table 20: Leaves moved by upward or downward orientation.

	Leaves moved (total/63)
Upward	23 – (37%)
Downward	25 – (40%)

Table 20 shows a comparison of percentage of leaves moved, out of a possible 63 (7 leaves of 3 species, with 3 levels of dry/wetness). 23 of 63 (37%) upward orientated and 25 of 63 (40%) downward orientated leaves were moved.

5.5 Discussion

The sizes of the leaves used (see Table 14) varied much more for sycamore than for c. lime and ash, with a combined average of length and width averages of 12.3cm, 5.5cm and 3.4cm respectively. Sycamore is by far the largest, with c. lime being just under half the size and ash being just over a quarter. It is worth noting that the standard deviation for sycamore leaves was far higher than that of c. lime and ash, at 3.38, 0.79 and 0.41 respectively.

Sycamore leaves showed average fan and no-fan drift distances of 0.42m and 0.87m respectively, an increase of 107%. C. lime leaves showed average fan and no-fan drift distances of 0.43m and 0.86m respectively, an increase of 100%. Ash leaves showed average fan and no-fan drift distances of 0.31m and 0.68m respectively, an increase of 119%. Leaf drop distance and percentage increase in drop distance with the fan did not correlate with the leaf length and width averages. C. lime leaves were the smallest in size and weight and showed the largest percentage increase in drop distance when the fan was on.

As expected, all species showed an increase in lateral drop distance between no-fan and simulated wind, with all being 100% or more. Fall characteristics observed were

also different for the three species, this was expected and is thought to be due to differences in their shapes. Ash was noted for typically being longer and narrower, whereas sycamore and c. lime shared more shape similarities in that their lengths were closer to their widths.

Ash showed the lowest no-fan drop distance yet the highest increase with the fan. Sycamore leaves had the heaviest average mass and the highest standard deviation yet fell in between c. lime and ash in terms of both drop distance and percentage increase with the fan. C. lime showed the highest no-fan drop distance yet the lowest increase with simulated wind as well as the lowest average mass and standard deviation.

Sycamore leaves had the highest average weight and standard deviation, at 0.868g and 0.522g respectively, these are notable when compared to 0.249g and 0.136g for ash and 0.185g and 0.047g for c. lime (shown in Table 18).

On the day of the "fully wetted" leaf mobility testing, the sycamore and ash required 6 additional sprays of water as they were notably less hydrated than the c. lime. It was also noted that some of the leaves curled up as they dried, altering their shape, aerodynamic properties, and potentially biological composition. This is in line with real world situations and is not believed to have affected the validity of the tests.

According to Table 17, ash had the lowest standard deviation with and without fan, while sycamore had the highest. It is worth noting that when the fan was on the standard deviation relative to the mean was much lower for all species, indicating that the simulated wind may have helped to concentrate the leaves into a more uniform group.

Looking at Figure 58, no straight trend lines could be fitted to the graph with enough confidence to suggest a strong correlation between leaf mass and drop distance. It can be said that most c. lime and ash leaves had a mass of less than 1g and dropped within 60cm of the origin. However, typically there only tends to be an increase in either drop distance or mass as shown by the points close to, yet higher up both axes. This could suggest that heavier leaves tend to fall closer to the origin while lighter leaves are able to travel further from the origin.

After comparing leaf masses and drop distances (Figure 58) with fall classes (Table 15) no clear links could be found.

Figure 59 to Figure 64 show the air speeds at which leaves were moved from ballast under various conditions, mainly the dryness/wetness of the leaves, the species and

the orientation (upward/downward). The highest wind speed observed in the tests was 4.5m/s, from the highest speed setting of the fan.

When comparing by species, sycamore had the highest total number of leaves moved under all conditions (26/42), followed by ash (13/42) and finally c. lime (9/42). This somewhat matches the scaling of fully wetted masses (see Table 18).

When comparing the orientation, more downward facing leaves were moved. This was unexpected and could possibly be due to the centre of gravity of the leaf being slightly higher when the leaves were in the downward facing position meaning that the wind was able to hit more of the leaves surface area.

Unfortunately, the tests used in this project were not designed to assess the number of leaves that are picked-up and sucked into the wheel-rail interface and squashed. One method that could be used to assess this would include using a high speed camera to record leaf movement at a full-scale test facility (i.e. Long Marston) with leaves deliberately placed around the line.

Suggestions for leaf corridor design

When considering suggestions for leaf corridor design, the findings from the leaf fall and mobility study indicate that the horizontal distance covered by leaves as they fall van vary dramatically. For every 2m of height, leaves can travel almost 1m horizontally under still conditions and much further in windy conditions. Therefore, a tree that is, say, 10m tall could drop a leaf that will cover approximately 5m horizontally, not accounting for the effects of wind. Wind could serve to wither increase or decrease this distance depending upon its direction. This means that higher a tree is (accounting for the base height of the tree relative to the track), the further it should be kept from a rail line.

Limitations

When measuring leaf sizes, only maximum length and widths were used. This did not show the true area of each leaf, considering their specific shapes.

One limitation observed during the leaf drop tests with simulated wind was that occasionally leaves would skid along the floor as they landed, providing they had enough residual horizontal velocity. This effect was uncommon and was averaged out, as shown by the distance between the maximum and mean values, see Figure 56.

Another limitation was observed where in some instances leaves were blown out of the path of the wind, in either the positive or negative y-axis. This could be because the simulated wind originated from a fan with a diameter of 40cm, and the column of

wind would disperse and spread outward (possibly producing small vortices) as it pushed toward the origin point.

During the "semi wetted" and "fully wetted" leaf mobility tests both the leaves and ballast started to dry out due to the simulated wind. To lessen this effect, the tests were completed as fast as possible and when necessary, the leaves and ballast were periodically re-sprayed until appropriately wetted.

Additionally, prior to the "fully wetted" testing the ash and sycamore leaves did not appear to be as hydrated as the c. lime leaves. To rectify this, an additional six sprays were applied to the ash and sycamore leaves prior to testing. It is possible that this means that ash and sycamore leaves absorb water more slowly than common lime and as a result, in the real world they may be more mobile.

Another factor that was not measured was the surface area of the leaves. However, some of the leaves had curled up when drying out, meaning a true area would have been extremely difficult to measure.

Strengths and weaknesses

The main strengths of this set of tests were; that it gave a clear comparison of three leaf species (sycamore, ash and common lime) under still and windy conditions. The test set-up was simple so that it could easily be repeated in the future with the same or other leaf species. Leaf masses were recorded and compared to drop distances, leaf area approximations were also calculated.

The main weaknesses of these tests were; only one drop height was chosen, only one simulated wind speed was chosen for the drop tests, only a column of wind was produced by the fan which may have led to inconsistent airflow.

The drop tests could have been improved by using a wind tunnel to simulate a wall of air with a constant speed for the drop tests. More leaf species could have been tested with a bigger range in sizes and shapes. Leaf area could possibly have been calculated more accurately using image processing software.

5.6 Conclusions

- Leaf mass and/or size did not appear to correlate with distance covered in either fan or no-fan conditions, therefore it is hypothesised that shape must play a larger role in causing leaves to fall in different classes (tumbling, periodic, steady, chaotic etc.) and thus affecting their horizontal distance covered.
- Ash showed the greatest increase in drop distance in windy conditions, followed by sycamore and c. lime, indicating leaf shape must play a larger role.

- Both sycamore and c. lime were able to absorb close to their own mass (increasing by an average of 99% and 93% respectively) in water as they were fully hydrated, however, ash was able to absorb an averaged additional 269% of its mass in water.
- Sycamore leaves were two times more likely to be blown off the ballast as ash, and almost three times more than c. lime across all orientations and hydration states.
- Dry leaves were two times more likely to be blown off the ballast than semi wetted leaves, and more than three times more than fully wetted leaves across all species and orientations.
- Upward orientated leaves were only slightly more likely (>10% difference) to be blown off the ballast than downward orientated leaves across all species and hydration states.
- Sycamore leaves have the largest area by far, almost 5 times larger more than c. lime and over 15 times more than ash.

6. LAYER FORMATION/BONDING HYPOTHESES TESTING

6.1 Introduction

There are several hypotheses regarding how leaves bond to the railhead, while resulting in low friction to the wheels. These are described in detail in section 2.7, as well as being recapped here and the following chapter along with chosen methods for mechanical testing and chemical analysis. The bonding hypotheses covered in this chapter are:

- Iron oxide driven
- Metallic substrate effects

Table 21 : Test rig utilisation for formation/bonding hypotheses

Method	Location	Bonding
HPT	Lab	✓
SUROS	Lab	✓
Torque measuring screwdriver	Lab + Field	✓

Multiple test methods and rigs were used in the formation/bonding analysis, some of which were useful in both investigations while others were more specific, these are shown above in Table 21.

6.2 Iron oxide driven

As described in section 2.7.1 of the literature review, this hypothesis involves the reaction between Fe ions and chemical components of leaves to form a third body layer. Through the high temperatures and pressures found in the wheel-rail interface (with the possible addition of supercritical water) leaf components bond to Fe ions which in turn bond to iron oxides (e.g. Fe_2O_3 and Fe_3O_4) and the railhead surface.

To investigate whether iron oxides are involved in the bonding of leaf layers or black layers to the railhead, two test processes were employed and are described with their respective results in succession below.

Test procedure – 1

The first test process used to investigate whether iron oxides are involved in the leaf layer formation process, involved the SUROS twin disc test rig (as described in section 2.6.4) which was used to test a mixture of blended sycamore leaf pieces and distilled water (sycamore-water) as well as sycamore mixed with distilled water and sodium EDTA (sycamore-EDTA). Sodium EDTA (Ethylenediaminetetraacetic acid) is a chelating

agent supplied as a water soluble white powder, that is widely used as a water softener as well as in many industries including, medicine, textiles and cosmetics. The reason it was chosen to investigate this hypothesis is because it binds to iron ions (Fe^{2+} and Fe^{3+}) and should prevent any free ions in the contact from interacting with the leaf matter to form a bonded, low μ inducing layer. If successful, the sodium EDTA should significantly reduce leaf layer formation, meaning the leaf matter is removed/ejected from the contact allowing friction to return to an expected level.

Blended brown sycamore leaves were added to distilled water at a ratio of 2wt.% leaf to 98wt.% water as this ratio was found to provide the most consistency for being fed into the contact during the test. The mixture was left for 24 hours to allow the leaf particles to absorb water and achieve a similar specific gravity, this was done in part to ensure the leaf particles fed correctly from a 25ml syringe, though a plastic tube to the contact.

The running parameters for the SUROS rig were set to 400rpm, 3% slip and a contact pressure of 900Mpa. The test procedure involved cleaning and mounting the discs, then running under load for 30s to run the disc surfaces in and establish a baseline friction level. The test substance was then drip fed into the top disc at a rate of one drop per second for 60s, with a further 210s of running to allow friction behaviour to develop. The total test time for each solution was 300s. The test was done for a total of two times each for sycamore-water and sycamore-EDTA.

Results

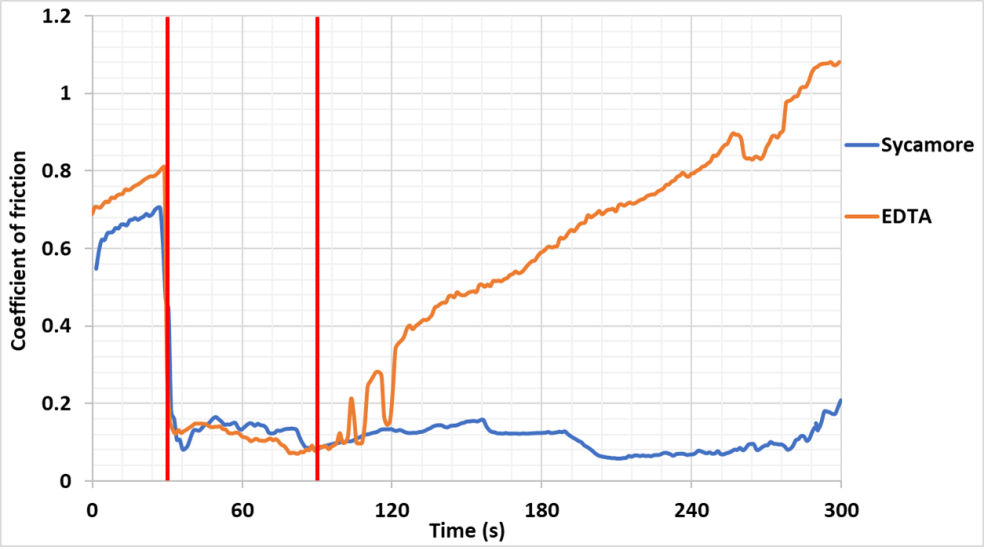

Figure 65: Averaged SUROS friction for sycamore-water and sycamore-EDTA.

Figure 65 shows the friction measured by the SUROS rig for sycamore-water and sycamore-EDTA. The lefthand vertical red line represents the 30s mark at which point

the solutions were added and the righthand red line represents the point at which the solutions stopped being added. This gives three phases to the test, the initial first 30s, the 60s where the solutions were added at 1 drop per second and the final 210s after the solutions had stopped being added. The average mass of contaminant added to the contact in the 60 seconds was measured to be 9.17g, equivalent to 0.15g per drop.

Table 22: Average friction levels for the different test phases

	0 – 30s	**30 – 90s**	**90 – 300s**
Sycamore-water	0.61	0.18	0.11
Sycamore-EDTA	0.75	0.12	0.62

Average friction levels for the three phases are shown in Table 22, where in the final 210s the sycamore-EDTA shows a return to normal friction levels while the sycamore-water remains low.

Test procedure – 2

The second test process involved submerging three R260 rail steel and three titanium specimens in tannic acid. Tannic acid refers to a specific form of tannin that has been used to generate black layers as a stand in for leaf layers in laboratory tests [142], [156], hence it being chosen to test this hypothesis. Tannic acid is also a known constituent of leaves [142], [157].

Originally supplied as a light brown powder, the tannic acid solution was mixed at a concentration of 5wt.% tannic acid powder to 95wt.% distilled water as per manufacturer recommendations. After being cleaned on all surfaces with acetone, the specimens were fully submerged in the tannic acid solution. After 30, 60 and 90 minute intervals the samples were removed and air dried. At these intervals the layer thicknesses were measured using an Eddy current probe, before being resubmerged in the tannic acid solution until the next measurement interval. 5 thickness measurements were taken at each interval at different points on the surface of the specimens and averaged to give a representative layer thickness. Between each eddy current probe measurement, the probe was checked against a reference surface that should read 0, to ensure no black layer had contaminated the probe surface, as well as being calibrated with plastic shims of a known thickness.

Results

Table 23 shows the black layer thickness on the R260 specimen measured using the eddy current probe.

Table 23: Black layer thickness growth on R260 at 30 minute intervals

Specimen	Avg. layer thickness (µm) at X minute intervals			
	0	30	60	90
R260	20	24	24	28

Initially, before the specimens were put in the tannic acid, both specimens were surface ground to give a comparable surface finish, then cleaned with acetone. Despite this, both gave readings when "clean", which could have been due to the surface roughness [158].

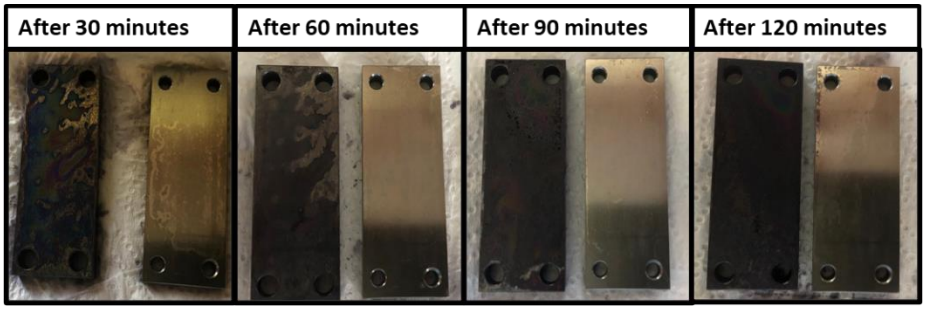

Figure 66: Black film formation on R260 and titanium at 30 minute intervals.

Figure 66 shows the gradual build-up of black layer on the R260 specimen, meanwhile no visible contamination was seen to be present on the titanium. The specimen on the left of each image are R260, while the specimen on the right are titanium.

Discussion

Despite the iron oxide driven hypothesis concerning leaf layer formation/bonding, the low µ and recovery behaviour is very telling in that it clearly shows an increase in friction for the sycamore-EDTA starting just after the 90s mark. When compared to the sycamore-water friction, the difference is very noticeable. The sycamore-water maintains a relatively consistent friction level of around 0.11, while the sycamore-EDTA increases to a value of 1.08, with an average of 0.62 for between 90s and 300s. The reason for the increase in friction to a coefficient of over 1 could be due to the removal of an iron oxide layer on the surface of the discs. EDTA's well known ability to capture iron ions (and by extension oxides) appears to be playing a key role here [159], [160]. Since iron oxides are known to reduce friction, it makes sense that the removal of the oxide surface layer would result in an increase in friction. It is reasonable to suggest that the increase in friction shown by the sycamore-EDTA solution indicates that a low µ inducing leaf layer was not formed and therefore bonding was prohibited.

From the second test, black layer appeared to form only on the R260 steel specimens, with no visible layer or contaminant seen on any of the titanium specimens (see Figure 66). Table 23 in shows the black layer thickness measured using the eddy current probe. The layer that formed on the R260 specimen increased by an average of 2.3µm every 30 minutes.

The change in colour of the tannic acid solution from yellow-brown to dark blue-black could be due to the formation of iron oxides as the acid reacts with the iron on the R260 surface. It could be possible that non-visible contamination/oxides were also being deposited/formed on the titanium as it was present in the same container of tannic acid, however, as stated no visible contamination was observed.

These observations suggest that the iron present in steel (R260 in this case) is crucially linked to the formation of the black layer and in turn leaf layers as they also contain amounts of tannins and tannic acid, supporting the iron oxide driven bonding hypothesis.

Strengths and weaknesses

Some of the strengths of this hypothesis testing include:

- The tannic acid method for forming a black layer is already established.
- The difference in layer formation on R260 and Ti is evident.

Some of the main weaknesses of the testing include:

- EDTA and water were not tested, this may have given more insight into any possible effects that EDTA would have on friction.
- Chemical compositions of the black layers formed in tests 1 & 2 were not compared, this could also have given a better understanding of how representable the tannic acid black layer is.

6.3 Metallic substrate effects

This hypothesis was also described in section 2.7.1 of the literature review, and states that the surface roughness is assumed to have an effect on the formation of the leaf layer on the railhead. A smoother surface should have a smaller total surface area than a rougher surface, which would give more area for leaf layers/adhesives to bond to. Measuring the surface roughness gives the clearest indication of the asperity sizes of a surface.

Test procedure

Three R260 steel and three titanium specimens were prepared, with one each having a ground flat (smoothest) surface finish, one each being sanded with 180 grit sandpaper (rougher) and the final two being sand blasted (roughest). The sandpapered specimens received 200 unidirectional passes in line with their longer dimension. The mean roughness average (Ra) of each specimen surface was measured using an Alicona InfiniteFocus SL optical 3D measurement system. Railhead roughness typically measures around 2.5µm for unused rail [161], so roughness values up to and around 2.5µm were desired.

Again, a tannic acid solution was used to grow a black layer on the steel and titanium specimens that was mixed at a concentration of 5wt.% tannic acid powder to 95wt.% distilled water. The same procedure used to test iron oxide hypothesis (Test procedure – 2) was used.

Results

Figure 67 shows the surface ground R260 specimen prior to being placed in the tannic acid (left), and just after it had been submerged (right).

Figure 67: Ground R260 specimen (left), and in tannic acid (right).

The specimens numbered 1 were surface ground, 2 were sanded and 3 were sand blasted. Table 23 shows the measured black layer thickness in 30 minute intervals, from 0 (just before specimens were placed in the tannic acid) to 90 minutes. The surface Ra shows the average roughness profile of the specimen surfaces in µm.

Table 24: Black layer thickness growth at 30 minute intervals

Specimen		Surface Ra (µm)	Avg. layer thickness (µm) at X minute intervals				Avg. growth rate (µm/min)
			0	30	60	90	
R260	1 – ground	0.573	20	24	24	28	0.438
	2 – sanded	1.037	21	24	36	36	0.517
	3 – sand blasted	1.512	28	32	34	38	0.585

The Ra values of the specimens increase in approximately 0.5µm increments between the ground, sanded and sand blasted surfaces for both R260 and titanium. The surface ground R260 and titanium specimens had Ra values of 0.573µm and 0.589µm respectively, while the sanded specimens were 1.037 µm and 1.007 µm respectively and the sand blasted specimens were 1.512 µm and 1.547 µm respectively. These values show a high consistency between R260 and titanium.

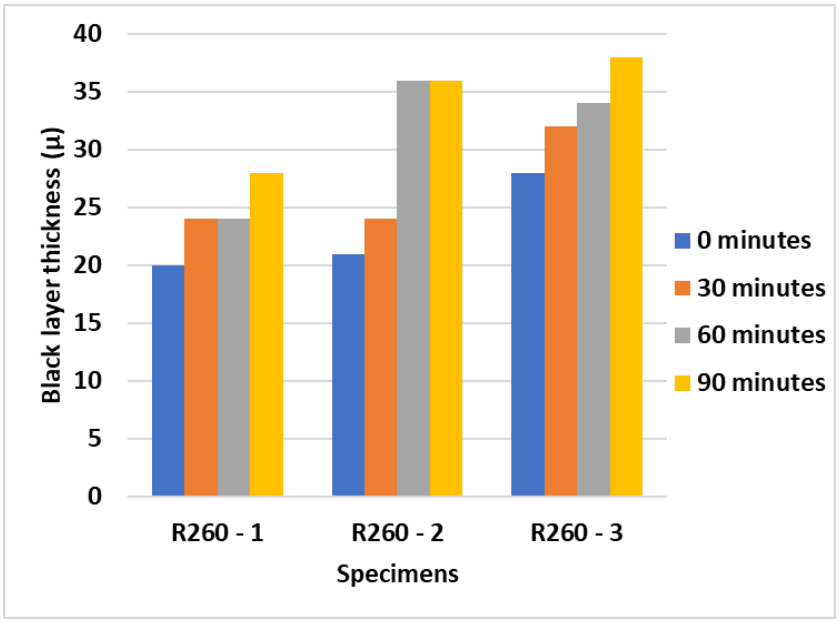

Figure 68: Layer formation thickness for R260.

Figure 68 shows data from Table 23, where the thickness of the R260 layers are shown. At each measurement, the thickness either increased or remained the same. The ground specimen has the smallest average layer thickness, followed by the sanded, and finally the sand blasted with the largest average.

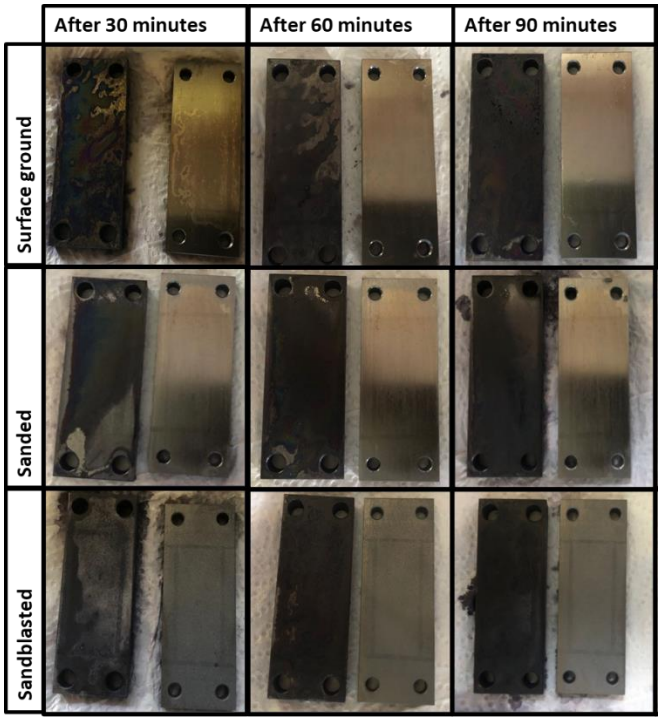

Figure 69: Black layer evolution by time and roughness.

Figure 69 shows the formation of black layers on R260 steel (left of each image) and titanium right of each image). The black layer is clearly formed on the R260, while distinctly not appearing on the titanium, which remained unchanged as before.

Discussion

A correlation between surface roughness and black layer thickness and rate of layer growth was observed. Looking at Figure 68, all three roughness' showed an increase in layer thickness between intervals except from 30-60 minutes for specimen 1 and 60-90 minutes for specimen 2, where the thickness remained the same. It is possible that at this point the surfaces had become saturated in the tannic acid derived layer and when the specimens were resubmerged in the tannic acid some of the layer was dissolved back into the solution.

Figure 68 also shows an increase in layer thickness and rate of layer formation that correlates with surface roughness. As surface roughness increases, so does the rate of layer formation. It is theorised that surfaces with a higher roughness have a higher real surface area [162], and this increase in surface area provides more opportunity for interaction with the tannic acid than if the surface was smoother and had a smaller true surface area. This increase in interaction means the black layer is formed more quickly.

During the experiment, the tannic acid went gradually from light yellow-brown (see, Figure 67 right) to a dark blue-grey in colouration (the same colour as the surface of

all the R260 specimens), strongly agreeing with Fe vs Ti. Observations of the black film growth on the specimen surfaces showed a visibly darker layer forming on the steel specimens, increasing in darkness and coverage every time the specimens were removed from the acid solution. This again supports the findings of the iron oxide driven hypothesis.

It should be noted that the black layer formed without any mechanical pressure or temperature increase, which has been found to be influential in other testing and may cause the layer to generate more quickly and/or thicker. The absence of mechanical pressure and increased temperature are representative of leaf layer formation when leaves land on the railhead and the water soluble tannins are secreted to form the black layer. This could mean that part of the reaction(s) that work in parallel to transform the leaf into a bonded black layer do not require train passes to occur. However, it is assumed that other reactions/processes occur that may or may not also require increased temperature and pressure caused by trains.

These findings support the hypothesis that an increase in surface roughness (and therefore an increase in total surface area) accelerates the rate of formation and total layer thickness.

While surface roughness is shown to have a link to layer formation rate, it may have a larger impact on the bond strength of the layer to the substrate. Further testing using tannic acid to generate layers and then the force required to remove a stud that has been glued to the layer should give the bond strength.

The tests are repeatable, and it is assumed that repeat tests would yield similar results.

Strengths and weaknesses

Some of the strengths of this hypothesis testing include:

- The tannic acid method for forming a black layer is already established.
- The rate of layer formation and layer thickness between the specimens of different roughness is consistent.

Some of the main weaknesses of the testing include:

- Only three surface roughness’ s were tested.
- Only R260 steel (representing the rail) was tested, future testing could also include wheel steel.

6.4 Conclusions

The iron oxide driven hypothesis was tested using the SUROS rig to compare leaf friction with and without the presence of a chelating agent (EDTA) to capture ferrous ions. It was found that when the chelating agent was present, the friction returned to clean contact levels, compared to leaf and water which remained low. This indicates that iron ions are involved in bonding (and therefore low μ), supporting the hypothesis. To further validate this hypothesis, rail steel and titanium specimens were placed in a tannic acid solution (as tannins/tannic acid are known leaf components), where a black layer quickly formed on the steel but not the titanium specimen. This again indicates that ferrous oxides/ions are involved in the bonding of the black layer.

The metallic substrate effects testing focused on the rate of formation of black layers on steel and titanium surfaces of different roughness' s using tannic acid to form the black layers. It found that the steel specimens with rougher surfaces generated thicker layers more quickly than those with smoother surfaces. This supports the hypothesis that a rougher surface with a higher true surface area, allows bonding to occur more quickly and possibly more strongly though this will require further testing. Again no visible layer was formed on the titanium specimens of any surface roughness.

Table 25 shows the conclusions reached for the layer formation hypotheses.

Table 25: Layer formation hypothesis conclusions.

Hypothesis	**Conclusion**
Iron oxide driven	Strongly agree
Metallic substrate	Strongly agree

7. LOW μ HYPOTHESES TESTING

7.1 Introduction

Leaf layer generation was either laboratory or field based, both of which came with their own benefits and drawbacks. Field testing was conducted at QRTC in Long Marston. Laboratory testing was carried out in various university tribology labs. The pendulum rig was used to test materials on the railhead, including water, leaves and preformed leaf layers.

Table 26: Test rig utilisation for low friction hypotheses

Method	Location	Low friction
HPT	Lab	✓
Pendulum	Lab + Field	✓
SUROS	Lab	✓

As shown in Table 26 two test rigs were used for generating the leaf layer in the laboratory; the HPT and twin disc SUROS test rigs. The HPT rig compresses test materials between two steel surfaces while applying torque, the resistance and movement of the specimens are closely monitored, and friction is calculated. The SUROS rig uses two counterrotating discs pressed against each other with a predetermined slip that is controlled by the rotating speed of the discs. Materials can be introduced to the contact, and the resulting effect on friction is measured and recorded.

The low μ hypotheses covered in this chapter are:

- Bulk leaves on the line
- Compressed leaf solid lubricant layer
- Viscous acid gel formation
- Supercritical water + high temperature and pressure
- Thin surface layers

7.2 Bulk leaves on the line

This hypothesis assumes that the number of leaves present on the railhead at the time of a wheel passing will have an effect on friction, possibly due to the leaves sliding over themselves. The leaves may also compact under a normal load and remain as several layers, which slide over one another and reduce friction. When large volumes of leaves are dumped on the line it may be possible that leaves land on top of each other on the

railhead. Simply put, this hypothesis aimed to answer the question; do more leaves mean lower friction?

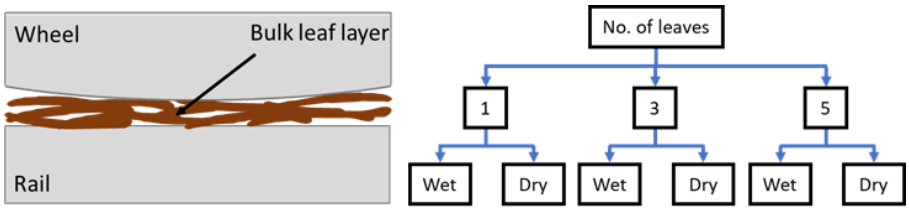

Figure 70: Bulk leaves on the line diagram

Since both wet and dry leaves are known to produce low friction levels, and train operators can and do suspend/delay trains after immediately heavy leaf fall [9], it was important to test both wet and dry leaves, see Figure 70 (right).

Test procedure

This hypothesis was tested using sycamore leaves and the Pendulum skid resistance rig, with 1, 3 and 5 leaves in the contact in both wet and dry conditions. The dry conditions simply involved placing the required number of leaves on the railhead and letting the pendulum fall and skid over them, replacing them in between repeats. The wet tests involved the same procedure, except the leaves had been soaked in water and sealed in a container for 24-48 hours prior to testing to ensure they were fully hydrated. Wet and dry railhead conditions were also tested to provide a reference point. In each case 8 repeats were done, the results were then converted to BRR values and averaged.

Results

The results of the pendulum tests are shown below in Table 26 and have been converted to BRR values using the method described in [163].

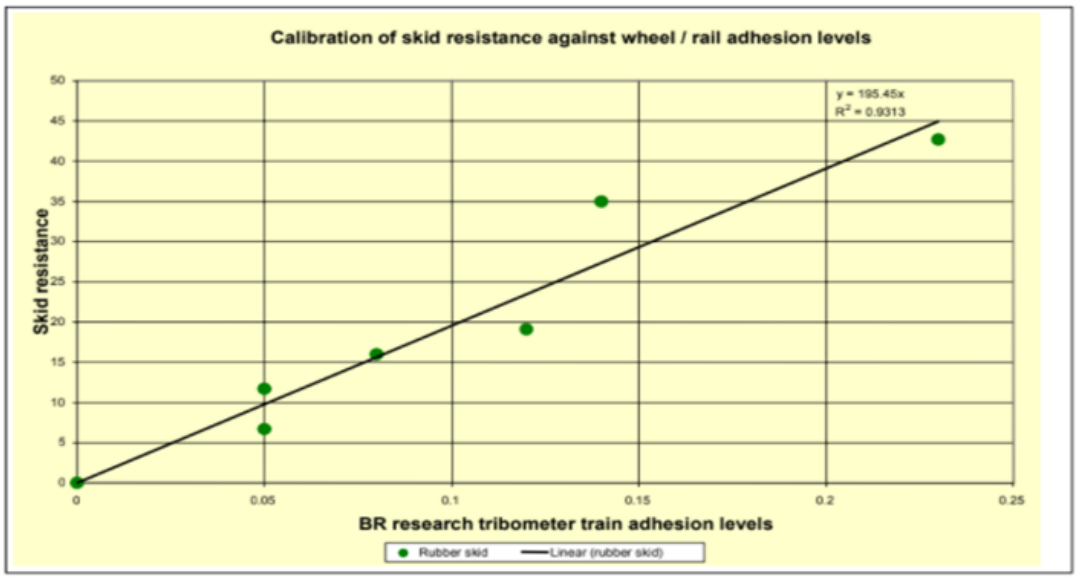

Figure 71: Pendulum reading to BRR tribometer conversion graph [163]**.**

Figure 71 shows the conversion that was used to convert pendulum skid resistance values to meaningful coefficient of friction values, that was developed by British Rail Research (BRR) [163].

Table 27: BRR converted pendulum values for sycamore leaves.

No. of leaves		BRR converted pendulum value								Avg.	St. dev.
		1	2	3	4	5	6	7	8		
Dry rail		0.37	0.32	0.33	0.37	0.38	0.35	0.38	0.33	0.35	0.02
Wet rail		0.12	0.11	0.11	0.13	0.14	0.15	0.12	0.12	0.13	0.01
Dry	**1**	0.38	0.35	0.35	0.24	0.34	0.25	0.32	0.15	0.30	0.07
	3	0.27	0.22	0.29	0.15	0.18	0.16	0.23	0.16	0.21	0.05
	5	0.31	0.23	0.28	0.19	0.17	0.31	0.28	0.33	0.26	0.05
Wet	**1**	0.09	0.13	0.15	0.15	0.21	0.18	0.13	0.18	0.15	0.04
	3	0.19	0.19	0.20	0.19	0.24	0.14	0.18	0.18	0.19	0.03
	5	0.26	0.29	0.28	0.26	0.23	0.23	0.20	0.16	0.24	0.04

A total of 8 tests were done for each number and wetness condition with the average and standard deviation shown in the table above. While the coefficient of friction values range from 0.13 up to 0.35, they still represent low adhesion similar to that measured on artificially generated layers at Long Marston.

It is worth noting that the tests were performed on a clean section of rail, though there likely was an oxide layer present on the surface. The effects of this oxide layer are not quantified as they are representative of real world conditions including leaves on the railhead.

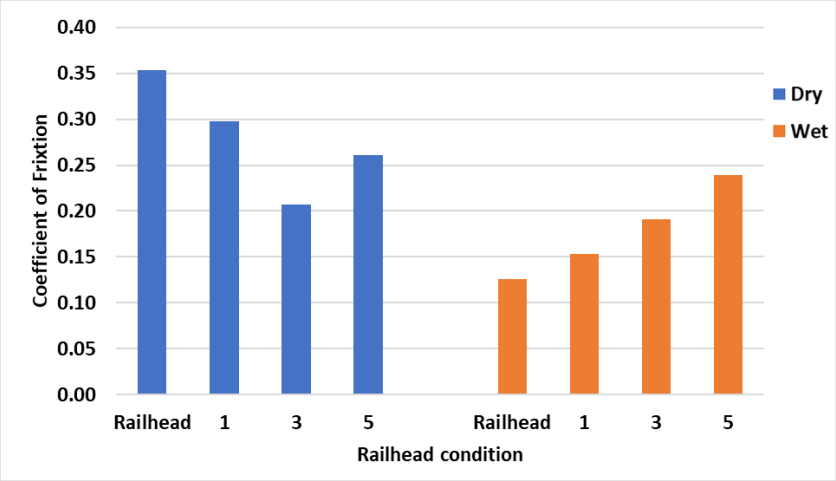

Figure 72: Wet and dry leaf friction.

Figure 72 shows the average friction levels, taken from the data in Table 26. In wet conditions the average friction increases from no leaves present steadily up to 5 leaves present. In dry conditions however, the lowest friction was shown when 3 leaves were present, followed by 5 leaves, 1 leaf and finally the bare railhead with the highest friction.

Discussion

Table 26 and Figure 71 show the BRR converted friction values measured by the pendulum skid resistance rig. As expected, the wet railhead gave much lower average friction than the dry railhead, at 0.13 and 0.35 respectively. Interestingly the wet leaves showed an increase in friction as more leaves were present, which could possibly be due to them tumbling over each other. It is more likely that the wet conditions cause the leaves to stick to one another and their higher thickness presents a more viscous shear for the pendulum to overcome, whereas the dry leaves slide over one another far more easily and produce lower friction. Dry leaf-leaf friction is lower than wet leaf-leaf friction. The latter makes sense as the increase in friction appears somewhat linear, as would the increase in leaf bulk thickness. During the experiment it was noticed that the wet leaves stuck to each other and resisted being pulled apart, almost giving the effect of them being one larger, thicker leaf.

The dry leaves show a different story, where more leaves seem to lead to lower friction with the exception of 5 leaves where the friction increased. This may also be due to more leaves forming a thicker bulk and reducing the space for the pendulum skid pad. While conducting the experiment it was noted that the dry leaves were a lot more brittle than the wet ones and frequently broke up into smaller pieces as the tests

progressed. The dry leaves were also able to slide over each other far more easily than the wet leaves, having much lower leaf-leaf friction.

Limitations for this test include the fact that the pendulum skid resistance rig is not as representative as other rigs when relating to the conditions found in real wheel-rail contacts. The contact pressure is far lower, the material taking place of a train wheel is rubber and not steel, the path of the pendulum glances the railhead instead of rolling along it.

However, that is not to say the test was a failure, as useful anecdotal information was obtained.

7.3 Compressed leaf solid lubricant layer

This hypothesis regards the solid lubricant theory in which the leaf layers prevent wheel-rail contact, acting as a solid lubricant (made only of leaf matter) and lowering friction in the contact. Both laboratory experiments and experiences from train operators support this theory [9].

Test procedure

A direct comparison of friction levels produced by 8 species of leaf matter as well as oak bark and graphite powder (a widely used solid lubricant) was conducted using the HPT rig. This additionally provided a useful opportunity to directly compare the friction reducing capabilities of different leaf species, as well as OBP which may be a suitable replacement for leaf matter in laboratory testing due to its commercial availability and consistency. An additional outcome of the tests was the generation of a small amount of leaf layer for FT-IR chemical analysis.

The top specimen is made of a piece of rail wheel steel while the bottom is made from a piece of rail steel (in this case R260) that has been machined to the shape and dimensions shown above in Figure 25 – left. The critical contact dimensions are shown on the right of Figure 25, with contact dimensions and predicted maximum torque and forces expected shown below in Table 27.

Table 28: Contact Dimensions and Predicted Force Requirements [140]**.**

Parameter	Value
Inner radius (mm)	5.25
Outer radius (mm)	9
Effective radius of friction (mm)	7.29
Contact area (mm^2)	169
Maximum normal load (@1000Mpa normal pressure) (kN)	168
Maximum torque (assuming 700Mpa shear stress) (Nm)	840

The procedure for HPT testing was taken from the literature [164] and is described in detail in the Appendix. Three repeats were conducted for each sample type, with a total of 30 tests in total, using 0.025g of leaf powder (or graphite/oak bark powder) plus 20µl of distilled water. The reason for the addition for the small amount of water was that it aided with the functionality of the testing, while only adding a relatively small amount of water.

The graphite powder used was a synthetic graphite powder with 99% purity and 7-11 micron average particle size. The OBP used was purchased as a commercial product.

Results

Figure 73 shows the friction measured by the HPT rig for clean rail (dry) and wet rail (water present), alongside the 2 leaf species, oak bark and graphite powder. The clean dry contact shows an initial sharp increase in friction from 0 to 0.6, before starting to level off and finishing at around 0.74. The wet contact friction also rises sharply to around 0.47, then a sharp drop before levelling off at around 0.23. Meanwhile all other test specimens show friction well below 0.1.

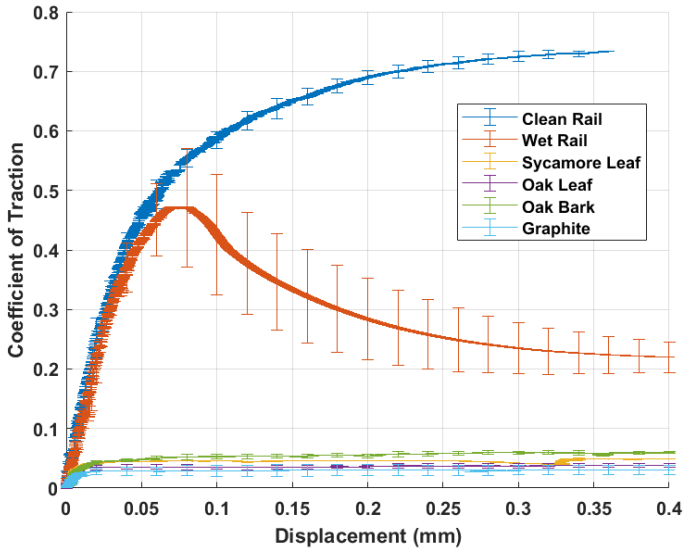

Figure 73: HPT friction levels of clean dry steel-steel contact, wet steel-steel, as well as sycamore leaf, oak leaf, oak bark and graphite powders.

Figure 74 shows the averaged curves for the 8 leaf species plus graphite and oak bark powders, with the dry and wet contact friction removed.

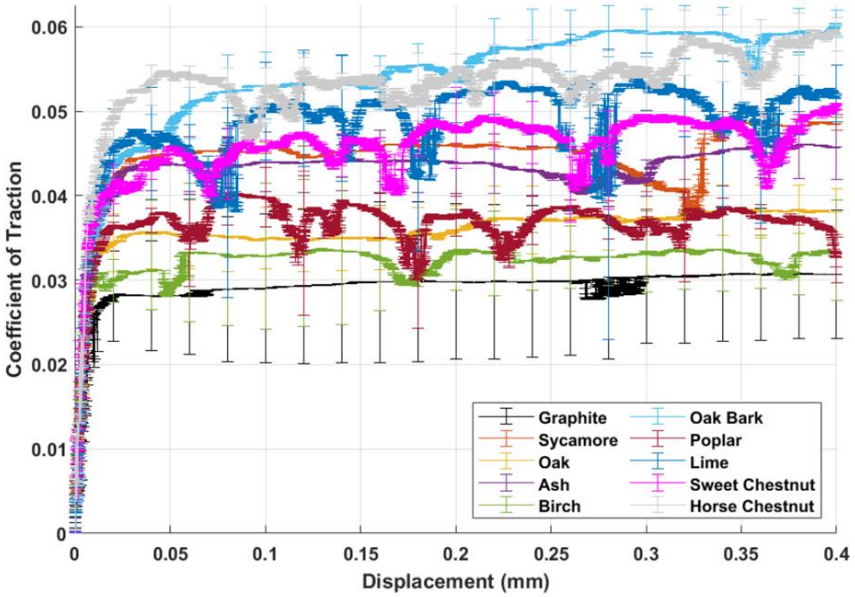

Figure 74: Average Coefficient of Traction for all materials tested.

The maximum friction observed was at 0.06, by horse chestnut and OBP, while the lowest was caused by graphite and at certain points silver birch powder. All of the friction shown in Figure 74 inhabits the region where braking would be affected, and the values are in good agreement with those from other research comparing friction of different leaf species [142]. They are also comparable to leaf layers measured in the laboratory and in the field, being lower than those measured with the pendulum rig (typical range for μ is 0.12-0.35 depending on the substance being tested and

environmental conditions), and the SUROS rig (typical range for μ is 0.05-0.15 for leaf mulch in water). It is expected that friction values for leaf matter in the HPT would be slightly different than those of other rigs and was intended more for comparing species with one another and solid lubricants.

To compare the friction levels of the different materials tested, the coefficient of traction between 0.05 and 0.4mm of displacement was isolated, this was averaged and is shown below in Table 29 alongside average and standard deviation for the three runs. The materials have been ranked by the average for the three run averages from lowest (graphite) to highest (common lime).

Table 29: CoT levels for materials studied.

Species	1st test	2nd test	3rd test	Average	St. dev.
Graphite	0.038	0.028	0.019	0.028	0.008
Poplar	0.035	0.034	0.032	0.034	0.001
English Oak	0.040	0.033	0.035	0.036	0.003
Sycamore	0.035	0.043	0.043	0.040	0.004
Silver Birch	0.029	0.059	0.034	0.041	0.013
Ash	0.040	0.045	0.041	0.042	0.002
Sweet chestnut	0.041	0.043	0.045	0.043	0.002
Horse chestnut	0.047	0.048	0.052	0.049	0.002
Oak bark powder	0.055	0.053	0.054	0.054	0.001
Common lime	0.082	0.040	0.043	0.055	0.019

As an addition to specific hypotheses investigation, a direct comparison of the friction behaviour of leaves of different species was carried out. The outcome of this could shed light on the validity of the "Troublesome tree" designations from the AWG manual [11].

Although leaf species can be ranked by their average friction values, it is notable that they are all still well within the ultralow region and when the standard deviation is considered, their behaviour is far less easy to distinguish.

FT-IR analysis

The leaf layers generated by the HPT rig were scanned using an FT-IR scanner to investigate whether layers of different species could be identified by their IR spectra.

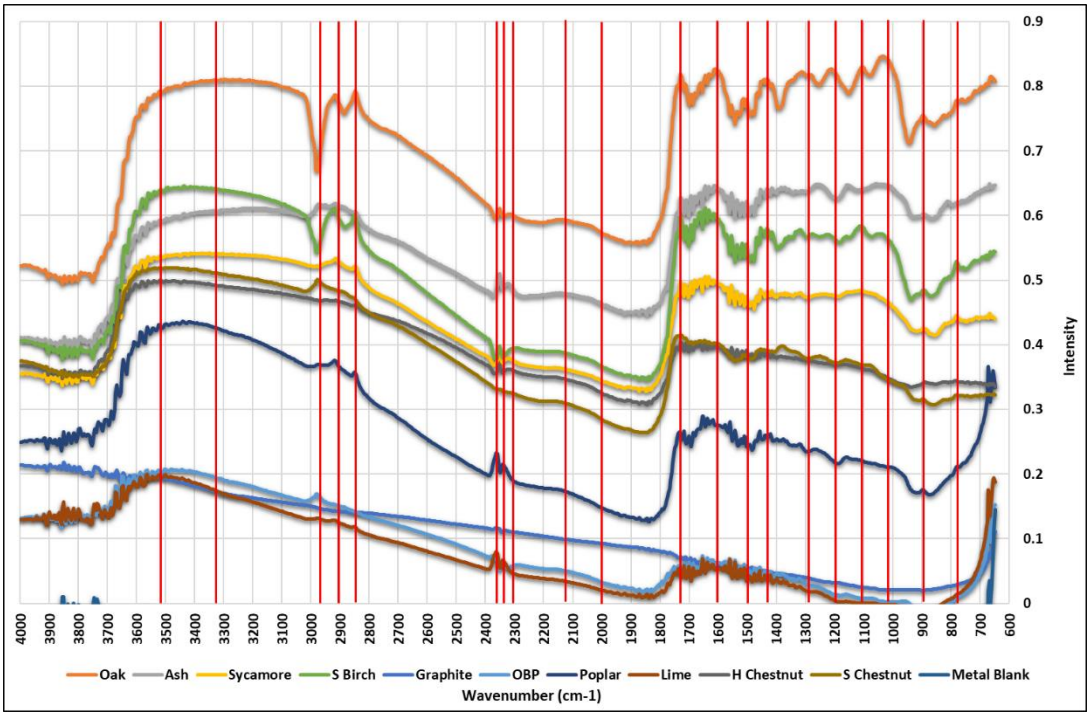

Figure 75: FT-IR spectra for rail specimens from HPT tests.

Figure 75 shows the FT-IR spectra collected on layers of the 8 species, plus graphite and oak bark powder and a metal blank (the blank should read 0 as metals cannot be detected by FT-IR). Each spectra shown above is the average of 3 readings taken at different points of the same samples. Significant peaks in the spectra are listed in Table 30 below, alongside wavenumber range, chemical assignments, species exhibiting the peaks and a reference to support the assignment.

Table 30: Wavenumber peak assignment for FT-IR spectra.

Wavenumber range (cm^{-1})	Chemical assignment	Species exhibiting peaks	Ref
790 – 840	C=C bending alkene	Oak, ash, sycamore, silver birch, OBP, poplar, lime, sweet chestnut	[165]
900	C-H bonding	Oak, ash, sycamore, silver birch, poplar, horse chestnut, sweet chestnut	None
1020	C-N stretching	Oak, ash, sycamore, silver birch	[135]
1100 – 1120	C-O stretching	Oak, sycamore, silver birch	[165]–[169]
1200	C-C, C-O,	Oak	[165]–[169]

	and C=O stretching		
1290	C-O stretching	Oak, ash, sycamore, silver birch, OBP	[165]–[169]
1380–1420	C-H bending, Aliphatic, and O-H phenolic	Oak, silver birch	[165], [166], [168], [169]
1700-1730	C=O	Oak, ash, sycamore, silver birch, OBP, poplar, lime, horse chestnut, sweet chestnut	[165]–[169]
2350 – 2370	Carbon dioxide (CO_2) \ (Artifact from device)	Oak, ash, sycamore, silver birch, OBP, poplar, lime, horse chestnut, sweet chestnut, graphite	[165]–[169]
2840 – 2980	CH stretching, Aromatic-CH_2-OH, Alkane	Oak, ash, sycamore, silver birch, OBP, poplar, lime, horse chestnut	[165]–[169]
3200 – 3550	O-H stretching (alcohol) Or Carboxylic acid	Oak, ash, sycamore, silver birch, OBP, poplar, lime, horse chestnut, sweet chestnut	[165]–[169]

Discussion

In Figure 74, all friction materials tested produced COT levels between approximately 0.06 and 0.02 which are well below the critical safety level of 0.1. The friction levels produced by the leaf powders are comparable to those of graphite powder. When the average frictions are scaled against graphite powder, poplar showed the lowest increase at only 21%, while common lime showed the greatest increase at 96%. OBP showed the second highest average friction, at 92% more than that of graphite. Though these numbers might sound large, it should be noted that all materials tested showed average friction levels of 0.055 and lower, and all but OBP and common lime falling into the exceptionally low ($0.02<\mu<0.05$) category [128].

With friction levels all being within 100% of graphite, it can be stated that leaf powders do act as solid lubricants in the contact when dry, and that it is likely this hypothesis is true and exists alongside other low μ hypotheses.

Since Fe, and elevated pressures and therefore temperatures were also present in the contact, it is possible that they would have also played a role in reducing friction. However, the fact remains that dry leaf powder was tested in a contact that resembles the wheel-rail contact and low adhesion was produced.

Analysis of the FT-IR spectra was not able to provide a reason why one leaf species would give different friction to another or identify a leaf layer from one particular species over another. Despite some peaks only being exhibited by a smaller number of species, there is still not enough to definitively identify a particular species.

7.4 Viscous acid gel formation (from a formed leaf layer)

This hypothesis involves a viscous acidic pectin gel being formed within the leaf layer, which is then released on the surface allowing the wheel to pass over and shear it [25]. FT-IR analysis has shown the presence of pectin and cellulose in leaves, both of which are water soluble and would be expected to be released in light rain or morning dew [9]. It has been presumed that the Fe ions assist the pectin transformation into pectin gel [25], thus preventing wheel rail contact and lowering friction via EHL (ElastroHydrodynamic Lubrication) under the right conditions.

Test procedure

Phosphate-Buffered Saline (PBS) solution can also be referred to as an acidity controller due to its ability to bring the pH of a solution to a neutral level (~7). PBS is a water based salt solution that contains water, sodium chloride, disodium hydrogen phosphate and in some cases potassium dihydrogen phosphate and potassium chloride. Its main applications include the medical and research fields. The presence of PBS ensures that the mixture formed in the contact cannot be acidic as the solution is immediately neutralised due to the excess of buffer. The pH is maintained at neutral (~7), inhibiting any acid gel formation. PBS is also non-toxic to most types of cells, including those found in leaves.

Testing for this hypothesis used the exact same test procedure as the iron oxide driven hypothesis, using the SUROS rig. The only difference was that the sample fed into the contact was 2wt.% blended brown sycamore leaves and 98wt.% PBS solution. Again, the mixture was left for 24 hours to allow the leaf particles to absorb water and achieve a similar specific gravity, meaning they fed correctly from a 25ml syringe and plastic tube. The sample feed rate was also 1 drop per second for 30s.

Results

Figure 76: Averaged SUROS friction for sycamore-water and sycamore-PBS

Figure 76 shows the average friction for sycamore-water and sycamore-PBS, which has been split into three phases using vertical red lines, similarly to Figure 65. In the first 30s the discs are run against each other under load to establish friction levels. For the following 60s the contaminants are fed into the contact at a rate of 1 drop per second. In the final 210s the discs continue to run under load to allow friction to naturally develop. In both cases the friction remained relatively low.

Table 31: Average friction levels for the different test phases

	0 – 30s	**30 – 60s**	**60 – 210s**
Sycamore-water	0.61	0.18	0.11
Sycamore-PBS	0.49	0.09	0.14

Table 31 shows the average coefficient of friction for the three test phases for sycamore-water and sycamore-PBS solution.

Discussion

As shown in Table 31 the initial running in friction levels were very similar (within 19% of each other). Between 30 and 60 seconds the sycamore-PBS friction was half of that of the sycamore-water, at 0.09 and 0.18 respectively. In phase 3 (final 210s) the sycamore-PBS rose to be 21% higher than sycamore-water, which is still classed as medium low [128]. The fact that the friction for sycamore-PBS did not return to clean dry levels and instead remained very similar to sycamore-water indicated that the addition of PBS had little to no effect. This finding casts serious doubt on the validity of the viscous acid gel formation hypothesis.

Although the friction generated by the sycamore and water did not fall unto the ultra-low (μ>0.05) category, it was in line with other leaf-water test results that typically reduce friction to 0.1 and lower. Further chemical analysis of leaf matter may reveal the relative quantity of acidic gels present in water saturated leaves and black leaf layers.

7.5 Supercritical water + high temperature and pressure

This hypothesis was covered in section 2.7.1 and states that water present in the wheel-rail interface is elevated to supercritical conditions where pressure is greater than 22.1 MPa and temperature is greater than 374 °C. Both of these conditions have been met in the HPT interface as the pressure applied (900MPa) in the test far exceeds the requirement for supercritical water, and previous testing with a thermocouple present near the contact showed an increase in temperature that should be enough to allow water to go supercritical. Under such conditions the microstructure of the material could change [147], creating a third body layer.

Test procedure

The HPT rig was used to create the bonded leaf layer(s) and examine the effects of supercritical water. These tests were done at room temperature (although thermal conditions were elevated in the HPT contact) using the exact same procedure as that used in section 7.3. The test procedure is described in 11.2 of the Appendix. In this case clean rail (dry metal-metal contact) and wet rail (water present in the contact) were also tested.

Results

Figure 73 from section 7.3 shows the HPT friction for clean rail (dry) and wet rail (water present), alongside the 2 leaf powder species, oak bark powder and graphite powder. The clean dry contact shows an initial sharp increase in friction from 0 to 0.6, before starting to level off and finishing at around 0.74. The wet contact friction also rises sharply to around 0.47, then a sharp drop before levelling off at around 0.23. Meanwhile, all other test specimens show friction well below 0.1.

Discussion

Water changes upon becoming supercritical, the hydrogen-bonded structure breaks down, becoming less polar. Relatively large amounts of organic compounds as well as permanent gases such as oxygen become available for chemical reaction. Diffusion rates are >100 times than those of water at room temperature [170]. Because more oxygen is present in the interface, the rate of oxide and other third body layer

formation would be accelerated. Oxides and third body (leaf) layers have been known reduce friction to dangerously low [59], [62], [64], [66], [67], [171].

Hydrogen peroxide is known to be formed during the reaction between water and oxygen on ferrous surfaces. H_2O_2 reacts with Fe to form various iron oxides. The formation of hydrogen peroxide during the oxidation of metals in supercritical water (containing dissolved oxygen) is crucial to this oxidation process [172]. If supercritical water is formed, then oxide formation will happen more quickly than compared to normal water oxide formation processes.

Future work could investigate the friction behaviour of water using the HPT rig at various pressures (and therefore temperatures) from 900MPa (as used in these tests) down to below the threshold for supercritical water. If there is a difference in friction for when water is supposed to be supercritical, this could further prove/disprove the hypothesis.

7.6 Thin surface layers

This hypothesis regards the leaf solid lubricant theory in which the leaf matter reacts with the metallic substrate to generate a thin organometallic compound layer (organic compounds reacted with iron oxides/ions) that prevents steel on steel contact and acts as a solid lubricant, lowering the coefficient of friction. This layer could exist above or underneath the compressed leaf solid lubricant layer as a separate unreacted layer. XPS is used for characterisation of thin surface layers. Literature precedence exist for rail and low adhesion applications with XPS used as the analysis tool. Access to a low adhesion site in the UK was granted and comparisons were made with data gathered in the field against the published data to identify key trends.

Test procedure

This hypothesis was assessed using XPS (X-ray Photoelectron Spectroscopy) analysis of leaf layers taken from a section of live track in the UK known for low adhesion and comparing them to artificial layers generated during field testing at the QRTC test track at Long Marston. C The QRTC leaf layer generation procedure is described below in section 7.7, where the friction of different leaf species is compared.

Figure 77: UK leaf layer (left) and QRTC layer (right).

Figure 77 shows leaf layers from live track in the UK and QRTC, which were scraped off the railhead and into a piece of aluminium foil (aluminium was chosen as it is not normally found in the wheel-rail interface and therefore would be easily identified and omitted from ESCA results) which was folded up and placed into sample bags to avoid any cross contamination. The live track layer had an inconsistent appearance, with a distinct dull black colouration. The QTRC layer had a smoother, more consistent appearance with black colouration along the contact width and squashed brown matter either side.

Results

Because the % atomic concentrations for oxygen (15-30%) and carbon (70-80%) were so high compared to the trace elements (>3.5%), they are shown separately in Figure 78 and Figure 79 for scaling purposes.

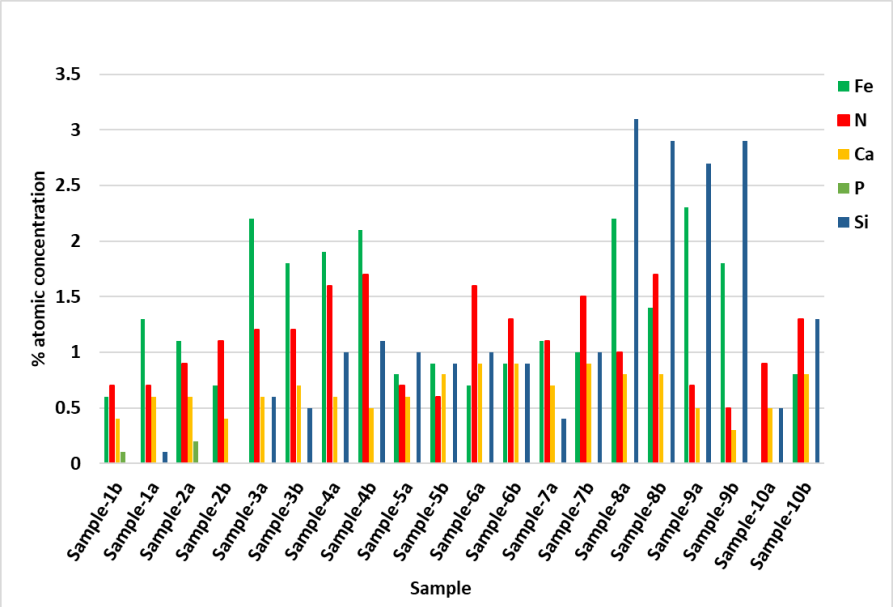

Figure 78: Trace elements % atomic content of live track leaf layers.

Figure 78 shows the % atomic concentrations for trace elements (Fe, N, Ca, P and Si) for scans of 10 black leaf layer samples from locations spread across an approximately 4km section of live track. Each sample was scanned twice so that any major inconsistencies would be apparent. Trace element concentration data was not available for the QRTC layer scrapings as a comparitive sample was not analysed using XPS.

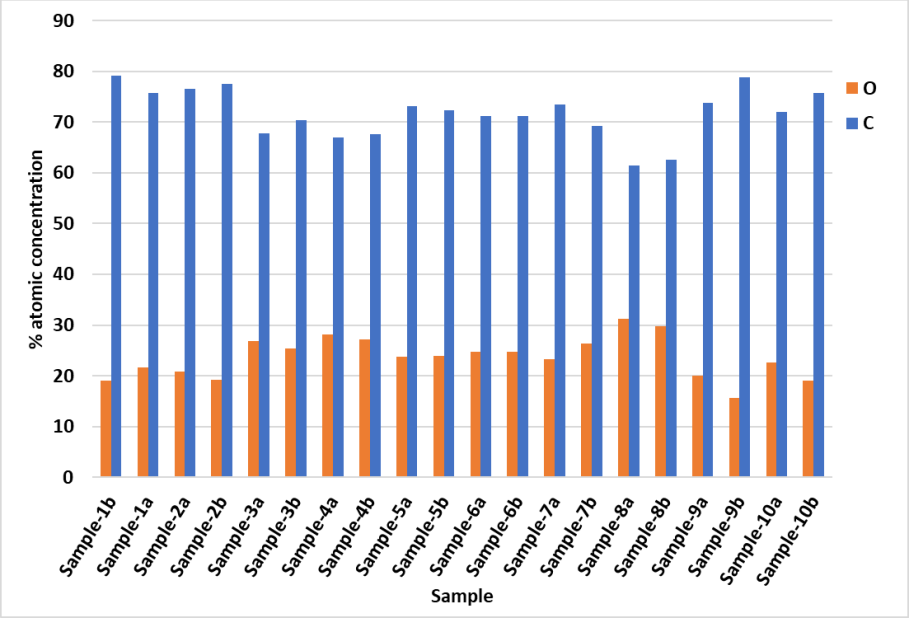

Figure 79: Carbon and oxygen % atomic content of UK leaf layers.

Figure 79 shows the O and C levels for the UK layer. The average oxygen concentration was 23.7% with a standard deviation of 3.9%, the average carbon concentration was 71.8% with a standard deviation of 4.8%.

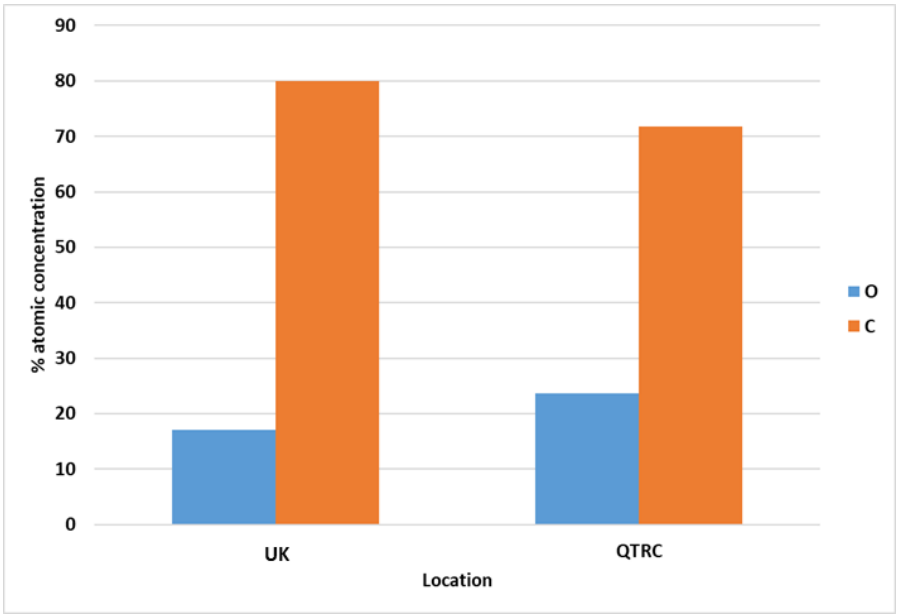

Figure 80: Carbon and oxygen % atomic content of UK and QRTC leaf layers [111].

Figure 80 compares the averaged % atomic concentrations of oxygen and carbon from the UK (blue bars) and QRTC (red bars) [111]. The average oxygen and carbon % atomic concentrations from QTRC were approximately 18% and 80% respectively.

Discussion

The variation in Si levels shown in Figure 78 indicates that sand and/or traction gel application was present at some locations but not others.

Figure 79 shows a high level of consistency between the carbon and oxygen concentrations of the 10 samples, both having standard deviations of less than 5%.

O and C % atomic concentrations from the UK are in good agreement with published data from QTRC where leaf layers were created, tested and shown to cause low adhesion. In the same paper it was reported that mainline track had detected Fe and Si, and that is in good agreement with the dataset from the UK [111]. XPS analysis confirms that there was a leaf layer present (as shown in Figure 3 from [111]), as its chemical composition was very similar. The largest oxygen component was seen at a binding energy of 533.1 eV, as could be expected in cellulose.

The key species noted for the high resolution carbon spectra from the UK are in good agreement with the data from the literature. These are listed below:

- C-C/C-H
- C-O/C-N
- C=O
- O-C-O
- O-C=O (carboxylate, COOH)

The XPS peaks attributed to C1s were analysed and found to agree strongly with those from the literature, where the binding energy of the peaks were attributed to C-C (284.8 ± 0.1eV), C=O (286.5 ± 0.1eV) and C-O (288.5 ± 0.1eV) [173].

In the UK data, Si is present in every sample which indicates that sanding was in operation (for braking) and/or the presence of traction gel, suggesting that low adhesion was experienced.

We have compared real mainline data with artificial layers known to cause low adhesion. They are chemically similar to those reported in the literature where leaf layers were created and demonstrated to negatively impact braking performance. The % atomic concentration levels observed from XPS analysis of artificially generated layers closely represent those of naturally occurring layers from the field.

As the XPS analysis only penetrates to a depth of approximately 10nm on the surface of the film, this gives us insight into the top of the upper layer where contact is made with the wheel and friction is reduced. The findings agree with published literature on

low adhesion. It is possible that below XPS penetration depth, the layer could be formed differently and that has not been explored currently. One possible method could involve using a Scanning Electron Microscope (SEM) to look at the cross section of layer fragments to see if there was a different chemical makeup at different depths.

This testing supports the thin surface layers hypothesis by showing that different pieces of black layer have different chemical compositions, which must have been created at different points in time by leaf matter being formed into a layer on top of other existing leaf layer in thin layers.

7.7 Field leaf layer generation

The aims of field testing were:

- Generate a representative leaf layer with specific leaf species.
- Test the friction of the layers of different species.
- Test the pull of force of different layers.
- Collect railhead scrapings/samples of the layers of different species.

The main aims of generating leaf layers in the field were to assess the conditions in which the layers did/did not form and identify any differences between leaf species under different conditions, generate leaf layer samples that can be chemically analysed and compare them to lab generated leaf layers. Where possible measure the thicknesses of the layers as well as the pull off force (using torque measuring screwdrivers) and the friction levels of the layers using the pendulum and tribometer rigs.

Figure 81: Vanguard shunter, pendulum rig and eddy current probe (left to right).

Testing the generation of leaf layers for the four different species (plus commercially sourced oak bark powder) in the field was extremely important and insightful. Full scale field testing was all conducted at QRTC. The locomotive used was a Vanguard shunter (see Figure 81, left) with tread brakes and two axles, therefore giving two wheel passes per loco pass. The tread brakes are different from most modern trains as they are fitted with inboard disc brakes. The tread brakes on the shunter at QRTC would prevent any

carry down via the wheels and may introduce brake dust and heat up the surface of the wheels slightly. This was noted but could not be avoided. Testing dates from 2020 to 2022 were:

- 26/11/20
- 20/1/21
- 21/1/21
- 17/2/21
- 19/2/21
- 30/3/21
- 14/4/21
- 12/5/21
- 18/1/22

One additional benefit of a spread in testing dates was a variation in weather/environmental conditions. Rainy days were avoided or cancelled, as previous testing under these conditions proved very difficult. This was due to excess water dispersing the leaf material out of the contact as well as further down the line. Additionally, very windy dates were avoided as leaf matter was easily blown off the railhead before the shunter could roll over and embed it.

Due to variation in weather conditions, the specific method (referring to number of rolling and braking wheel passes) was changed slightly for each day. Individual assessment and judgement were used, based on how the layer appeared to be forming. If the leaf matter appeared to be compacting and bonding to the railhead, fewer rolling passes would be used and braking passes would be employed sooner. For the same reasons it was not always possible to test all leaf types on every test date.

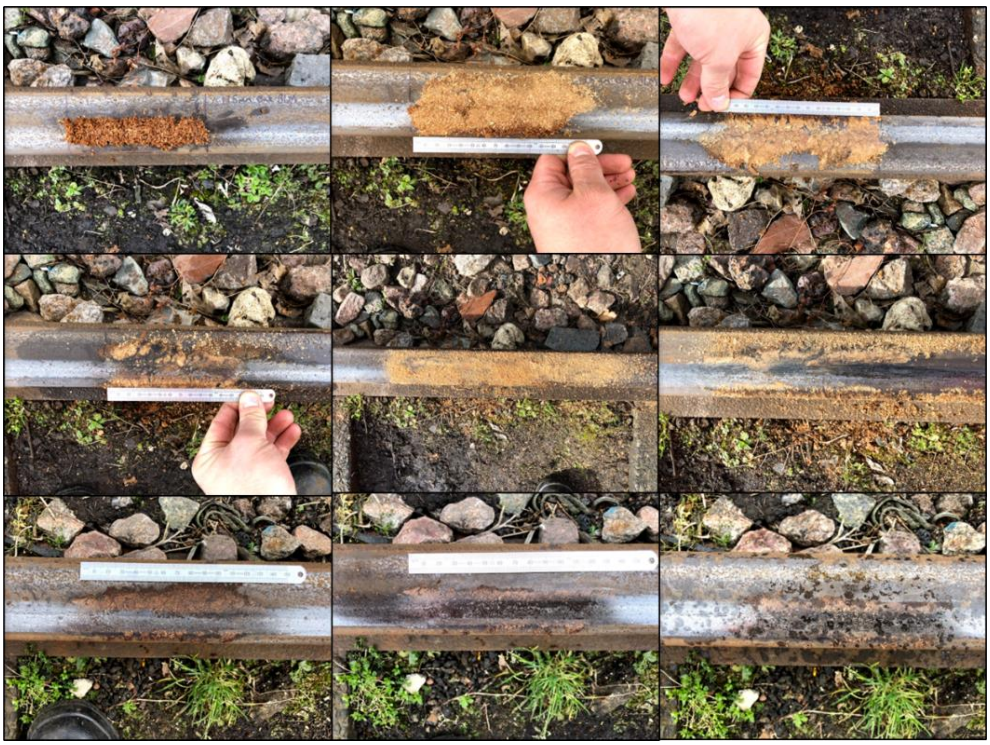

Figure 82: Leaf layer generation steps, from top left to bottom right.

Typically, successful leaf layer generation involved the following steps (as shown in Figure 82):

1. Clean the railhead using a railhead scrubber with a wire wheel brush, this is optional but does improve chances of successful bonding by removing other railhead contaminants.
2. Mix the brown leaf mulch with a small amount of water, until it reaches the consistency of damp sand and is able to hold itself together on the railhead. The amount of water required also depends on the environmental conditions;
    a. If windy, more water may be needed to keep the leaf mulch in place and prevent it from drying out too quickly.
    b. If sunny, the leaf mulch may need lightly spraying with water between train passes.
    c. If cold/frosty, not much more water is required.
    d. If heavily raining, the chances of success are significantly reduced.
3. Apply generously to the railhead, particularly on the running band and lightly press down so that the leaf matter is not blown off by any wind.
4. Roll over with a train 3-4 times, checking the development between each pass & axle passes.
5. If successful, a compact biscuit type layer will be formed (see upper right image of Figure 82), at this point the layer should be lightly misted, followed shortly by 4-6 braking passes. Fully sliding passes are preferential as they were observed as speeding up the transformation of the layer from brown to black. This indicates that a high pressure combined with mechanical shearing are two components that are important in forming the black layer.
6. If the layer begins to break apart during the braking passes, more leaf mulch may be required along with a light spray of water (see middle centre and right image of Figure 82).
7. Continue with braking passes until the bonded black leaf layer is formed (see lower three images of Figure 82).

The procedure outlined above is intended as a rough guide and would likely require individual interpretation and adjustment depending upon the prevailing weather and experimental setup. Additionally, it is worth noting that the train used was a shunter with two axles and tread brakes, which must be considered when counting the number of wheel passes.

Table 32: BRR converted average leaf layer friction values from Long Marston.

Species	BRR leaf layer CoF
Oak	0.17
Sycamore	0.17
Ash	0.14
OBP	0.14

Table 32 shows the average BRR converted Pendulum friction values of leaf layers made using oak, sycamore, ash and OBP. All layers measured were fully formed and were dry at the time.

The field leaf layer generation was successful as brown and black leaf layers were generated for all leaf species tested. The friction of the layers was measured using the pendulum rig and converted to BRR values, with friction values being between 0.14 and 0.17 which are low for the pendulum rig and are in line with natural leaf layers measured at known low adhesion hotspots. The pull off force was measured using torque measuring screwdrivers, however due to issues with implementation and inconsistent results they have been omitted from this project. Railhead scrapings were collected and used for FT-IR comparison in section 7.6.

Strengths and weaknesses

Some of the strengths of this testing are that; it used full-scale rail equipment including a shunter and full-scale track, it was conducted in the field and therefore was subject to representative environmental conditions, the progression of leaf material from leaf mulch to brown layer to bonded black layer was clearly shown and reported on, and friction, layer thickness and contamination scrapings were obtained and compared to 'natural' leaf layers.

Some of the weaknesses of this testing are that; a tread braked vehicle was used which may have introduced brake dust and the pull off testing did not yield any usable results.

7.8 Conclusions

It is assumed that real world leaf layers exhibit a combination of all of the hypotheses described in this chapter, except from the acid gel hypothesis. It could be speculated that the hypotheses mechanisms will occur in the following order: bulk leaves on the line, compressed leaf solid lubricant layer, supercritical water + high temperature and pressure and finally thin surface layers.

The bulk leaves on the line hypothesis was tested using a combination of 1, 3 and 5 wet and/or dry leaves using a section of rail and the pendulum skid resistance rig. It was found that wet rail gave the lowest friction while dry rail gave the highest. 1 wet leaf gave low friction, which increased steadily for 3 and then 5 leaves. 1 dry leaf gave high friction, which was lowered for 3 leaves, but then increased for 5 leaves. The exact reason for this was unclear however it was noted that wet leaves stuck to each other while dry leaves did not. In both wet and dry conditions 5 leaves gave higher friction than 3 leaves, possibly due to an effect of their "bulkiness", however, further testing would be needed to confirm this, possibly using the FSR. In conclusion, an increase in the number of leaves present on the railhead leads to a reduction in friction if the leaves are dry but an increase in friction if the leaves are wet.

The compressed leaf solid lubricant layer testing used the HPT rig to test 8 leaf powders against OBP and graphite powder (an established solid lubricant). It found that the friction levels were comparable between leaf and graphite powders, which all exhibited varying degrees of stick-slip. We can say that it is likely that this hypothesis is valid. At this point there is not enough distinction between the friction levels of each species to definitively state which species cause lower friction than others.

The viscous acid gel hypothesis testing used the SUROS rig to test leaf in water against leaf in PBS solution (acidity regulator), where the pH should be neutralised. It was found that the friction both with and without the acidity regulator remained low, suggesting that the presence of an acidic gel does not have much impact the friction. Therefore, we can say that this hypothesis is likely untrue, however more testing would be able to confirm this. This additional work could include more chemical analysis of leaves and black leaf layers with a specific focus on the presence of acidic pectin gels, and/or more testing using the same method as above (mechanical testing plus chemical analysis), but with additional leaf species.

The supercritical water + high temperature and pressure hypothesis used HPT data comparing a clean dry contact to a wet contact. It is known that the conditions of the HPT rig are high enough to send water supercritical, and under these conditions water is known to degenerate and then form into H_2O_2 which is known to react with iron to form iron oxides, which are known to bond with leaf matter to form the black leaf layer. Therefore, we can say that this hypothesis is likely true, but more work would be needed to fully confirm, such as chemical analysis of the specimens after testing with water to identify the oxides present and if possible, the presence of H_2O_2.

The thin surfacer layers hypothesis involved using XPS to analyse black leaf layer scrapings taken from a section of railway known for low μ. Since XPS only penetrates the top 10nm of a surface, and different layers were observed we can say that this hypothesis is likely valid. More work involving using a Scanning Electron Microscope (SEM) may be able to prove this conclusively.

From testing on all rigs, as well as in the field at Long Marston it was found that fully formed black leaf layers require a combination of; leaves, water (relatively low levels work better), steel (for the iron content), elevated temperatures and pressures, plus mechanical rolling and/or sliding. The correct weather is also crucial, during strong wind and rain no layers could be made at QRTC.

Table 33 below shows the conclusions reached for the low μ hypothesis.

Table 33: Low μ hypothesis conclusions.

Hypothesis	**Conclusion**
Bulk leaves on the line	Somewhat supports
Compressed leaf solid lubricant	Strongly supports
Viscous acid gel	Disproves
Supercritical water + high temperature and pressure	Somewhat supports
Thin Surface layers	Somewhat supports

8. CRCL STUDY AND MODEL DEVELOPMENT

8.1 Introduction

Several companies provide low adhesion prediction services, similar to weather forecasts, however, they are commercially sensitive, and the methods used are closely guarded.

145he rail industry aims to manage low adhesion effectively and efficiently (particularly those caused by leaf layers) by changing timetables, keeping drivers informed and planning more effective mitigation such as cleaning the rail. Several companies offer low adhesion prediction services, similar to weather forecasts, however, these do not account for specific physical features and present tree species. MetDesk is an example of a low adhesion prediction service that uses a temporal format rather than a spatial format (see section 2.5.3) and operates similarly to a weather forecast. Therefore, a model is needed that can account for these, providing those involved in track, infrastructure and vegetation management with more detailed information on where and why there might be a higher risk of low adhesion due to leaf layer formation, therefore with a spatial format.

This chapter describes the development of a model for predicting the risk of low adhesion for specific rail sites (and not on specific days). Initially based on a case study of the Chiltern Railways Company Limited (CRCL) network, this model is intended to be rolled out onto other networks and locations. The model utilises inputs from field vegetation surveys, online sources such as Google Maps and Street View, as well as laboratory testing (including detailed analysis of leaf chemistry) to create a comprehensive spatial low adhesion forecast. It is intended to have a simple, modular design, with open source technology so end users can make small adjustments for their specific needs. The outputs from the model will be displayed in an easily accessible and understandable manner (i.e. heat maps comparable to weather forecasts), enabling informed decisions to be made regarding vegetation management and railhead cleaning techniques.

Throughout the development process assumptions were made, some of which are detailed in the section 8.6.1.

Overview of CRCL

The case study route chosen is part of the Chiltern Railways network. CRCL, founded in 1996, is a TOC owned by Arriva UK Trains. CRCL operate inter-city and regional stopping services, see Figure 83 below.

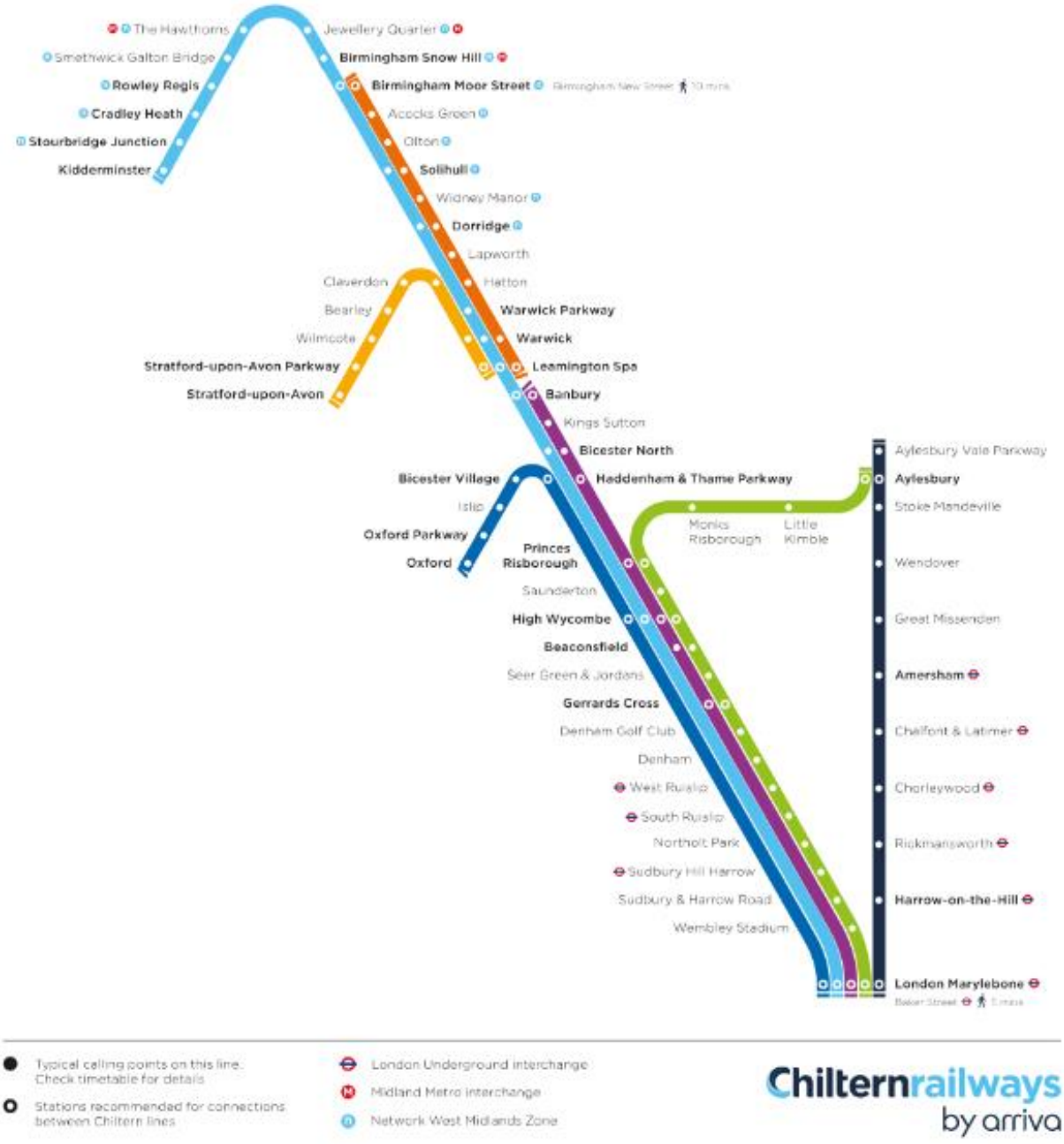

Figure 83: CRCL Network Map [174]

Analysis of CRCL wheel slip data was carried out. This data was collected from the 'COMPASS' incident management software and the On Train Data Recorders (OTDRs).

8.2 Aims, objectives and deliverables

Aims

The aim of this study was to investigate data (provided by CRCL) on WSP activation to identify high, medium and low risk sites (based on historical WSP events). Then study these locations to find any patterns and/or trends in the parameters. Once the key parameters have been identified, produce a model using one half of the location data, then validate using the second half of the data.

Objectives

To ensure optimal usage, application and modification of the model, the following objectives apply:

- Identify trends in the WSP data regarding location, frequency, timing (date and time).
- Research and decide on a set of parameters that the model shall assess locations on.
- Conduct vegetation surveys of CRCL locations.
- Develop the model using half of the locations and rank the parameters.
- Validate the parameter ranking on the second half of the locations.

Allow the user to input new wheel slip incident data to update the model' s inputs.

Deliverables

The model is designed to deliver:

- A risk category rating for each location analysed.
- A suggestion on which parameters are more likely to need attention to resolve the risk issue.

It is noted that the weather data gathered and displayed earlier in this thesis does not inform the model directly and was intended to widen the understanding of leaf induced low adhesion as a whole.

8.3 Model specification

To ensure optimal usage, application and modification of the model, the following requirements apply. The model shall:

- Be simple enough to allow the user to update location information.

- Ensure railhead contamination risk is easily determined using basic site observations (e.g. proximity of vegetation to track) and simple measurement tools (e.g. tape measure, infrared thermometer).
- Have an open, modular design that can be adapted/incorporated into a larger autumn performance tool.
- Allow users to input new WSP data to update the model, for both vegetation state and WSP activation.
- Have a spatial resolution of one station per analysis, or approximately one station in cases where the location is not at a station.
- Have minimum WSP data input requirements that include; location, time, date, attribution (reason for activation) and headcode.

The model assesses low adhesion risk using certain parameters, with a specific scoring mechanism. Parameters are split into fixed and temporal. Fixed parameters will not change between assessments and include:

- Local terrain – track gradient, whether the track is in a cutting/flat/embankment
- Signal diagram information – speed limits, number of services, location of signals etc.

Temporal parameters may change over time and include:

- Distance of treeline from the outside rail, linear spread/density of treeline etc.

Each parameter is expected to contribute to the risk of leaf layers formation and wheel slip occurrence. The magnitude of and relationship between parameters is still unknown.

8.4 Methodology

The model development involved the following stages:

a) Receive WSP raw data
b) Analyse the raw data to help with identification of key locations
c) Parameter selection
d) Model set-up
e) Signal diagram analysis
f) Site investigation
g) Weighting and scoring adjustments
h) Model validation and refinement

The rough order of operations is listed above, though they were not followed specifically in that order as some of the outcomes of the later stages affected earlier stages.

Receive WSP raw data

The data sample used consisted of 109 instances of WSP activation between January 2018 and October 2020. Though this number may seem small for a whole fleet, it is worth noting that CRCL is a relatively small TOC and the available data set reflected this. The raw data was analysed to identify trends in three main areas: date, time of day and location. Date information was used to establish when in Autumn the model would be most effective. Time information should be used to aid RHTT timetabling. Location data was the most prominent factor and was used to investigate track and lineside features that contribute to a higher risk of leaf layers forming.

Data points identified from the raw data included: the date and time of occurrence, headcode (for timetable investigation), the name of the nearest station, delay (mins) and cost (£). Originally the severity of the delays was considered, including the duration and cost, however, this led to a largely complicated model as subsequent delay to preceding trains was difficult to quantify. Therefore, only the frequency was used to inform the model as it was found to provide enough meaningful information. It could be possible that the delay severity and cost could be incorporated into the model in the future.

Analyse the raw data to help with identification of key locations

Figure 84 shows monthly WSP activation between January 2018 and October 2020.

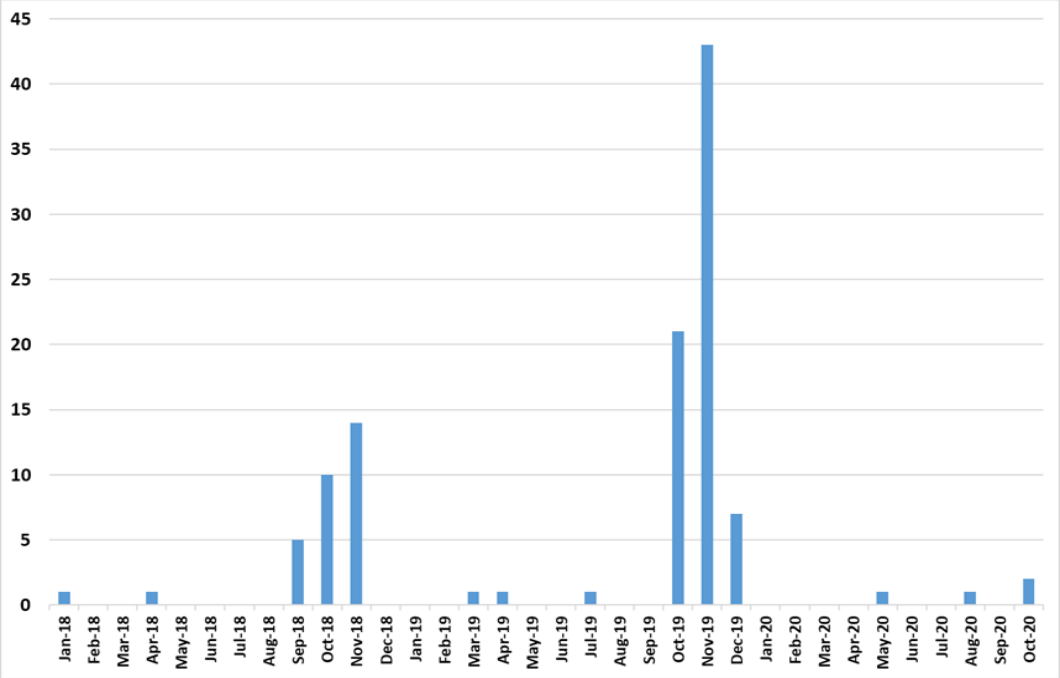

Figure 84: Month vs frequency of WSP activation

Figure 84 shows that the WSP activation most frequently occurred in September-November 2018 and October-December 2019. This is in line with what is generally considered the Autumn season (late September to late December), indicating that the model will be most effective between September and December. The reason the month versus frequency was investigated was to see if any insight could be found to give extra supplementary information alongside the model. The model is designed to be spatial and work alongside a temporal model (such as MetDesk for example).

Autumn weather in 2019 was noted for having notably high rainfall in large parts of the UK (fifth wettest on record) and a mixture of cooler than average and warmer than average days.

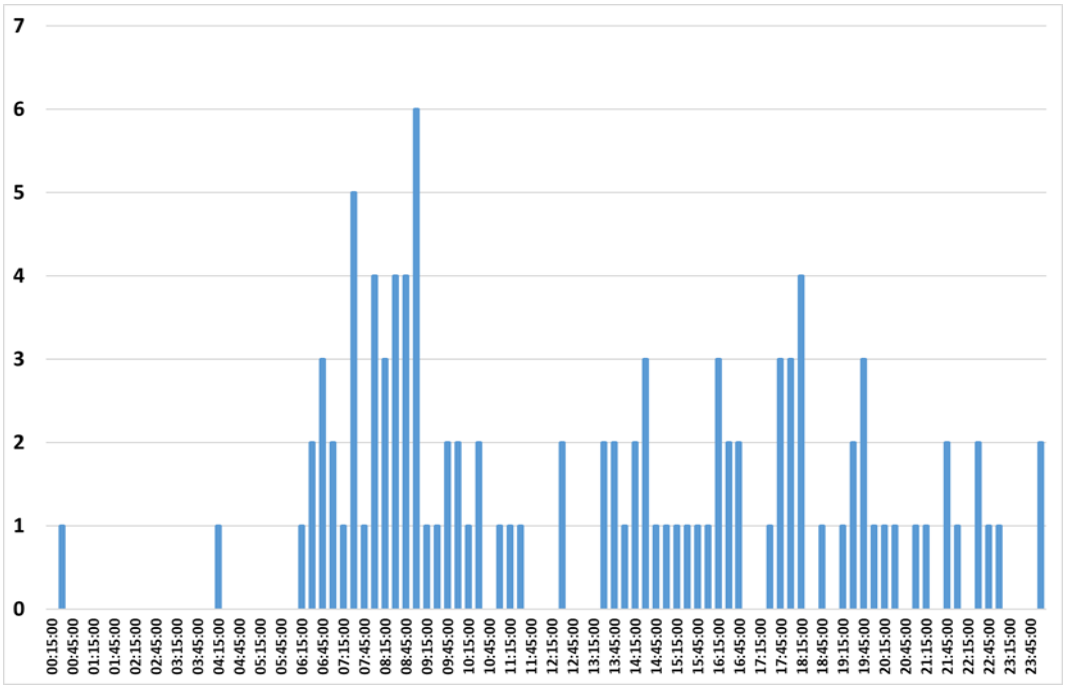

Figure 85: Time of WSP activation

Figure 85 shows WSP activation throughout the day, broken into 15-minute segments, with notable peaks between 6:45 and 9:00am, coinciding with delay trends seen in literature [175]. Trends in the afternoon/evening are less notable and range from approximately 14:30 to 19:45.

Identification of key locations

Locations were first organised by the number of delays, as shown in Figure 86, and have been arbitrarily split into low (0-2), medium (3-6) and high (7+) categories. Originally the severity of the delays were also investigated, however the amount of information gathered in the WSP activation spreadsheet did not contain enough information to fully explore the effects of the severity of each incident [176].

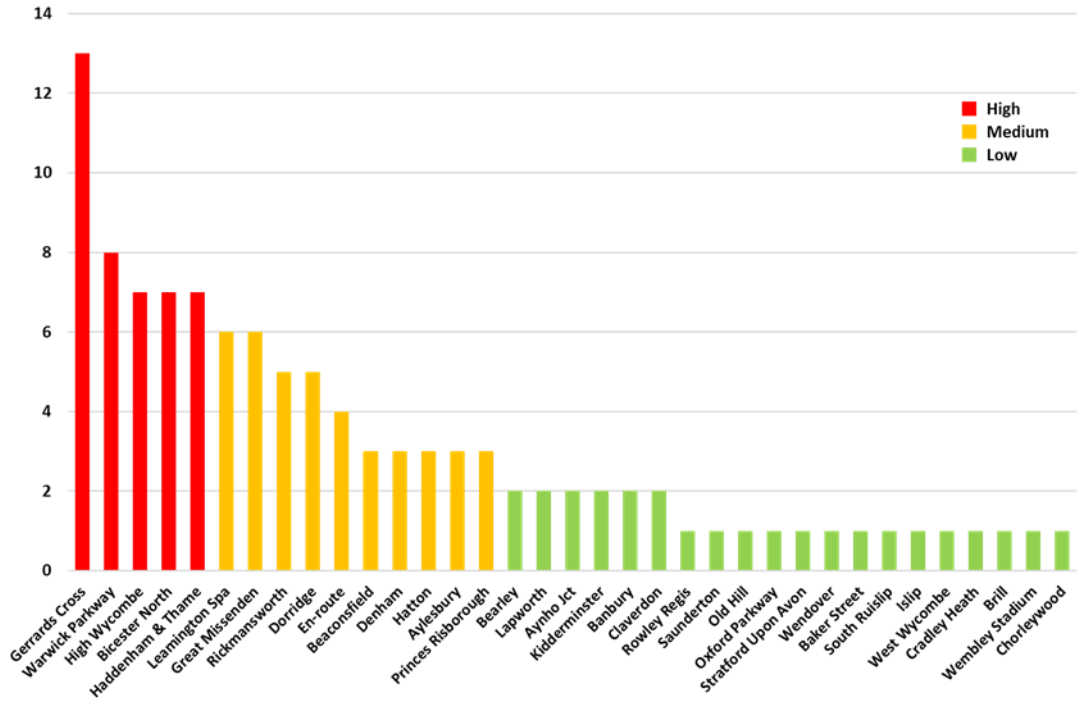

Figure 86: Frequency of delays per location

The thresholds were chosen primarily to give reasonable sized groups, though this is something that could easily be altered should the end user decide.

Delay duration was also investigated to give a combined value for each location, however, no meaningful conclusions or links could be drawn from this approach. Ultimately it was decided that the number of delays per location was the most appropriate route to pursue, as the model was initially designed to predict the likelihood of a leaf induced low adhesion incident and not the necessarily the scale of the incident.

Parameter selection

The model assesses low adhesion risk using certain parameters, with a specific scoring mechanism. Parameters are split into fixed and temporal. Fixed parameters will not change between assessments and include:

- Local terrain - track gradient, whether the track is in a valley/flat/raised
- Signal diagram information - speed limits, number of services etc.

Temporal parameters may change over time and include:

- Distance of treeline from the outside rail, linear spread/density of treeline etc.

Each parameter is expected to contribute to the risk of leaf layer formation and wheel slip occurrence. The magnitude of and relationship between parameters is still unknown. As the model is rolled out onto other networks and the data feeding into it increases, it is possible that stronger trends may become evident that could identify certain parameters more clearly and link them to trends in the WSP activation frequency.

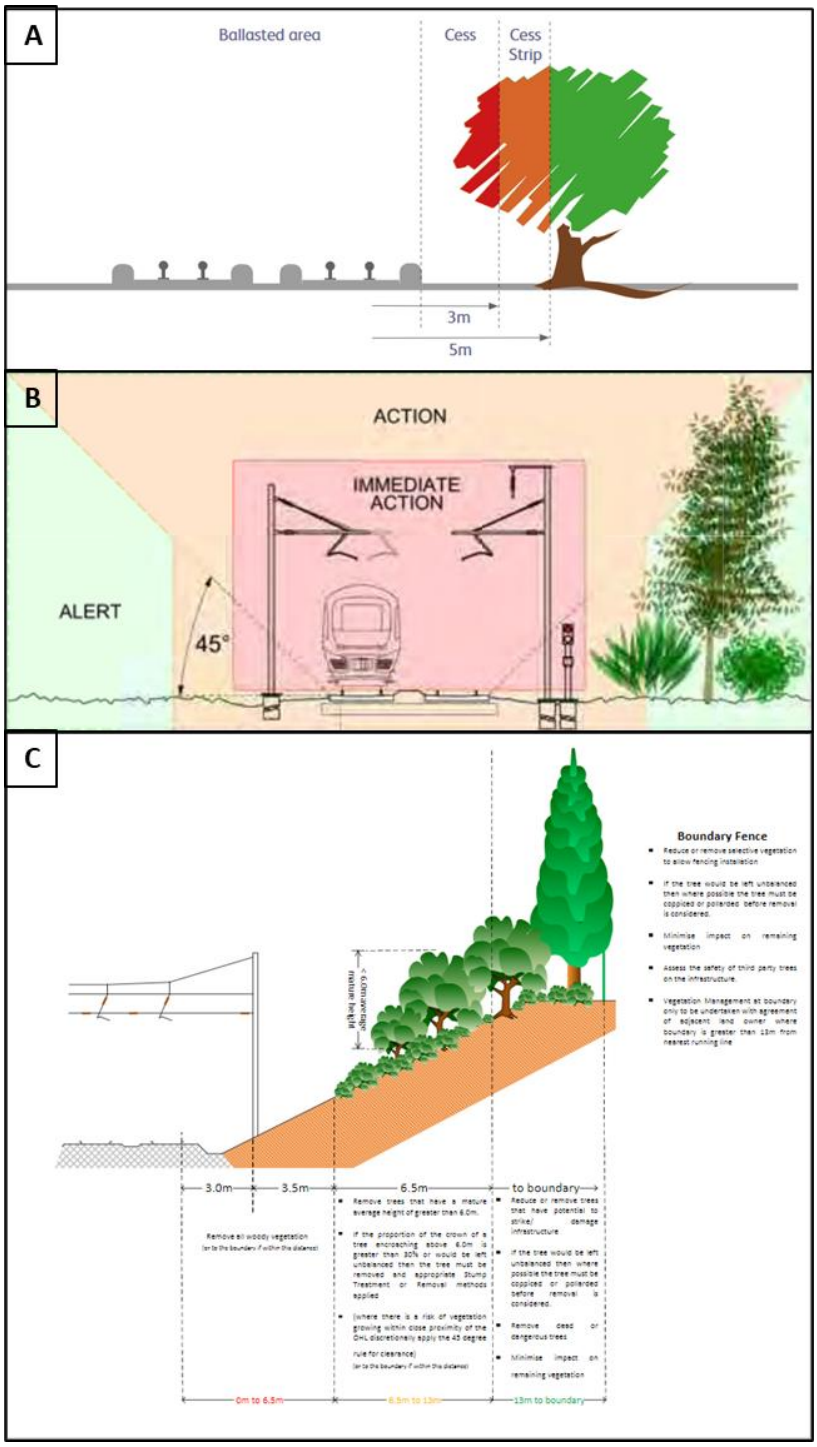

Figure 87: Figures taken from the Varley report [177]**.**

Vegetation distance parameters were chosen based in part on the trackside vegetation standards outlined in pages 18, 19 and 24 of the Varley report [177] and shown above in A, B and C of Figure 86.

Model set-up

Microsoft Excel was chosen for the development of the model due to its ease of use and prevalence. It also allows the model to remain transparent to the end user, enabling them to adjust/input new data as it becomes available.

Parameter		Range				Weighting
		3	2	1	0	
Delay frequency						
Tree coverage	Tree species	-	-	Problematic species present	Problematic species not present	5
	Overhanging the line (overhanging/not overhanging)	-	-	overhanging	not overhanging	3
	Linear spread (or density) along the line (packed or spread)	high	medium	low	no trees	10
	Distance from track in m	less than 3m	between 3m and 5m	between 5m and 10m	over 10m	6
	Depth of trees (away from track)	over 10m	between 3m and 10m	less than 3m or single tree depth	no trees	9
Local terrain	Embankment/flat/cutting-shallow sides/cutting-steep sides	steep, high cutting	medium cutting	flat, no cutting	track is raised	8
Key track features	Gradient	1/265 or steeper	between 1/265 and 1/429	less steep than 1/429	flat	7
	Train speed limits	100 or greater	99 - 75	74 - 60	59 or less	2
Service	No. of lines running through station	4	3	2	1	1
Local area	Rural or urban	-	-	Rural	Urban	4
Total						

	<=	49
	between	50
		101
	>=	102

Figure 88: Scoring mechanism and parameters of the model

Parameters are listed in rows with locations as columns, with a total score shown at the bottom, see Figures Figure 88 and Figure 89. The weightings for parameters are shown in the right most column of Figure 88. All parameters have possible scores in integers ranging from 0-1 or 0-4, where a higher number represents more risk.

The parameters shown above were chosen based on information on vegetation management guidance taken from the Varley report [173], examples of which are shown above in Figure 86. This information describes things such as;

- The distance vegetation should be from the edge of the ballasted area before it is considered dangerous.
- The area immediately surrounding the line, tree corridor and Overhead Line Equipment (OLE) action requirements zones for vegetation.

- Boundary fence and embankment distance specifications.

The gradient and speed limit parameters were included as a result of conversations between the researcher and train drivers and other TOC staff members that explained that low adhesion was expected more so at locations with a higher gradient. The remaining parameters were chosen based on the vegetation surveys carried out (both online and in person) by the author, as well as on cab rides on the CRCL network.

Parameter		Case Study Sites																	
		1 - Gerrards Cross	2 - High Wycombe	3 - Beaconsfield	4 - Great Missenden	5 - Princes Risborough	6 - Claverdon	7 - Leamington Spa	8 - Beasley	9 - Hatton	10 - Old Hill	11 - Chorleywood	12 - Lapworth	13 - Wembley Stadium	14 - Rowley Regis	15 - Wendover	16 - Ilslip	17 - Kidderminster	18 - Oxford Parkway
Delay frequency		3	3	2	2	2	2	2	2	2	1	1	1	1	1	1	1	1	1
Tree coverage	Tree species	1	1	1	1	1	1	1	1	1	1	1	1	1	1	1	1	1	1
	Overhanging the line (overhanging/not overhanging)	1	1	1	1	0	1	1	1	0	1	1	0	0	1	0	1	0	0
	Linear spread (or density) along the line (packed or spread)	3	3	2	3	1	1	1	1	1	2	2	2	2	2	1	1	2	1
	Distance from track in m	3	3	3	3	2	3	2	3	2	3	3	2	2	3	3	3	2	2
	Depth of trees (away from track)	3	1	2	1	1	1	1	1	2	2	2	3	2	1	1	2	1	1
Local terrain	Embankment/cutting/shallow sides/cutting/steep sides	3	3	3	2	1	1	1	1	1	2	1	2	2	1	1	1	2	1
Key track features	Gradient	3	1	3	1	3	0	3	0	0	3	3	1	3	3	3	0	0	0
	Train speed limits	3	2	3	2	2	3	2	1	2	0	1	3	3	0	2	3	0	0
Service	No. of lines running through station	3	3	3	0	3	0	2	0	2	1	0	1	3	0	0	0	0	0
Local area	Rural or urban	0	0	0	1	1	1	0	1	1	0	1	1	0	0	1	1	1	1
Total		137	103	118	96	76	63	74	59	63	102	99	98	101	84	79	72	66	48

Figure 89: Group 1 locations with scores

Figure 89 shows a screenshot of Group 1 from the model with the first 18 locations assessed, their scores are shown at the bottom.

Signal diagram analysis

Signal diagrams were provided by CRCL and contained information on fixed/permanent track features that were considered for the model (e.g. gradient, speed limits and number of platforms). Signal diagrams for all but three locations were available, and where unavailable an educated, yet conservative estimation was used with a tendency towards giving a higher score as opposed to a lower one. The diagrams provided invaluable and otherwise unobtainable information on physical track features.

Site investigation

A site investigation and vegetation survey was carried out on the CRCL network to investigate multiple locations to assess tree information (i.e. leaf types, vegetation density, proximity to track etc.) and other physical parameters (e.g. topography, bridges, tunnels). The researcher personally visited most of the locations on the CRCL network to conduct the vegetation survey, though not all locations could be visited due to a two day time constraint. At each location/station, photographs were taken of the vegetation at the station and track at entrance/exit. Immediately following each visit, notes were taken, including the species of trees/plants that were observed, the level of vegetation coverage and any other notable physical features. Distances between vegetation and track were calculated using the images that were taken. Present tree species were compared to those defined as "problematic" or not [3].

For each site/location the 'most severe' readings were taken, for example, if a station was covered in vegetation on one side and free of vegetation on the other, it would still receive a score based on the side with heavy vegetation. Locations only received one set of scores each.

Weighting and scoring adjustments

Locations assessed using the model were split into two groups. The first group had the total score thresholds adjusted so that the scores matched the average delay rating as closely as possible.

The weighting factors were defined using Group 1 and then validated using Group 2. Several mathematical approaches for ranking the weighting factors were trialled before settling on the one that gave the best fit of total scores to frequency delay scores. The

best fitting method that was used to calculate parameter weighting scores involved going parameter by parameter and summarising the scores for all locations in each delay frequency category. This gave 3 total numbers for each parameter, one for the sum of locations with a delay rating of 3 ("high"), one for those with a delay rating of 2 ("medium") and one for those with a delay rating of 1 ("low"). The "high" total numbers were divided by the "medium" total numbers, and the "medium" total numbers were divided by the "low" total numbers, the latter was then subtracted from the former. This produced a numerical value for each parameter on which they could be ranked against each other in integers from 1-10 where 10 represents the most and 1 represents the least influential parameter. When applied to Group 2, the model predicted location scores that closely matched the delay scores, the user can then look back at the parameter scores and identify what action should be taken for mitigation.

An example of the parameter weighting method for the Tree species parameter that was used on Group 1 involved;

1. Parameter = Tree species
2. Sum of 'high' frequency locations = 2
3. Sum of 'medium' frequency locations = 7
4. Sum of 'low' frequency locations = 9
5. Sum of 'high' frequency locations/ sum of 'medium' frequency locations = 2/7 = 0.29
6. Sum of 'medium' frequency locations/ sum of 'low' frequency locations = 7/9 = 0.78
7. 0.29-0.78 = 0.49
8. When compared to the other parameters, 0.49 came 5th out of 10

This method was used on all parameters and the final scores were ranked against one another (in integers of 1 to 10) in size order of smallest to largest. The parameter 'no. of lines running through station' was given a score of 1 meaning it had the least influence on the risk score, while the parameter 'linear spread (or density) along the line (packed or spread)' was given a score of 10 meaning it had the largest influence.

8.5 Results

Model validation and refinement

Table 34 shows the parameter ranking following the mathematical analysis. The most influential parameter was found to be the linear density of trees along the track, while

the least influential was the number of lines running through the location (station, junction etc.).

Table 34: Parameters with ranked weighting factors

Parameter	Rank
Linear spread (or density of trees) along the line (packed or spread)	10
Embankment/flat/cutting-shallow sides/cutting-steep sides	9
Depth of trees (away from track)	8
Gradient	7
Rural or urban	6
Distance from track in m	5
Tree species	4
Train speed limits	3
Overhanging the line (overhanging/not overhanging)	2
No. of lines running through the location	1

Figure 90 shows the validation using Group 2, where for all but 1 location (Warwick Parkway, possibly due to out of date vegetation information as this site was not visited in the vegetation survey) the score at the bottom was the same or greater than the frequency delay score. The default overestimation of the risk was deliberately intended as a safety precaution, of course this may lead to false positives though it is better that these locations are checked just in case.

Once the Group 2 locations (the control group that was randomised and had the delay frequency scores removed when assessing parameters) were analysed, score colour thresholds (see bottom of Figure 88) were checked to ensure higher risk sites were red, medium risk sites were amber and lower risk sites were green.

Parameter		Cross Check Sites																
		West Wycombe	Cradley Heath	Stratford Upon Avon	Brill	Aylesbury	Bicester North	Rickmansworth	Saunderton	South Ruslip	Haddenham & Thame	Warwick Parkway	Banbury	Denham	Dorridge	Aynho Jct
Delay frequency		1	1	1	1	2	3	2	1	1	3	3	2	2	2	2
Tree coverage	Tree species	1	1	1	0	1	1	1	1	1	1	1	1	1	1	1
	Overhanging the line (overhanging/not overhanging)	1	0	1	0	1	0	0	1	0	1	1	1	1	1	1
	Linear spread (or density) along the line (packed or spread)	2	0	2	2	1	3	1	1	1	3	2	2	3	1	1
	Distance from track in m	3	2	3	2	3	3	2	2	3	3	3	3	3	3	3
	Depth of trees (away from track)	1	1	2	1	1	2	1	1	1	2	1	1	3	1	1
Local terrain	Embankment/flat/cutting-shallow sides/cutting-steep sides	1	1	2	1	1	1	1	1	1	2	1	1	1	1	1
Key track features	Gradient	1	3	0	3	0	3	3	3	0	0	3	2	3	2	2
	Train speed limits	1	1	0	3	0	3	0	3	3	3	0	3	3	1	2
Service	No. of lines running through station	1	1	2	1	2	1	1	1	3	2	1	2	2	3	3
Local area	Rural or urban	1	1	0	1	0	0	0	1	0	1	1	0	1	0	1
Total		77	62	82	81	55	107	66	79	59	102	89	85	124	72	78

Figure 90: Group 2 locations with scores

Figure 90 shows how the model fits the Group 2 locations, where all but one location gives the same or higher risk ranking when compared to the delay frequency. Warwick Parkway is an anomaly with a delay frequency score of 3-high but a risk score of 86, which is in the medium category. It is possible that due to the fact Warwick Parkway was not visited in the vegetation survey (due to time constraints for CRCL and the researcher) and instead relied on Google Maps images, the data used could be out of date hence an incorrect overall score might have been assigned.

8.6 Discussion

A comprehensive low adhesion risk prediction model validated with wheel slide delay data from the CRCL network has been compiled with the aim of approval low adhesion performance, especially during Autumn months. Assumptions had to be made, so there are limitations to the accuracy, repeatability and reliability of the model. For example, wheel slip events were assumed to have happened at the stations listed but could have occurred outside of the station limits. Not all wheel slip incidents will have resulted from low adhesion caused by leaf layers. Efforts were made to remove those not directly attributable to leaf fall, but some may have been missed.

The model can now be used by CRCL and NwR to focus remediation techniques at any given location within the model' s scope. The model can also be rolled out to be used on other routes (this would require some additional field/observational work to feed into the model for a new route). There is potential for this to feed into machine learning for predicting low adhesion.

Suggestions for leaf corridor design

Using the outcomes of the model development and vegetation surveys, suggestions for leaf corridor design include the following. Where possible reduce the linear density of the treeline, keeping trees more spaced out in the direction of the line as this was found to be the most influential parameter. Target any vegetation that extends toward the line, with special attention to any vegetation that is overhanging the line. Despite all species tested showing very similar friction levels, sycamore trees should be removed due to their large leaves, also older trees should be removed as they typically generate more leaves than smaller, younger trees.

8.6.1 Assumptions

Necessary assumptions and limitations were used. These were out of the authors control in some instances (e.g. historical data).

For example, wheel slip events were assumed to have happened at the stations listed but could have occurred outside of the station limits. Not all wheel slip incidents will have resulted from low adhesion caused by leaf layers. Efforts were made to remove those not directly attributable to leaf fall, however, some could have been missed.

It is noted that vegetation surveys were carried out in October 2021 and therefore vegetation levels are likely different to those at the time of each WSP instance.

When performing the mathematical analysis of the parameters, all parameters were analysed using the same process regardless of whether they were scored from 0-1 or 0-3. This was due to the inherent complexity of the issue and did not appear to cause any issues with the final result. It is possible that a more complex method could account for this however one was not found during the model development.

There may be far more causes of contamination to the railhead, however, this model is intended to be as simple as possible and also to focus specifically on leaf contamination.

8.7 Conclusions

- A comprehensive low adhesion risk prediction model validated with wheel slide delay data from the CRCL network has been compiled with the aim of improving low adhesion performance, especially during Autumn months.
- The model can now be used by CRCL and Network Rail (NwR) to focus remediation techniques at any given location within the model' s scope. The model can also be rolled out to be used on other routes (this would require some additional field/observational work to feed into the model for a new route).
- Figure 88 and Table 34 both display the ranked parameters that were found as an outcome of the mathematical analysis of the Group 1 data.
- Figure 90 shows how the model fits the Group 2 locations, where all but one location gives the same or higher risk ranking when compared to the delay frequency. Warwick Parkway is an anomaly.
- Historic WSP activation most frequently occurred in September-November 2018 and October-December 2019, indicating that the model will be most effective between September and December.
- Historic WSP activation data analysis showed notable peaks between 6:45 and 9:00am, and slightly smaller peaks between 14:30 and 19:45.

Strengths

The main strengths of the model are that:

- It predicts a risk rating for a rail location and classifies it as either low, medium or high, it has a bias toward overpredicting the risk which is intended as a safety measure.
- It only requires basic input information that should be able to be gathered by a person with minimal additional training.
- The ranked parameters give the end user the best idea of where to begin with their vegetation management plan.

Weaknesses

The main weaknesses of the model include:

- The user interface has not yet been developed.
- Warwick Parkway produced an anomalous result with a risk rating that did not match the frequency of WSP activation.
- The original data input that the model was developed with only takes into account the frequency of WSP activation at a given location.
- The original data fed into the model assumes that the location designated to WSP activation occurred at a station, though this could be improved if more precise location information is provided.
- There are currently no clear definitions for 'high', 'medium' and 'low' density for things like linear spread, though this could be changed in the future by providing example images for the end user to reference.

8.7.1 Planned Model Development

- Development of model software (i.e. generation of heatmap) and design of user interface (including how to easily edit the model – admins only)
- Roll-out across a second trial Train Operating Company (TOC) network, with a view to nationwide implementation after a second successful trial
- Additional input data from existing low adhesion forecasting models (e.g. NwR)
- Automatic updates to incident data from TOC records WSP activations (e.g. integration with Porterbrook Class 377 remote OTDR)
- Updated vegetation surveys (obtainable from NwR)

9. GENERAL DISCUSSION

9.1 Introduction

The seven overall benefits of this research into understanding and modelling low adhesion risk in the wheel-rail interface are:

1. Identification of the key hypotheses for the formation/bonding and low friction mechanisms of leaf layers.
2. Greater insight into which hypotheses are valid, and which are either invalid or require more investigation.
3. A better understanding of how to successfully generate a black leaf layer during field testing.
4. More understanding of leaf fall dynamics, more specifically the relationship between drop height and horizontal distance covered.
5. A better understanding of the physical parameters responsible for contributing to the risk of leaf layer formation and therefore low adhesion occurring.
6. An open source, location based model for assessing the risk of leaf layer induced low adhesion.
7. Suggestions for leaf corridor design, using the results and data collected in this work.

This chapter discusses the work described in the previous chapters, highlighting any important findings. Outcomes of the experimental work are linked to the low adhesion risk assessment model where possible.

9.2 Testing approaches

9.2.1 Friction

Several approaches were used when measuring the friction of leaf substances (whole leaves, leaf mulch, leaf powders, black leaf layers) both in the laboratory and in the field. Some methods were applicable to both lab and field settings, such as the pendulum skid resistance rig. The two main methods for generating low μ and measuring friction in laboratory settings involved the SUROS and HPT rigs.

SUROS vs HPT

Both the SUROS and HTP rigs were used to test hypotheses for bonding and low μ as they represent the conditions found in the wheel-rail interface. The literature review

revealed that leaf matter testing with the SUROS rig (and other twin disc rigs) is well established, and friction values typically range from 0.01-0.15 (usually below 0.1) depending on the chosen slip and contact pressure. Through operational experience the most influential parameter was found to be the method of delivery of the leaf matter. The SUROS tribometer was typically chosen when testing required liquids being introduced to the contact, including leaf extracts and solid leaf particles/powders suspended in liquids. This was due to the layout of the rigs comparatively open design with limited access to the upper disc and to a lesser extent the contact while running. While the SUROS tribometer is capable of producing leaf layers, its main functions are to monitor friction and wear behaviours.

Meanwhile leaf friction measured by the HPT tribometer is less well established, typical friction values fall in the 0.02-0.06 range. This again is largely driven by the contact pressures, type of contaminant tested and the fact that materials being tested are squashed between two platens under normal and axial loads. This typically ensures test materials are retained in the contact, whereas with the SUROS tribometer materials are very easily ejected. For this reason, it was possible to test comparatively dry (20µl water added) leaf and graphite powders that could not be tested in the SUROS tribometer without the addition of water which would have its own effects. The black leaf layers produced by the HPT tribometer were more beneficial for analysis as they were formed on a flat surface as opposed to the circumferential edge of a relatively small (47mm diameter). The tight radius of the discs affected measurements (as flat surfaces are strongly preferred) and prevented them from fitting into the XPS analysis chamber.

Testing of the bonding and low µ hypotheses would not have been possible without the use of both of these rigs.

Lab vs field

Artificial leaf layers can be generated either in the lab or the field (at heritage or test tracks) and allow for more control over the species present in the layer, the railhead condition (clean/contaminated/specific railhead material (R260 steel alloy)) and the weather conditions (real or simulated). In the context of this work, where species were not being compared sycamore was chosen for leaf layer generation as it is very common and is known in the industry as a "troublesome tree species" for low adhesion in the railway, though other species were tested and compared. At QRTC, the railhead was cleaned using a railhead scrubber prior to each new set of leaf layer tests,

to remove the majority of dust and oxides present and give a repeatable railhead condition. The railhead was also wiped with paper towels to remove any loose dust or dirt post scrubbing. Weather was found to be a crucial aspect of the success or failure of field leaf layer generation, heavy rain and strong winds immediately caused the tests to be abandoned as the leaf matter on the railhead was either washed away, prevented from bonding due to excess water, or blown off the railhead. In cases of light rain and/or wind there was a chance of success, though it was reduced and required modification to the test procedure. For example, a wetter mulch may be needed to stay on the railhead and braking passes may be used sooner before the leaf matter sticks to the wet wheels and is carried down the line.

Field generated layers are either artificially or naturally generated, both of which offer multiple benefits over laboratory generated layers, including accurate representation of real railway environmental and physical conditions, inclusion of other contaminants such as oxides, brake dust, grease and other biological matter. Naturally generated layers are, as the name suggests, generated by real trains on real track without any deliberate effort, and have been observed on UK track from the north of Scotland down to the south of England.

Lab generated layers offer a far higher level of control over all test parameters, including the type of contact (twin disc, pin on disc, HPT, pendulum, FSR (wheel on rail) etc.), speeds feeds and pressures of the contact, number of repetitions, materials used to simulate wheel-rail, contaminant state (whole leaves, mulches/powders, liquid solutions) and ambient conditions. As described above the two main lab based rigs used for this work were the SUROS and HPT.

Hypotheses

The results of the bulk leaves on the line hypothesis proved that wet leaves give lower friction than dry leaves and that wet leaves stick to each other, but dry leaves do not. Therefore, multiple wet leaves may initially cause slightly higher friction than multiple dry leaves, this occurs before the leaves are squashed and formed into a black leaf layer.

When comparing dry leaf powders to solid lubricants, very comparable friction levels were found, indicating that leaves behave in a similar way to dry lubricants. This similarity strongly supports the leaf powders as solid lubricants hypothesis.

The viscous acid gel hypothesis was disproved as a result of the SUROS testing with sycamore-water and sycamore-PBS solution, where very similar friction levels were

observed. If acidic gels were present then the PBS solution would have neutralized them and allowed friction to return to its previous level, however, this was not the case. Though, to be completely certain, chemical analysis on the surface of the discs could provide more valuable information, such as whether any leaf material managed to remain on the surfaces of the discs and if so, what its chemical composition is.

The supercritical water + high temperature and pressure hypothesis compared HPT data on clean dry rail (up to $\mu = 0.7$) and wet rail, showing lower friction (up to $\mu = 0.48$) for the wet conditions. It is likely that the water in the HPT contact reaches supercritical conditions, where it has already been established that water can become H_2O_2, and thus react with the steel substrate to form oxides that could either react with leaf matter to form leaf layers or provide low μ themselves.

The thin surfacer layers hypothesis used XPS analysis of natural field leaf layers, where different chemicals/elements were found at different locations of the sample leaf layers. This supports the thin surface layer hypothesis. SEM analysis of leaf layers would be the ideal next step for this line of investigation.

9.2.2 Leaf layer formation/bonding

Two layer formation/bonding hypotheses were tested, iron oxide catalyst and metallic substrate effects. The iron oxide catalyst hypothesis used two testing approaches, both of which proved to be successful in that they clearly showed a difference in leaf layer formation with and without iron or iron ions present. The first testing method used the SUROS rig to compare the friction of sycamore-water against sycamore-EDTA (a chelating agent), where the sycamore-water showed low friction during and after it was fed into the contact, indicating the formation of a low μ layer. During the sycamore-EDTA test, friction increased immediately after the sycamore-EDTA stopped being fed into the contact, indicating no low μ layer was formed. Despite this clear result, chemical analysis (possibly XPS or FT-IR) could shed further light on the effectiveness of EDTA and metal ions in forming a leaf layer. The second test involving submersing steel (R260) and titanium specimens in tannic acid and monitoring the progress of any black layer formation. A black layer was observed on the R260 but not on the titanium, indicating that some component of the steel was reacting with the tannic acid, and this was assumed to be iron. Again despite the success of this test, chemical and friction analysis of the black layer would reveal exactly which oxides were forming on the steel, and what effect this might have on friction. Future research into this hypothesis could investigate other substrate materials, such as aluminium or

stainless steel which also contains iron but is known for its resistance to oxide formation.

The metallic substrate effects hypothesis investigated the difference in black layer formation on surfaces with different roughness' s and found that rougher surfaces grew black layers at a faster rate than smoother surfaces. The same method (involving tannic acid) was used to grow the black layers. While these results strongly support the hypothesis, ideal next steps would include a wider range in surface roughness' s, possibly involving sections of railhead that are brand new, have been ground or are severely worn.

A successful method for assessing bond strength would be required to fully understand leaf layer formation and bonding. A method was trialled using a torque measuring screwdriver, however, success was very limited in the field. The method involved gluing a metal stud to the leaf layer, then using a torque measuring screwdriver to record the torque at which the layer broke away from the railhead. In the field this method only worked in dry conditions and on some fully formed leaf layers. The results were also difficult to record and interpret.

More work will always be needed to fully confirm these hypotheses and where possible quantify their effects. This could include;

- More chemical analysis of black leaf layers from different species, alongside a friction comparison.
- Chemical analysis of the tannic acid black layer and comparison to lab and naturally generated layers.
- Microscopic analysis to compare lab and field leaf layers.

9.2.3 Leaf fall/mobility

The findings from the leaf fall study showed no correlation between leaf size and/or mass and the horizontal distance covered by falling leaves in wind and no-wind conditions. However, during windy conditions ash travelled the furthest distance, followed by sycamore and common lime. Sycamore leaves were more likely to be blown around on the ballast than ash and common lime. These findings suggest that ash should be considered as troublesome tree species alongside sycamore, due to the fact that sycamore is more likely to move around the track area due to wind and ash travels further horizontally when falling.

Ideally, future work would involve analysing more leaf species with a wider range of sizes and masses. Leaf surface areas could also be calculated or measured more accurately, possibly with the use of image processing. More simulated wind speeds and different drop heights could be investigated as well.

9.3 Low adhesion risk from different tree species

Low adhesion risk from different tree species comes as a result of a combination of; species prevalence, prevailing weather, possible differences in the chemical composition of leaves, differences in the sizes and shapes of different leaves. Weather conditions play a huge roll in the times that leaves fall (linked in particular to a drop in temperature and strong winds), the mobility of leaves on the ground and the hydration state of leaves.

Testing has shown that wet leaves are far more likely to stick to one another, and other surfaces such as ballast, sleepers and/or the railhead. Once on the railhead they can have multiple effects including being run over by a train and forming a leaf layer (thus reducing friction directly), retaining moisture on the railhead (thus accelerating oxide formation and reducing friction indirectly) or being run over and compressed onto a pre-existing leaf or oxide layer.

HPT results have shown that all leaves tested were capable of reducing friction to low ($\mu < 0.1$) or even exceptionally low ($\mu < 0.05$) levels, meaning the risk of low adhesion is more driven by the likelihood of a leaf to reach the railhead in the first place. This means that understanding leaf layer formation requires a better understanding of leaf fall timings, and mobility.

9.4 Autumn data collection

Autumn data collection provided invaluable insight into the time of year that leaf abscission occurs, and leaves are dumped in large quantities. A strong correlation was also observed between leaf abscission and a drop in ambient temperature, which agrees with the literature. The major leaf fall occurred within a 2-3 week period, during which the average friction measured on the railhead at a heritage line dropped by 32% while the leaf layer thickness increased by over 600%. These findings suggest the most beneficial time for using the model would be prior to leaf fall (typically mid-October), and that vegetation management would ideally take place beforehand to reduce the number of leaves present on and around the track. Severe storms are also a key driver in leaf fall that should be anticipated and should be predicted by other adhesion

forecasting tools (i.e., MetDesk' s tool, that provides a more weather based perspective) that the model would work alongside.

The information on the time of year that leaves drop and what weather markers to look for that indicate leaf fall is imminent can be used alongside the low μ prediction model. Once the leaves have fallen the risk of leaf layer formation will increase dramatically, this is when the model predictions will be most useful.

9.5 Suggestions for leaf corridor design

Suggestions for leaf corridor design draw on the outcomes of chapters 4, 5 and 8. Since heavy leaf fall is expected to occur when the ambient temperature drops (usually mid-October), it would be beneficial to carry out vegetation management measures beforehand. This should reduce the volume of leaves in the leaf corridor, thus lowering the potential for leaves to reach the railhead and form a low μ layer.

The findings of the leaf fall and mobility study would suggest that in order to calculate the distance trees should be kept from the track area, a minimum of 1m horizontal distance should be given for every 2m of tree height.

The outcomes of the model development and vegetation surveys suggest that where possible, the linear density of the treeline should be reduced as this was found to be the most influential parameter linked to WSP activation. Any vegetation extending out towards the track should be removed, especially that which overhangs the track. Despite all species tested showing very similar friction levels, sycamore trees should be removed due to their large leaves, also older trees should be removed as they typically generate more leaves than smaller, younger trees.

9.6 Model and summary

The low adhesion prediction model was developed initially using historical WSP activation data and then Google Maps and vegetation surveys. It was always intended to be a static model, that provides a risk assessment score for a specific location using simple data points that can be collected and input to the model relatively easily.

It must be fed fresh data on both WSP activation and vegetation state at regular intervals (ideally annually), or when vegetation is treated/altered. New WSP activation data will ensure that the model has up to date information on which locations are experiencing low μ and the new vegetation data will ensure that the parameter rankings and location risk scores are up to date. Every time a location receives vegetation treatment, its parameter scores will change and so will its risk rating.

The model will also draw on the outcomes of the testing described in this work, such as the leaf fall timing and linked weather conditions (drop in temperature and/or severe storms). Additionally, when vegetation management is planned it would be advisable to, where applicable, reduce the linear density of the treeline as this was found to be the most influential parameter as well as eliminate any vegetation overhanging the line. Another key finding was that once a leaf layer has formed, specific leaf species present is somewhat irrelevant as they are all capable of significantly reducing friction to low or even exceptionally low levels.

In summary, the model is currently in a state where it is ready to be applied to other networks for further validation and finer development tweaks. Steps for improvement include; developing the user interface, devising a robust vegetation and physical track feature survey for the customer to use to score locations and perhaps a refinement of the parameter ranking mathematical process.

10. CONCLUSIONS

The main aims of this project were to widen the understanding of leaf induced low adhesion, and develop a location based model for predicting low adhesion risk in the wheel-rail interface. To achieve this, hypotheses for leaf layer bonding mechanisms and low μ were identified from the literature review and tested. It is assumed that real leaf layers found in the field exhibit combinations of the hypotheses described in this thesis. To develop the low adhesion prediction model, a case study was carried out on historical WSP data that was supplied by CRCL.

The hypotheses were tested using a combination of laboratory and field experiments, as well as chemical analysis (XPS and FT-IR) of authentic and artificially created black leaf layers.

The model for predicting low adhesion took data on WSP activation, identified locations with high and low activation then assessed each location to identify parameters that contribute to the risk. These parameters were then mathematically assessed and ranked based on their effects.

This chapter will state the key findings of the project, as well as any benefits to the rail industry and any future work that is needed.

10.1 Bonding hypotheses

The two bonding hypotheses identified were "iron oxide driven" and "metallic substrate effects", the findings were:

- The iron oxide driven hypothesis testing provided a clear indication that iron oxides are involved in both the bonding and low adhesion of leaves. When an iron capturing chelating agent was present, the friction returned to and increased above levels prior to insertion into the contact.
- The second iron oxide driven hypothesis testing also indicated that iron plays a crucial role in the development of a black layer and by association a leaf layer.
- The metallic substrate effects showed that the surface roughness played a role in the formation rate of black layers, where a smoother surface formed a black layer at a slower rate than a rougher surface.

10.2 Low μ hypotheses

The five low μ hypotheses identified were "bulk leaves on the line", "compressed leaf solid lubricant layer", "viscous acid gel formation", "supercritical water + high temperature and pressure" and "thin surface layers", the findings were:

- The bulk leaves on the line hypothesis testing showed that wet leaves gave lower friction than dry leaves, however, more wet leaves in the contact increase friction.
- The compressed leaf solid lubricant layer testing found that leaf powders were able to reduce friction to levels similar to those of established solid lubricants. Therefore, it is likely that leaves in the wheel-rail contact do act as solid lubricants.
- The results of the viscous acid gel testing cast serious doubt on the validity of the hypothesis, as when the leaf mulch in the simulated wheel-rail contact was brought to a neutral pH level, the friction remained at a similarly low level to the control (sycamore and water).
- Water in the wheel-rail contact is well established for reducing friction, this alongside evidence that when supercritical H_2O can break down and form H_2O_2. H_2O_2 is known to react with ferrous materials to form iron oxides which can bond to leaf materials to form leaf layers. This supports the supercritical water + high temperature and pressure for bonding hypothesis.
- XPS analysis of thin leaf layers collected from the field found them to be chemically similar to other leaf layers that have been known to cause low adhesion.
- From testing on all rigs, as well as in the field at Long Marston it was found that fully formed black leaf layers require a combination of; leaves, water (relatively low levels work better), steel (for the iron content) plus rolling and/or sliding.

10.3 Low adhesion model

The development of the low adhesion risk assessment model included:

- A comprehensive low adhesion risk prediction model validated with wheel slide delay data from the CRCL network has been compiled with the aim of improving low adhesion performance, especially during Autumn months. The model can now be used by CRCL and Network Rail (NwR) to focus remediation techniques at any given location within the model's scope. The model can also be rolled

out to be used on other routes (this would require some additional field/observational work to feed into the model for a new route).

- Parameters were found to be responsible for risk in the following order (higher risk first):
    1. Linear spread (or density of trees) along the line (packed or spread)
    2. Embankment/flat/cutting-shallow sides/cutting-steep sides
    3. Depth of trees (away from track)
    4. Gradient
    5. Rural or urban
    6. Distance from track in m
    7. Tree species
    8. Train speed limits
    9. Overhanging the line (overhanging/not overhanging)
    10. No. of lines running through the location

10.3.1 Leaf corridor design

When considering leaf corridor design, the findings of the leaf drop tests and the low adhesion risk assessment model development would suggest:

- Where possible reduce the linear density of the treeline, keeping trees more spaced out in the direction of the line.
- Target any vegetation that overhangs or reaches towards the line or a place where it may contact the train.
- Despite all species tested showing very similar friction levels, sycamore trees should be removed due to their large leaves, also older trees should be removed as they typically generate more leaves than smaller, younger trees.
- Vegetation management should be more effective if carried out before the significant leaf fall, typically starting in mid-October and sudden drop in ambient temperature should be considered as a marker indicating imminent leaf fall.
- For every 2m of height, leaves can travel almost 1m horizontally under still conditions and much further in windy conditions. This means that higher a tree is (accounting for the base height of the tree relative to the track), the further it should be kept from a rail line (or cess ideally) with a minimum of 1m distance per 2m height.

10.4 Further work

There are many possible avenues for furthering this line of research and development, the most immediate considerations could include:

- Development of model software (i.e. generation of heatmap) and design of user interface (including how to easily edit the model – admins only).
- Roll-out the model across a second rail network, with possible further implementation after a second successful trial.
- Integration of the model into/with existing low adhesion forecasting models (e.g. NwR).
- Further investigation into and development of a species-friction database to provide more justification for troublesome/not-troublesome species classification.
- Further analysis of bonding and low μ hypotheses to further validate or disprove them.

References

[1] "Passengers – Network Rail." https://www.networkrail.co.uk/communities/passengers/ (accessed Feb. 12, 2018).

[2] "Rail industry finance (UK) | ORR Data Portal." https://dataportal.orr.gov.uk/statistics/finance/rail-industry-finance/ (accessed Sep. 07, 2022).

[3] AWG and RSSB, "Adhesion Manual Edition 6.0," 2018. Accessed: May 29, 2018. [Online]. Available: https://www.rssb.co.uk/rgs/oodocs/rdg-awg manual iss 6.pdf

[4] "ADHERE (ADHEsion REsearch challenge)." https://www.rssb.co.uk/en/what-we-do/key-industry-topics/adhesion/adhere-adhesion-research-challenge (accessed Sep. 21, 2022).

[5] C. F. Fulford, "Review of low adhesion research," 2004.

[6] RAIB, "Buffer stop collision at Chester station 20 November 2013," *Rail Accident Report*, 2013.

[7] RAIB, "Station overrun at Stonegate, East Sussex 8 November 2010," *Rail Accident Report*, 2011.

[8] "Interim report 01/2022: Collision between passenger trains at Salisbury Tunnel Junction - GOV.UK." https://www.gov.uk/government/news/interim-report-012021-collision-between-passenger-trains-at-salisbury-tunnel-junction (accessed Nov. 22, 2022).

[9] K. Ishizaka, S. Lewis, and R. Lewis, "The low adhesion problem due to leaf contamination in the wheel/rail contact: Bonding and low adhesion mechanisms," *Wear*, vol. 378–379, pp. 183–197, 2017, doi: 10.1016/j.wear.2017.02.044.

[10] M. Harmon and R. Lewis, "Review of top of rail friction modifier tribology," *Tribology - Materials, Surfaces and Interfaces*, vol. 10, no. 3. pp. 150–162, 2016. doi: 10.1080/17515831.2016.1216265.

[11] AWG and RSSB, "Managing Low Adhesion," 2018.

[12] W. Poole and RSSB, "Characteristics of Railhead Leaf Contamination. Summary Report.," 2007.

[13] R. N. McInnes *et al.*, "Mapping allergenic pollen vegetation in UK to study environmental exposure and human health," *Science of The Total Environment*, vol. 599–600, pp. 483–499, Dec. 2017, doi: 10.1016/j.scitotenv.2017.04.136.

[14] "Aerial Photography | LiDAR | GIS data | Bluesky." https://www.bluesky-world.com/ (accessed Feb. 13, 2019).

[15] "UK rail maps schematic and geographic." http://www.projectmapping.co.uk/Reviews/ukrailmapsschema.html (accessed Feb. 14, 2019).

[16] Forestry Commission, “NFI preliminary estimates of quantities of broadleaved species in British woodlands, with special focus on ash 1 NFI preliminary estimates for broadleaved species and ash,” 2012.

[17] “Ash dieback (Hymenoscyphus fraxineus) - Forest Research.” https://www.forestresearch.gov.uk/tools-and-resources/fthr/pest-and-disease-resources/ash-dieback-hymenoscyphus-fraxineus/ (accessed Aug. 10, 2022).

[18] R. Parker and Z. Fang, *Adhesion & Adhesives. Book*. 1966.

[19] D. Cosgrove, “Assembly and enlargement of the primary cell wall in plants,” *Annu Rev Cell Dev Biol*, vol. 13, no. 1, pp. 171–201, Nov. 1997, doi: 10.1146/annurev.cellbio.13.1.171.

[20] B. Ridley, M. O’Neill, and D. Mohnen, “Pectin structure and biosynthesis, and oligogalacturonide-related signaling,” *Phytochemistry*, vol. 57, no. 6, pp. 929–967, Jul. 2001, doi: 10.1016/S0031-9422(01)00113-3.

[21] D. Mohnen, “Pectin structure and biosynthesis,” *Curr Opin Plant Biol*, vol. 11, no. 3, pp. 266–277, 2008, doi: 10.1016/j.pbi.2008.03.006.

[22] B. R. Thakur, R. K. Singh, A. K. Handa, and M. A. Rao, “Chemistry and uses of pectin — A review,” *Crit Rev Food Sci Nutr*, vol. 37, no. 1, pp. 47–73, Feb. 1997, doi: 10.1080/10408399709527767.

[23] N. Wellner, M. Kačuráková, A. Malovíková, R. Wilson, and P. Belton, “FT-IR study of pectate and pectinate gels formed by divalent cations,” *Carbohydr Res*, vol. 308, no. 1–2, pp. 123–131, Mar. 1998, doi: 10.1016/S0008-6215(98)00065-2.

[24] A. Kawabata, S. Sawayama, H. Nakahara, and T. Kamata, “Mechanism of Association of Various Demethylated Pectins by Calcium Ions,” *Agric Biol Chem*, vol. 45, no. 4, pp. 965–973, Apr. 1981, doi: 10.1080/00021369.1981.10864628.

[25] P. M. Cann, “The ‘“leaves on the line”’ problem—a study of leaf residue film formation and lubricity under laboratory test conditions,” *Tribol Lett*, vol. 24, no. 2, pp. 151–158, 2006, doi: 10.1007/s11249-006-9152-2.

[26] “Cellulose - The Difference Between Cellulose and Starch - Breaking the Vicious Cycle.” http://www.breakingtheviciouscycle.info/knowledge_base/detail/cellulose-the-difference-between-cellulose-and-starch/ (accessed Feb. 22, 2019).

[27] D. Argyropoulos, H. Sadeghifar, C. Cui, and S. Sen, “Synthesis and Characterization of Poly(arylene ether sulfone) Kraft Lignin Heat Stable Copolymers,” *ACS Sustain Chem Eng*, vol. 2, no. 2, pp. 264–271, Feb. 2014, doi: 10.1021/sc4002998.

[28] A. Koriakin, H. Nguyen, D. Kim, and C. Lee, “Thermochemical Decomposition of Microcrystalline Cellulose Using Sub- and Supercritical Tetralin and Decalin with Fe3O4,” *Ind Eng Chem Res*, vol. 54, no. 18, pp. 5184–5194, May 2015, doi: 10.1021/acs.iecr.5b00763.

[29] S. Mitsuru, F. Zhen, F. Yoshiko, A. Tadafumi, and K. Arai, “Dissolution and Hydrolysis of Cellulose in Subcritical and Supercritical Water,” 2000, doi: 10.1021/IE990690J.

[30] N. Somashekara, Z. M. Saiyed, and C. N. Ramchand, “Biochemistry of Railhead Leaf Film Contamination,” 2006.

[31] J. Crowe, T. Bradshaw, and P. Monk, *Molecular shape and structure 2: the shape of large molecules*. Oxford: Oxford University Press, 2006.

[32] Z. Li, O. Arias-Cuevas, R. Lewis, and E. Gallardo-Hernández, "Rolling–Sliding Laboratory Tests of Friction Modifiers in Leaf Contaminated Wheel–Rail Contacts," *Tribol Lett*, vol. 33, no. 2, pp. 97–109, Feb. 2009, doi: 10.1007/s11249-008-9393-3.

[33] A. Naseem, S. Tabasum, K. Zia, M. Zuber, M. Ali, and A. Noreen, "Lignin-derivatives based polymers, blends and composites: A review," *Int J Biol Macromol*, vol. 93, pp. 296–313, Dec. 2016, doi: 10.1016/J.IJBIOMAC.2016.08.030.

[34] B. M. Upton and A. M. Kasko, "Strategies for the Conversion of Lignin to High-Value Polymeric Materials: Review and Perspective," *Chem Rev*, vol. 116, no. 4, pp. 2275–2306, Feb. 2016, doi: 10.1021/acs.chemrev.5b00345.

[35] A. Toledano Zabaleta, "Lignin extraction, purification and depolymerization study," 2012.

[36] R. J. A. Gosselink *et al.*, "Lignin depolymerisation in supercritical carbon dioxide/acetone/water fluid for the production of aromatic chemicals," *Bioresour Technol*, vol. 106, pp. 173–177, Feb. 2012, doi: 10.1016/J.BIORTECH.2011.11.121.

[37] J. E. Holladay, J. J. Bozell, J. F. White, and D. Johnson, "Top Value-Added Chemicals from Biomass - Volume II—Results of Screening for Potential Candidates from Biorefinery Lignin," 2007.

[38] M. Rahman, J. Tsukamoto, Md. M. Rahman, A. Yoneyama, and K. Mostafa, "Lignin and its effects on litter decomposition in forest ecosystems," *Chemistry and Ecology*, vol. 29, no. 6, pp. 540–553, Aug. 2013, doi: 10.1080/02757540.2013.790380.

[39] T. Yong and Y. Matsumura, "Reaction Kinetics of the Lignin Conversion in Supercritical Water," *Ind Eng Chem Res*, vol. 51, no. 37, pp. 11975–11988, Sep. 2012, doi: 10.1021/ie300921d.

[40] Y. Nagamatsu and M. Funaoka, "Structural Control of Lignin-Based Polymers and the Design of Recyclable Lignocellulosic Composites," *Adhesion society of Japan*, vol. 37, no. 12, pp. 479–486, 2001.

[41] Z. Yuan, S. Cheng, M. Leitch, and C. Xu, "Hydrolytic degradation of alkaline lignin in hot-compressed water and ethanol," *Bioresour Technol*, vol. 101, no. 23, pp. 9308–9313, Dec. 2010, doi: 10.1016/J.BIORTECH.2010.06.140.

[42] K. Okuda, X. Man, M. Umetsu, S. Takami, and T. Adschiri, "Efficient conversion of lignin into single chemical species by solvothermal reaction in water– p -cresol solvent," *Journal of Physics: Condensed Matter*, vol. 16, no. 14, pp. S1325–S1330, Apr. 2004, doi: 10.1088/0953-8984/16/14/045.

[43] † Mitsumasa Osada, † Takafumi Sato, ‡ Masaru Watanabe, § and Tadafumi Adschiri, and ‡ Kunio Arai*, †, "Low-Temperature Catalytic Gasification of Lignin and Cellulose with a Ruthenium Catalyst in Supercritical Water," 2003, doi: 10.1021/EF034026Y.

[44] K. Ishizaka, "Confirmation Review," Sheffield, 2017.

[45] D. N.-S. Hon, *Chemical modification of lignocellulosic materials*. M. Dekker, 1996.

[46] T. Fletcher and E. Harris, “Destructive Distillation of Douglas Fir Lignin,” *J Am Chem Soc*, vol. 69, no. 12, pp. 3144–3145, Dec. 1947, doi: 10.1021/ja01204a505.

[47] A. Austin and C. Ballaré, “Dual role of lignin in plant litter decomposition in terrestrial ecosystems.,” *Proc Natl Acad Sci U S A*, vol. 107, no. 10, pp. 4618–22, Mar. 2010, doi: 10.1073/pnas.0909396107.

[48] D. Gillon, R. Joffre, and A. Ibrahima, “Initial litter properties and decay rate: a microcosm experiment on Mediterranean species,” *Canadian Journal of Botany*, vol. 72, no. 7, pp. 946–954, Jul. 1994, doi: 10.1139/b94-120.

[49] J. Melillo, J. Aber, and J. Muratore, “Nitrogen and Lignin Control of Hardwood Leaf Litter Decomposition Dynamics,” *Ecology*, vol. 63, no. 3, pp. 621–626, Jun. 1982, doi: 10.2307/1936780.

[50] Jr. H. V. Marsh, H. J. Evans, and G. Matrone, “Investigations of the Role of Iron in Chlorophyll Metabolism. II. Effect of Iron Deficiency on Chlorophyll Synthesis,” *Plant Physiol*, vol. 38, no. 6, p. 638, Nov. 1963, doi: 10.1104/PP.38.6.638.

[51] N. Nykvist, “Leaching and Decomposition of Litter V. Experiments on Leaf Litter of Alnus glutinosa, Fagus silvatica and Quercus robur,” *Oikos*, vol. 13, no. 2, p. 232, 1962, doi: 10.2307/3565087.

[52] H. Staaf, “Release of Plant Nutrients from Decomposing Leaf Litter in a South Swedish Beech Forest,” *Holarctic Ecology*, vol. 3, pp. 129–136, 1980.

[53] C. Otto and L. M. Nilsson, “Why Do Beech and Oak Trees Retain Leaves Until Spring?,” 1981. Accessed: Feb. 11, 2019. [Online]. Available: https://www.jstor.org/stable/3544134

[54] M. Witkamp and J. Olson, “Breakdown of Confined and Nonconfined Oak Litter,” *Oikos*, vol. 14, no. 2, p. 138, 1963, doi: 10.2307/3564969.

[55] K. Ishizaka, “The Low Adhesion Problem due to Leaf Contamination in the Wheel/Rail Contact: Bonding and Low Adhesion Mechanisms,” The University of Sheffield, Sheffield, 2019.

[56] R. Lewis and J. Masing, “Static wheel/rail contact isolation due to track contamination”, doi: 10.1243/095440906X77919.

[57] B. White, “Using Tribo-Chemistry Analysis to Understand Low Adhesion in the Wheel-Rail Contact,” The University of Sheffield, 2018.

[58] J. Suzumura, Y. Sone, A. Ishizaki, D. Yamashita, Y. Nakajima, and M. Ishida, “In situ X-ray analytical study on the alteration process of iron oxide layers at the railhead surface while under railway traffic,” *Wear*, vol. 271, no. 1–2, pp. 47–53, 2010, doi: 10.1016/j.wear.2010.10.054.

[59] T. Misawa, K. Hashimoto, and S. Shimodaira, “The mechanism of formation of iron oxide and oxyhydroxides in aqueous solutions at room temperature,” *Corros Sci*, vol. 14, no. 2, pp. 131–149, Jan. 1974, doi: 10.1016/S0010-938X(74)80051-X.

[60] H. Zhu, F. Cao, D. Zuo, L. Zhu, D. Jin, and K. Yao, “A new hydrothermal blackening technology for Fe 3 O 4 coatings of carbon steel,” *Appl Surf Sci*, no. 254, pp. 5905–5909, 2008, doi: 10.1016/j.apsusc.2008.03.184.

[61] H. Chen, M. Ishida, and T. Nakahara, “Analysis of adhesion under wet conditions for three-dimensional contact considering surface roughness,” *Wear*, vol. 258, no. 7–8, pp. 1209–1216, Mar. 2005, doi: 10.1016/J.WEAR.2004.03.031.

[62] D. Godfrey, “Iron oxides and rust (Hydrated iron oxides) in tribology,” *Journal of the Society of Tribologists and Lubrication Engineers*, vol. 55, no. 2, pp. 33–37, 1999, Accessed: Feb. 25, 2019. [Online]. Available: https://search.proquest.com/docview/226949422/fulltextPDF/814366A73A4D4D78PQ/1?accountid=13828

[63] N. Basavegowda, K. Mishra, and Y. R. Lee, “Synthesis, characterization, and catalytic applications of hematite (α-Fe2O3) nanoparticles as reusable nanocatalyst,” *Advances in Natural Sciences: Nanoscience and Nanotechnology*, vol. 8, no. 2, p. 025017, Jun. 2017, doi: 10.1088/2043-6254/AA6885.

[64] M. C. Pereira, L. C. A. Oliveira, and E. Murad, “Iron oxide catalysts: Fenton and Fentonlike reactions – a review,” *Clay Miner*, vol. 47, no. 3, pp. 285–302, Sep. 2012, doi: 10.1180/CLAYMIN.2012.047.3.01.

[65] S. D. Jojoa-Sierra, J. Herrero-Albillos, M. P. Ormad, E. A. Serna-Galvis, R. A. Torres-Palma, and R. Mosteo, “Wüstite as a catalyst source for water remediation: Differentiated antimicrobial activity of by-products, action routes of the process, and transformation of fluoroquinolones,” *Chemical Engineering Journal*, vol. 435, May 2022, doi: 10.1016/J.CEJ.2022.134850.

[66] T. Nakahara, K. Baek, H. Chen, and M. Ishida, “Relationship between surface oxide layer and transient traction characteristics for two steel rollers under unlubricated and water lubricated conditions,” *Wear*, vol. 271, no. 1–2, pp. 25–31, May 2011, doi: 10.1016/J.WEAR.2010.10.030.

[67] Y. Berthier *et al.*, “The role and effects of the third body in the wheel-rail interaction,” *Fatigue Fracture of Engineering Materials and Structures*, vol. 27, no. 5, pp. 423–436, May 2004, doi: 10.1111/j.1460-2695.2004.00764.x.

[68] K. Ishizaka, “Basic Tribology of Leaf-related Material and Basic Material Analysis,” Sheffield, 2018.

[69] U. Niinemets, O. Kull, and J. Tenhunen, “An analysis of light effects on foliar morphology, physiology, and light interception in temperate deciduous woody species of contrasting shade tolerance.,” *Tree Physiol*, vol. 18, no. 10, pp. 681–696, Oct. 1998.

[70] H. K. Lichtenthaler *et al.*, “Photosynthetic activity, chloroplast ultrastructure, and leaf characteristics of high-light and low-light plants and of sun and shade leaves.”

[71] H. Lichtenthaler, “Adaptation of leaves and chloroplasts to high quanta fluenee rates.,” *Proceedings of the Fifth International Congress on Photosynthesis*, 1981.

[72] H. K. Lichtenthaler, “The Unequal Synthesis of the Lipophilic Plastidquinones in Sun- and Shade Leaves of Fagus silvatica L.,” *Zeitschrift für Naturforschung B*, vol. 26, no. 8, pp. 832–842, Aug. 1971, doi: 10.1515/znb-1971-0819.

[73] O. Bjorkman, N. Boardman, J. Anderson, S. Thorne, D. Goodchild, and N. Pyliotis, “Effect of light intensity during growth of Atriplex patula on the capacity of photosynthetic reactions, chloroplast components and structure,” *Annu Rep Dep Plant Biol Carnegie Inst*, 1971.

[74] T. Sariyildiz and J. Anderson, “Variation in the chemical composition of green leaves and leaf litters from three deciduous tree species growing on different soil types,” *For Ecol Manage*, vol. 210, no. 1–3, pp. 303–319, May 2005, doi: 10.1016/J.FORECO.2005.02.043.

[75] “soil | Definition of soil in English by Oxford Dictionaries,” 2019. https://en.oxforddictionaries.com/definition/soil (accessed Feb. 06, 2019).

[76] T. Sariyildiz and J. Anderson, “Interactions between litter quality, decomposition and soil fertility: a laboratory study,” *Soil Biol Biochem*, vol. 35, no. 3, pp. 391–399, Mar. 2003, doi: 10.1016/S0038-0717(02)00290-0.

[77] B. Clayden, “Soils of the Exeter District.,” *Soils of the Exeter District.*, 1971.

[78] L. S. Sonon, D. E. Kissel, and U. Saha, “Cation Exchange Capacity and Base Saturation.”

[79] “Nitrogen Basics-The Nitrogen Cycle Agronomy Fact Sheet Series.”

[80] “Soil map for England and Wales — World Reference Base 2006 Level 1 Version | UK Soil Observatory | Natural Environment Research Council.” http://www.ukso.org/wrb/WRB_England_Wales.html (accessed Feb. 27, 2019).

[81] “Thermo Scientific XPS: What is XPS.” https://xpssimplified.com/whatisxps.php (accessed May 31, 2018).

[82] T. Yamashita and P. Hayes, “Analysis of XPS spectra of Fe2+ and Fe3+ ions in oxide materials,” *Appl Surf Sci*, vol. 254, no. 18, pp. 2441–2449, 2008, doi: 10.1016/j.apsusc.2007.09.063.

[83] J. Andrade, “X-ray Photoelectron Spectroscopy (XPS),” in *Surface and Interfacial Aspects of Biomedical Polymers*, Boston, MA: Springer US, 1985, pp. 105–195. doi: 10.1007/978-1-4684-8610-0_5.

[84] Y. Zhu, U. Olofsson, and R. Nilsson, “A field test study of leaf contamination on railhead surfaces,” *Rail and Rapid Transit*, vol. 228, no. 1, pp. 71–84, 2014, doi: 10.1177/0954409712464860.

[85] “Raman spectroscopy in more detail.” http://www.renishaw.com/en/raman-spectroscopy-in-more-detail--25806 (accessed Jun. 01, 2018).

[86] “DoITPoMS - TLP Library Raman Spectroscopy - Advantages and disadvantages.” https://www.doitpoms.ac.uk/tlplib/raman/advantages_disadvantages.php (accessed Jun. 01, 2018).

[87] J. B. Bates, “Fourier Transform Infrared Spectroscopy,” *Science*, vol. 191. American Association for the Advancement of Science, pp. 31–37, 1976. doi: 10.2307/1741844.

[88] ThermoFisher, “FTIR Basics - TR.” https://www.thermofisher.com/tr/en/home/industrial/spectroscopy-elemental-isotope-analysis/spectroscopy-elemental-isotope-analysis-learning-center/molecular-spectroscopy-information/ftir-information/ftir-basics.html (accessed May 30, 2018).

[89] A. Rohman, Sismindari, Y. Erwanto, and Y. B. Che Man, “Analysis of pork adulteration in beef meatball using Fourier transform infrared (FTIR) spectroscopy,” *Meat Sci*, vol. 88, no. 1, pp. 91–95, May 2011, doi: 10.1016/J.MEATSCI.2010.12.007.

[90] “X-Ray Diffraction – XRD – Particle Analytical.” http://particle.dk/methods-analytical-laboratory/xrd-analysis/ (accessed Mar. 01, 2019).

[91] RSSB and T. Johnson, “Understanding aerodynamic influences of vehicle design on wheel/rail contamination: Summary report,” 2007.

[92] J. Garforth, “Woodland trust autumn analysis document.,” 2016.

[93] F. Chmielewski and T. Rötzer, “Response of tree phenology to climate change across Europe,” *Agric For Meteorol*, vol. 108, no. 2, pp. 101–112, Jun. 2001, doi: 10.1016/S0168-1923(01)00233-7.

[94] A. Menzel *et al.*, “European phenological response to climate change matches the warming pattern,” *Glob Chang Biol*, vol. 12, no. 10, pp. 1969–1976, Oct. 2006, doi: 10.1111/j.1365-2486.2006.01193.x.

[95] N. Delpierre *et al.*, “Modelling interannual and spatial variability of leaf senescence for three deciduous tree species in France”, doi: 10.1016/j.agrformet.2008.11.014.

[96] A. Menzel, “Plant Phenological Anomalies in Germany and their Relation to Air Temperature and NAO,” *Clim Change*, vol. 57, no. 3, pp. 243–263, 2003, doi: 10.1023/A:1022880418362.

[97] F. Addicott, “Environmental factors in the physiology of abscission.,” *Plant Physiol*, vol. 43, no. 9 Pt B, pp. 1471–9, Sep. 1968.

[98] T. Koike, “Autumn coloring, photosynthetic performance and leaf development of deciduous broad-leaved trees in relation to forest succession,” *Tree Physiol*, vol. 7, no. 1-2-3–4, pp. 21–32, Dec. 1990, doi: 10.1093/treephys/7.1-2-3-4.21.

[99] N. Bréda, R. Huc, A. Granier, and E. Dreyer, “Temperate forest trees and stands under severe drought: a review of ecophysiological responses, adaptation processes and long-term consequences,” *Ann For Sci*, vol. 63, no. 6, pp. 625–644, Sep. 2006, doi: 10.1051/forest:2006042.

[100] C. Smart, “Gene expression during leaf senescence,” *New Phytologist*, vol. 126, no. 3, pp. 419–448, Mar. 1994, doi: 10.1111/j.1469-8137.1994.tb04243.x.

[101] J. Keskitalo, B. Bergquist, P. Gardeström, and S. Jansson, “A cellular timetable of autumn senescence,” *Plant Physiol*, vol. 139, Jan. 2005.

[102] K. Nagase, “A Study of Adhesion Between the Rails and Running Wheels on Main Lines: Results of Investigations by Slipping Adhesion Test Bogie,” *Proc Inst Mech Eng F J Rail Rapid Transit*, vol. 203, no. 1, pp. 33–43, Jan. 1989, doi: 10.1243/PIME_PROC_1989_203_206_02.

[103] Met Office, "• Average wind speed UK 2001-2021 | Statista." https://www.statista.com/statistics/322785/average-wind-speed-in-the-united-kingdom-uk/ (accessed May 24, 2022).

[104] A. R. Hemsley, Imogen. Poole, and Linnean Society of London. Palaeobotany Specialist Group., "The evolution of plant physiology : from whole plants to ecosystems," p. 492, 2004.

[105] "Leaves - Network Rail." https://www.networkrail.co.uk/running-the-railway/looking-after-the-railway/delays-explained/leaves/ (accessed Aug. 10, 2022).

[106] S. Basu, "Modeling and Dynamics of Falling Leaves." Chapel Hill, North Carolina, 2006.

[107] S. B. Field, M. Klaus, M. G. Moore, and F. Nori, "Chaotic dynamics of falling disks," *Nature*, vol. 388, no. 6639, pp. 252–254, 1997, doi: 10.1038/40817.

[108] W. Liu, P. Luo, W. Qi, S. Lu, and H. Cui, "IOP Conference Series: Earth and Environmental Science Study on Airflow Characteristics of Train Induced by Piston Effect in Subway Tunnel Study on Airflow Characteristics of Train Induced by Piston Effect in Subway Tunnel", doi: 10.1088/1755-1315/237/3/032120.

[109] L. Evelyn Buckley-Johnstone, "Wheel/Rail Contact Tribology: Characterising Low Adhesion Mechanisms and Friction Management Products," The University of Sheffield, 2017.

[110] H. Rahmani, D. Gutsulyak, L. Stanlake, B. Stoeber, and S. Green, "Carrydown of liquid friction modifier," *Proc Inst Mech Eng F J Rail Rapid Transit*, vol. 236, no. 9, pp. 1124–1134, Oct. 2022, doi: 10.1177/09544097221076258/ASSET/IMAGES/LARGE/10.1177_09544097221076258-FIG3.JPEG.

[111] J. L. Lanigan, P. Krier, L. B. Johnstone, B. White, P. Ferriday, and R. Lewis, "Field trials of a methodology for locomotive brake testing to assess friction enhancement in the wheel/rail interface using a representative leaf layer:," *https://doi.org/10.1177/0954409720973135*, vol. 235, no. 9, pp. 1053–1064, Nov. 2020, doi: 10.1177/0954409720973135.

[112] RSSB, "Annual Safety Performance Report 2001/02," 2002.

[113] I. Flynn, B. Haddock, and Network Rail, "2015 National Autumn Review." 2016.

[114] I. Flynn, B. Haddock, and Network Rail, "2015 National Autumn Review." 2016.

[115] D. J. Watkins, "Exploring adhesion with British Rail's Tribometer Train," *Railway Engineering Journal*, 1975.

[116] D. J. Watkins, "Exploring adhesion with British Rail's Tribometer Train," *Railway Engineering Journal*, 1975.

[117] P. Murkin and A. Veal, "An Investigation of Possible Meteorological Factors Affecting Low Rail Adhesion Events in Autumn 2003," 2005.

[118] "Low adhesion forecast - Met Office." https://www.metoffice.gov.uk/services/transport/railways/low-adhesion-forecast (accessed Apr. 08, 2019).

[119] V. Chapman, "Met Office Adhesion Services and Research." Birmingham, 2019.

[120] U. Olofsson, Y. Zhu, S. Abbasi, R. Lewis, and S. Lewis, “Tribology of the wheel–rail contact – aspects of wear, particle emission and adhesion,” *Vehicle System Dynamics*, vol. 51, no. 7, pp. 1091–1120, 2013, doi: 10.1080/00423114.2013.800215.

[121] O. Arias-Cuevas and Z. Li, “Field investigations into the adhesion recovery in leaf-contaminated wheel–rail contacts with locomotive sanders,” *Proc Inst Mech Eng F J Rail Rapid Transit*, vol. 225, no. 5, pp. 443–456, Sep. 2011, doi: 10.1177/2041301710394921.

[122] M. Omasta, M. Machatka, D. Smejkal, M. Hartl, and I. Křupka, “Influence of sanding parameters on adhesion recovery in contaminated wheel–rail contact,” *Wear*, vol. 322–323, pp. 218–225, Jan. 2015, doi: 10.1016/J.WEAR.2014.11.017.

[123] R. Lewis and U. Olofsson, “Mapping rail wear regimes and transitions,” *Wear*, vol. 257, no. 7–8, pp. 721–729, Oct. 2004, doi: 10.1016/J.WEAR.2004.03.019.

[124] R. Lewis and U. Olofsson, *Wheel-rail interface handbook*. CRC Press, 2009.

[125] U. Olofsson and K. Sundvall, “Influence of leaf, humidity and applied lubrication on friction in the wheel-rail contact: Pin-on-disc experiments,” *Proc Inst Mech Eng F J Rail Rapid Transit*, vol. 218, no. 3, pp. 235–242, May 2004, doi: 10.1243/0954409042389364.

[126] U. Olofsson and R. Lewis, *Handbook of railway vehicle dynamics*. CRC/Taylor & Francis, 2006.

[127] E. Gallardo-Hernández and R. Lewis, “Twin disc assessment of wheel/rail adhesion,” *Wear*, vol. 265, no. 9–10, pp. 1309–1316, Oct. 2008.

[128] G. Vasic, F. J. Franklin, A. Kapoor, and V. Lucanin, “Laboratory simulation of low-adhesion leaf film on rail steel,” *International Journal of Surface Science and Engineering*, vol. 2, no. 1/2, p. 84, 2008, doi: 10.1504/IJSURFSE.2008.018970.

[129] O. Arias-Cuevas, Z. Li, R. Lewis, and E. Gallardo-Hernández, “Laboratory investigation of some sanding parameters to improve the adhesion in leaf-contaminated wheel—rail contacts,” *Proc Inst Mech Eng F J Rail Rapid Transit*, vol. 224, no. 3, pp. 139–157, May 2010, doi: 10.1243/09544097JRRT308.

[130] S. Lewis, R. Lewis, J. Cotter, X. Lu, and D. Eadie, “A new method for the assessment of traction enhancers and the generation of organic layers in a twin-disc machine,” *Wear*, vol. 366–367, pp. 258–267, Nov. 2016, doi: 10.1016/J.WEAR.2016.04.030.

[131] M. Harmon *et al.*, “Evaluation of the coefficient of friction of rails in the field and laboratory using several devices,” in *11th International conference on contact mechanics and wear of rail/wheel systems (CM2018)*, 2018, pp. 364–373.

[132] R. Lewis, S. Lewis, Y. Zhu, S. Abbasi, and U. Olofsson, “The modification of a slip resistance meter for measurement of railhead adhesion,” *Proc Inst Mech Eng F J Rail Rapid Transit*, vol. 227, no. 2, pp. 196–200, 2012, doi: 10.1177/0954409712455147.

[133] S. Lewis, R. Lewis, and U. Olofsson, “An alternative method for the assessment of railhead traction,” *Wear*, vol. 271, no. 1–2, pp. 62–70, May 2011, doi: 10.1016/J.WEAR.2010.10.035.

[134] R. Brookes, “Wheel rail interface technology management; autumn performance trials,” 2003.

[135] W. Zhang, J. Chen, X. Wu, and X. Jin, “Wheel/rail adhesion and analysis by using full scale roller rig,” *Wear*, vol. 253, no. 1–2, pp. 82–88, Jul. 2002, doi: 10.1016/S0043-1648(02)00086-8.

[136] P. Hyde, D. Fletcher, A. Kapoor, and S. Richardson, “Full scale testing to investigate the effect of rail head treatments of differing pH on railway rail leaf films,” 2008.

[137] “HAROLD - University of Huddersfield.” https://research.hud.ac.uk/institutes-centres/irr/harold/ (accessed Sep. 21, 2022).

[138] Zhou, Brunskill, Pletz, Daves, Scheriau, and Lewis, “Real time measurement of dynamic wheel-rail contacts using ultrasonic reflectometry”, doi: 10.1115/1.4043281.

[139] R. Lewis and U. Olofsson, “Basic tribology of the wheel-rail contact,” in *Wheel-Rail Interface Handbook*, 2009. doi: 10.1533/9781845696788.1.34.

[140] M. Evans, W. A. Skipper, L. Buckley-Johnstone, A. Meierhofer, K. Six, and R. Lewis, “The development of a high pressure torsion test methodology for simulating wheel/rail contacts,” *Tribol Int*, vol. 156, p. 106842, Apr. 2021, doi: 10.1016/J.TRIBOINT.2020.106842.

[141] K. Edalati, Z. Horita, and T. G. Langdon, “The significance of slippage in processing by high-pressure torsion,” *Scr Mater*, vol. 60, no. 1, pp. 9–12, Jan. 2009, doi: 10.1016/J.SCRIPTAMAT.2008.08.042.

[142] H. Chen and S. Hibino, “Evaluation test of tangential force coefficient under different types of fallen leaves,” *12 th International Conference on Contact Mechanics and Wear of Rail/Wheel Systems (CM2022)*, Sep. 2022.

[143] N. El Mansouri, A. Pizzi, and J. Salvadó, “Lignin-based wood panel adhesives without formaldehyde,” *Holz als Roh- und Werkstoff*, vol. 65, no. 1, pp. 65–70, Feb. 2007, doi: 10.1007/s00107-006-0130-z.

[144] P. Dongre *et al.*, “Lignin-Furfural Based Adhesives,” *Energies (Basel)*, vol. 8, no. 8, pp. 7897–7914, Jul. 2015, doi: 10.3390/en8087897.

[145] P. Platt, V. Allen, M. Fenwick, M. Gass, and M. Preuss, “Observation of the effect of surface roughness on the oxidation of Zircaloy-4,” *Corros Sci*, vol. 98, pp. 1–5, Sep. 2015, doi: 10.1016/J.CORSCI.2015.05.013.

[146] D. Fletcher, “Thermal contact stress and near surface rail cracks.,” in *The ninth international conference on contact mechanics and wear of rail/wheel systems*, 2012, pp. 470–479.

[147] Y. Cao *et al.*, “Concurrent microstructural evolution of ferrite and austenite in a duplex stainless steel processed by high-pressure torsion,” *Acta Mater*, vol. 63, pp. 16–29, Jan. 2014, doi: 10.1016/J.ACTAMAT.2013.09.030.

[148] D. A. Rigney, “Transfer, mixing and associated chemical and mechanical processes during the sliding of ductile materials,” *Wear*, vol. 245, no. 1–2, pp. 1–9, Oct. 2000, doi: 10.1016/S0043-1648(00)00460-9.

[149] G. Baumann, K. Knothe, and H.-J. Fecht, “Surface modification, corrugation and nanostructure formation of high speed railway tracks,” *Nanostructured Materials*, vol. 9, no. 1–8, pp. 751–754, Jan. 1997, doi: 10.1016/S0965-9773(97)00162-1.

[150] A. R. Imre, U. K. Deiters, T. Kraska, and I. Tiselj, “The pseudocritical regions for supercritical water,” *Nuclear Engineering and Design*, vol. 252, pp. 179–183, Nov. 2012, doi: 10.1016/J.NUCENGDES.2012.07.007.

[151] D. Fletcher, “Thermal contact stress and near surface rail cracks.,” in *The ninth international conference on contact mechanics and wear of rail/wheel systems*, 2012, pp. 470–479.

[152] “Sheffield Supertram | Worldwide Trams Wiki | Fandom.” https://trams.fandom.com/wiki/Sheffield_Supertram (accessed Sep. 07, 2022).

[153] “Google Maps.” https://www.google.com/maps/@53.395456,-1.5171584,13z (accessed Sep. 07, 2022).

[154] J. Crick and Michigan State University Extension, “How weather affects fall colors - MSU Extension.” 2016. Accessed: Jul. 22, 2022. [Online]. Available: https://www.canr.msu.edu/news/how_weather_affects_fall_colors

[155] A. Almaskati, “Understanding Low Adhesion Caused by ‘Leaves on the Line,’” MEng, The University of Sheffield, 2020.

[156] T. Ido and H. Chen, “The removal effect of citric acid on black leaf layer on rail surface caused by fallen leaves,” in *12 th International Conference on Contact Mechanics and Wear of Rail/Wheel Systems (CM2022)*, Sep. 2022.

[157] M. Watson, B. White, J. Lanigan, T. Slatter, and R. Lewis, “The composition and friction-reducing properties of leaf layers,” *Proceedings of the Royal Society A*, vol. 476, no. 2239, Jul. 2020, doi: 10.1098/RSPA.2020.0057.

[158] K. Kalyanasundaram and P. B. Nagy, “A simple numerical model of the apparent loss of eddy current conductivity due to surface roughness,” *NDT & E International*, vol. 37, no. 1, pp. 47–56, Jan. 2004, doi: 10.1016/J.NDTEINT.2003.08.005.

[159] W. Sunda and S. Huntsman, “Effect of pH, light, and temperature on Fe–EDTA chelation and Fe hydrolysis in seawater,” *Mar Chem*, vol. 84, no. 1–2, pp. 35–47, Dec. 2003, doi: 10.1016/S0304-4203(03)00101-4.

[160] C. J. Rudolph, E. W. McDonagh, and R. K. Barber, “Effect of EDTA Chelation on Serum Iron,” *Journal of Advancement in Medicine*, vol. 4, no. 1, pp. 39–45, 1991.

[161] M. B. Marshall, R. Lewis, R. S. Dwyer-Joyce, U. Olofsson, and S. Björklund, “Experimental characterization of wheel-rail contact patch evolution,” *J Tribol*, vol. 128, no. 3, pp. 493–504, Jul. 2006, doi: 10.1115/1.2197523.

[162] R. N. Wenzel, “Resistance of solid surfaces to wetting by water,” *Ind Eng Chem*, vol. 28, no. 8, pp. 988–994, Aug. 1936, doi: 10.1021/IE50320A024/ASSET/IE50320A024.FP.PNG_V03.

[163] “Guidance on Wheel / Rail Low Adhesion Measurement.” https://www.rssb.co.uk/standards-catalogue/catalogueitem/gmgn2642%20iss%201 (accessed Dec. 07, 2022).

[164] W. Skipper, “Sand Particle Entrainment and its Effects on the Wheel/Rail Interface,” The University of Sheffield, Sheffield, 2021.

[165] M. A. Pantoja-Castro, H. González-Rodríguez, M. A. Pantoja-Castro, and H. González-Rodríguez, "STUDY BY INFRARED SPECTROSCOPY AND THERMOGRAVIMETRIC ANALYSIS OF TANNINS AND TANNIC ACID", Accessed: Jun. 15, 2022. [Online]. Available: www.relaquim.com

[166] V. Viswanath, V. V. Leo, S. Sabna Prabha, C. Prabhakumari, V. P. Potty, and M. S. Jisha, "Thermal properties of tannin extracted from *Anacardium occidentale L* . using TGA and FT-IR spectroscopy," *Nat Prod Res*, vol. 30, no. 2, pp. 223–227, Jan. 2016, doi: 10.1080/14786419.2015.1040992.

[167] T. Wahyono, D. A. Astuti, I. Komang, G. Wiryawan, I. Sugoro, and A. Jayanegara, "Fourier Transform Mid-Infrared (FTIR) Spectroscopy to Identify Tannin Compounds in The Panicle of Sorghum Mutant Lines", doi: 10.1088/1757-899X/546/4/042045.

[168] C. G. Boeriu, D. Bravo, R. J. A. Gosselink, and J. E. G. van Dam, "Characterisation of structure-dependent functional properties of lignin with infrared spectroscopy," *Ind Crops Prod*, vol. 20, no. 2, pp. 205–218, Sep. 2004, doi: 10.1016/J.INDCROP.2004.04.022.

[169] "IR Spectrum Table." https://www.sigmaaldrich.com/GB/en/technical-documents/technical-article/analytical-chemistry/photometry-and-reflectometry/ir-spectrum-table (accessed Jun. 15, 2022).

[170] K. Johns, "Supercritical fluids - a novel approach to magnetic media production?," *Tribol Int*, vol. 31, no. 9, pp. 485–490, 1998, doi: 10.1016/S0301-679X(98)00052-8.

[171] D. Gutsulyak, L. Stanlake, and H. Qi, "Twin disc evaluation of third body materials in the wheel/rail interface," in *11th International conference on contact mechanics and wear of rail/wheel systems (CM2018)*, 2018, pp. 339–349.

[172] C. Zhang *et al.*, "Acceleration of oxidation process of iron in supercritical water containing dissolved oxygen by the formation of H 2 O 2," *J Chem Phys*, vol. 8, p. 85104, 2018, doi: 10.1063/1.5032264.

[173] K. jie Rong, Y. long Xiao, M. xue Shen, H. ping Zhao, W. J. Wang, and G. yao Xiong, "Influence of ambient humidity on the adhesion and damage behavior of wheel–rail interface under hot weather condition," *Wear*, vol. 486–487, p. 204091, Dec. 2021, doi: 10.1016/J.WEAR.2021.204091.

[174] "Our stations | Chiltern Railways." https://www.chilternrailways.co.uk/routes-and-destinations (accessed Jan. 17, 2022).

[175] H. Sun, J. Wu, L. Wu, X. Yan, and Z. Gao, "Estimating the influence of common disruptions on urban rail transit networks," *Transp Res Part A Policy Pract*, vol. 94, pp. 62–75, Dec. 2016, doi: 10.1016/J.TRA.2016.09.006.

[176] "2019: A year in review - Met Office." https://www.metoffice.gov.uk/about-us/press-office/news/weather-and-climate/2019/weather-overview-2019 (accessed Dec. 09, 2022).

[177] RSSB, "Valuing nature – a railway for people and wildlife… The Network Rail Vegetation Management Review," 2018.

[178] C. Chang, B. Chen, Y. Cai, and J. Wang, "An experimental study of high speed wheel-rail adhesion characteristics in wet condition on full scale roller rig," in *11th International*

conference on contact mechanics and wear of rail/wheel systems (CM2018), 2018, pp. 115–122.

[179] K. Ishizaka, S. Lewis, D. Hammond, and R. Lewis, “Investigation of leaf chemistry and leaf layer: low adhesion mechanism,” in *11th International conference on contact mechanics and wear of rail/wheel systems (CM2018)*, 2018, pp. 419–430.

[180] H. Chen, T. Furuya, S. Fukagai, S. Saga, K. Murakami, and T. Ban, “Survey occurrence of wheel slipping/sliding caused by fallen leaves on the test line,” in *11th International conference on contact mechanics and wear of rail/wheel systems (CM2018)2*, 2018, pp. 140–146.

[181] F. Tuinstra and J. L. Koenig, “Raman Spectrum of Graphite,” *The Journal of Chemical Physics Journal of Applied Physics Journal of Applied Physics Journal of Applied Physics Applied Physics Letters THE JOURNAL OF CHEMICAL PHYSICS*, vol. 53, no. 3, pp. 1126–1130, 1970, doi: 10.1063/1.2818692.

[182] “ESTERIFIED | English meaning - Cambridge Dictionary.” https://dictionary.cambridge.org/dictionary/english/esterified (accessed Nov. 22, 2022).

11. Appendix

11.1 Paper grading table

Table 35: Paper grading table

Reference	Reference letter	Category		Criteria							Total
		Primary	Secondary	1	2	3	4	5	6	7	
[32]	A	Friction testing	Lab	y	y	y	n	n	y	n	4
[25]	A	Friction testing	Lab	y	y	y	n	n	y	n	4
[127]	A	Friction testing	Lab	y	y	y	n	n	y	n	4
[178]	A	Friction testing	Lab	n	y	n	y	y	y	n	4
[132]	A	Friction testing	Lab	y	y	y	n	y	y	n	5
[131]	A	Friction testing	Lab	n	y	y	y	y	y	n	5
[171]	A	Friction testing	Lab	n	y	y	n	y	y	n	4
[179]	B	Friction testing	Lab	n	y	y	n	y	y	n	4
[180]	C	Friction testing	Lab	n	y	n	y	y	y	y	5
[125]	A	Friction testing	Lab	y	y	y	n	y	y	n	5
[133]	A	Friction testing	Lab	y	y	y	n	y	y	n	5
[102]	A	Friction testing	Field	y	y	n	n	y	y	y	5
[84]	A	Friction testing	Field	y	y	n	n	y	y	n	4
[132]	B	Friction testing	Field	y	y	y	n	y	y	n	5
[131]	B	Friction testing	Field	n	y	y	y	y	y	n	5
[133]	B	Friction testing	Field	y	y	y	n	y	y	n	5
[32]	D	Leaf fall mechanics	Leaf entrainment	y	y	y	n	y	y	n	5
[102]	B	Leaf fall Mechanics	Leaf entrainment	y	y	n	n	y	y	y	5
[53]	C	Leaf fall Mechanics	When	y	n	n	y	y	y	n	4
[180]	A	Leaf fall mechanics	When	n	y	n	n	y	y	y	5
[53]	B	Leaf fall Mechanics	How	y	y	n	y	y	y	n	5
[32]	B	Chemistry	Analysis Techniques	y	y	y	n	n	y	n	4

[25]	C	Chemistry	Analysis Techniques	y	y	y	n	n	y	n	4
[181]	A	Chemistry	Analysis Techniques	y	y	y	n	y	y	n	5
[58]	A	Chemistry	Analysis Techniques	y	n	n	y	y	y	n	4
[82]	A	Chemistry	Analysis Techniques	y	y	y	n	y	y	n	5
[179]	A	Chemistry	Analysis Techniques	n	y	y	n	y	y	n	4
[74]	A	Chemistry	Leaf fall and condition	y	y	n	y	y	y	n	5
[53]	A	Chemistry	Leaf fall and condition	y	y	n	y	y	y	n	5
[84]	B	Mechanisms	Bonding	y	y	n	n	n	y	n	3
[179]	C	Mechanisms	Bonding	n	y	y	n	y	y	n	4
[180]	B	Mechanisms	Bonding	n	y	n	y	y	y	y	5
[12]	A	Mechanisms	Bonding	n	y	y	y	y	y	n	5
[32]	C	Mechanisms	Low μ	y	y	y	n	y	y	n	5
[84]	C	Mechanisms	Low μ	y	y	n	n	n	y	n	3
[25]	B	Mechanisms	Low μ	y	y	y	n	n	y	n	4
[127]	B	Mechanisms	Low μ	y	y	y	n	n	y	n	4
[12]	B	Mechanisms	Low μ	n	y	y	y	y	y	n	5
[133]	C	Mechanisms	Low μ	y	y	y	n	y	n	n	4
[32]	E	Bond strength testing	Lab	y	y	n	n	y	y	y	5
[127]	C	Bond strength testing	Lab	y	y	y	n	n	y	n	4

11.2 HPT test procedure

1. Record material being tested, time and date, ambient temperature and humidity, contact inner and outer radii.
2. Insert the upper and lower specimens into the rig.
3. Enter the information from step 1 into the test program and begin the script.
4. Check the alignment of the specimens at 0°, 40° and -40°, insert contact paper between specimens to ensure consistent pressure is being applied at each angle.
5. Use callipers to measure the inner and outer radii of the upper specimen and update the script if necessary.
6. Use acetone to clean contacting surfaces.
7. Run the script with no contaminant present to prevent strain hardening from occurring in the actual test run using the following steps:

a. Rotate bottom specimen to 0° and raise until it contacts the upper specimen.

b. Increase the contact pressure to 900 MPa.

c. Lower specimen begins to rotate in positive direction.

d. Lower specimen stops rotating when either:

i. The shear contact stress reaches ±950 MPa.

ii. The sweep angle moves by ± 2°.

iii. The slip between contact faces is detected as quick angular movement with negligible change in shear stress. This is usually the most reached condition.

e. Once the positive rotation is complete, the lower specimen will rotate back in the negative direction, ending using the same criteria for the positive case.

f. Repeated the process with the lower specimen starting at positive and negative 30°.

8. Carry out two dry test passes at -30° and -20°, ensuring that the contact surfaces are fully run in. This is done to allow for a comparison between a dry interface and one with leaf matter present. The dry test sweep procedure is:

g. The lower specimen is raised until it comes into contact with the upper specimen.

h. The pressure in the contact is increased to 900 MPa.

i. Data logging starts.

j. The lower specimen is rotated in the positive direction through 0.4 mm at 0.1 °/s.

k. Once the test sweep has reached the final position the data logging stops.

l. Contact shear stress reaches zero and the lower specimen is lowered.

m. Once both dry runs are complete, apply leaves to the contact as follows: insert 0.025 g of leaf powder into the contact, next apply 20 µl of distilled water onto the leaf powder. Perform one additional run in order to condition the leaf layer. Apply a further 20 µl of water and run the test again.

9. Perform a further three test runs with the lower specimen at -10°, 0°, and 10°, using the same procedure as shown in 9.